ACCSCIENCE PUBLISHING

Tumor Discovery

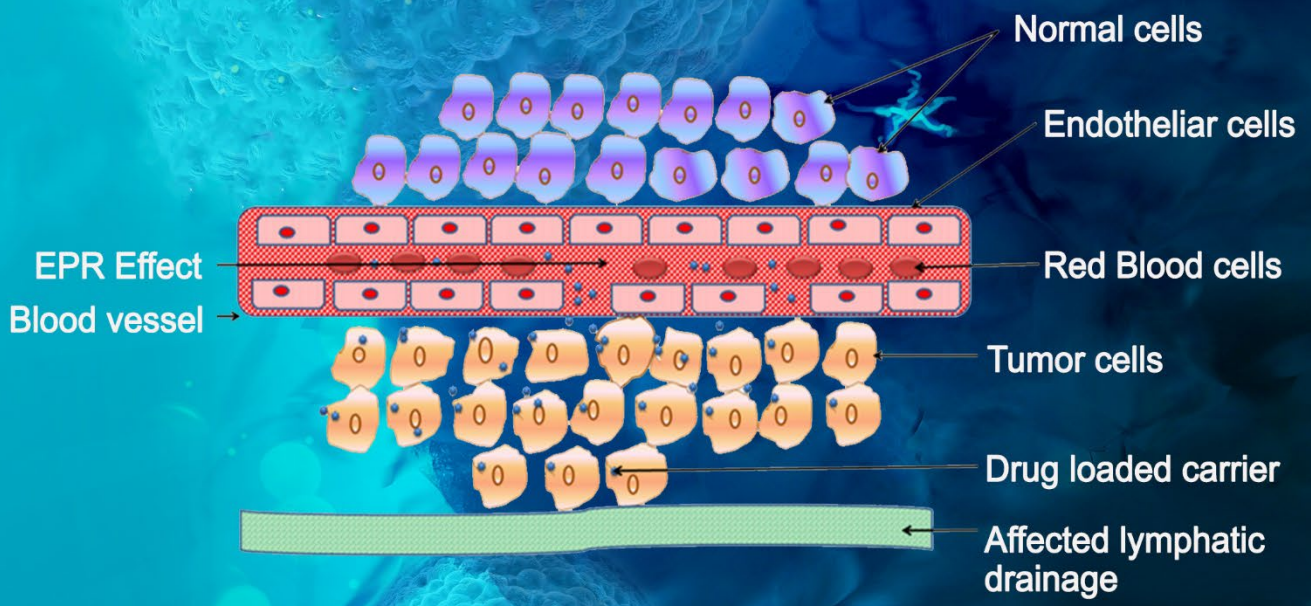

Targeted drug delivery approaches for the management of tumors

ISSN: 3060-8597 (Print)
ISSN: 2810-9775 (Online)
Volume 2 • Issue 3
November 2023

ACCSCIENCE PUBLISHING

Tumor Discovery

Print ISSN: 3060-8597
Online ISSN: 2810-9775

Tumor Discovery is a peer-reviewed and open-access journal that aims to present new cancer research with strong emphasis on fundamental and translational studies. *Tumor Discovery* covers topics such as etiology and pathogenesis of cancer, mechanisms and molecular pathways underlying cancer initiation and progression, tumor metastasis, etc.

Scan to access website:

Scan to submit papers:

About the Publisher

AccScience Publishing is a publishing company based in Singapore. We publish a range of high-quality, open-access, peer-reviewed journals and books from a broad spectrum of disciplines.

Contact Us

Managing Editor
td.office@accscience.sg

AccScience Publishing
8 Burn Road, #15-03 Trivex, Singapore 369977.

Volume 2 • Issue 3 • November 2023
ISSN 3060-8597 (print) ISSN 2810-9775 (online)

TUMOR DISCOVERY

ACCSCIENCE PUBLISHING

Access Science Without Barriers

TUMOR DISCOVERY

ISSN: 3060-8597 (print)
ISSN: 2810-9775 (online)

Editorial and Production Credits

Publisher: AccScience Publishing
Managing Editor: Zoe Zhang
Production Editor: Sharmila Velapasamy
Journal Development Editor: Felicia Wang
Special Issue Commissioning Editor: Hannah Zhang
Article Layout and Typeset: Sinjore Technologies (India)
Cover Design: ProPub (China)

For all advertising queries, contact td.office@accscience.sg.

Supplementary file

Supplementary files of articles can be obtained at https://accscience.com/journal/TD/2/3.

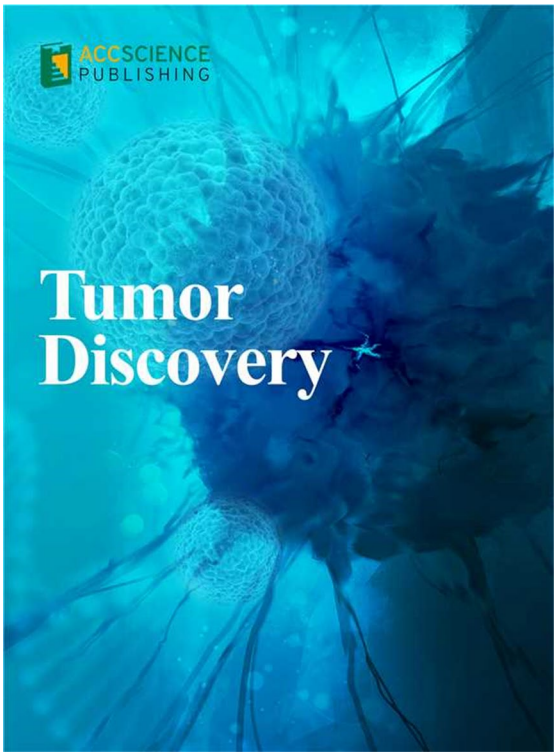

Tumor Discovery

Editorial Board

ACCSCIENCE PUBLISHING

Volume 2 | Issue 3 | November 2023 |

Tumor Discovery

https://accscience.com/journal/TD

CONTENTS

ACCSCIENCE PUBLISHING

Tumor Discovery

REVIEW ARTICLE

Targeted drug delivery approaches for the management of tumors

Shashi Kiran Misra[1], and Kamla Pathak[2]*

[1]Department of Pharmacy, School of Pharmaceutical Sciences, Chhatrapati Shahu Ji Maharaj University, Kanpur, Uttar Pradesh, India

[2]Department of Pharmacy, Faculty of Pharmacy, Uttar Pradesh University of Medical Sciences, Saifai, Etawah, Uttar Pradesh, India

Abstract

The treatment of tumors requires specific and selective drug delivery approaches capable of efficiently eliminating the root cause of oncogenesis. In this context, targeted drug delivery strategies are the preferred choice due to their exceptional recognition of tumor cell biology and their high transfection efficacy within the tumor microenvironment. The emergence of nanoscale techniques has marked significant milestones in the successful management of various types of tumors. The development of targeted delivery approaches for tumor therapeutics has gained momentum over the past few decades. However, in contrast to the plethora of successful pre-clinical studies, only a limited number of passively targeted nanocarriers have been approved for clinical use, and none of the actively targeted nanocarriers have advanced beyond clinical trials. This review delves into the major molecular principles associated with tumorigenesis, including active targeting, passive targeting, and cell-mediated targeting. It also explores the biological barriers (systemic, biological, and cellular) encountered in tumor drug delivery. Moreover, the review examines various tumor-targeted drug delivery systems that have been developed over the past decade. These systems encompass polymeric nanoparticles (micelles, nanoparticles, dendrimers, and polyplexes), lipid-based carriers (solid lipid nanoparticles, nanostructured lipid carriers, nanoemulsion), vesicular systems (liposomes, niosomes, aquasomes, and phytosomes), and inorganic nanocarriers (iron oxide nanoparticles, quantum dots, carbon-based nanoparticles, and mesoporous silica nanoparticles), all designed for the alleviation of tumors.

Keywords: Oncogenesis; Transfection efficacy; Microenvironment; Biological barriers; Nanocarriers

***Corresponding author:**
Kamla Pathak
(kamlapathak5@gmail.com)

Citation: Misra SK, Pathak K, 2023, Targeted drug delivery approaches for the management of tumors. *Tumor Discov*, 2(3): 1356. https://doi.org/10.36922/td.1356

Received: July 23, 2023

Accepted: September 15, 2023

Published Online: October 25, 2023

1. Introduction

Tumors are defined as abnormal growth of cells that proliferate and differentiate more rapidly than normal cells and do not undergo programmed cell death. Tumors can be classified as benign (non-harmful) or malignant (neoplasm and cancerous). Although benign tumors can grow large and do not invade neighboring cells/tissues in other parts of the body, they can be life-threatening if they compress vital organs, including blood vessels or nerves[1]. In contrast, malignant tumors exhibit high aggressiveness, invade adjacent tissues, and have the potential to spread through the body's vascular systems

(circulatory and lymphatic systems). It is estimated that every year, approximately 10 million individuals suffer from malignant tumors, and around 1.3 million of them succumb to the disease. Advanced medical and pharmaceutical strategies, including surgical procedures, radiotherapy, chemotherapy, and targeted drug delivery systems, have contributed to a reduction in mortality rates over the past 5 years.

According to a report by the Personalized Medicine Coalition report (2017–2023), the introduction of personalized medicine has proven to be a successful approach in oncology, constituting approximately 50% of Food and Drug Administration-approved antitumor therapeutics. Malignant tumors, commonly referred to as cancers, exhibit six hallmarks, including the activation of the proliferative signaling pathway, the inhibition of growth suppressors, resistance to cell death, the acquisition of replicative immortality, the promotion of angiogenesis, and the facilitation of metastasis. These hallmarks play pivotal roles in the development of tumors and cancer[2]. In a nutshell, tumor cells exhibit highly differentiated and disordered tissue structures, along with anomalous vasculature compared to normal cells. The deprivation of essential nutrients and oxygen supply results in increased interstitial pressure within cells, leading to an acidic and hypoxic environment. Hypoxia-inducible transcription factors (hif1 and hif2) are implicated in promoting distant metastasis and mediating the progression of tumor cells[3].

Moreover, disorganized tumor cells exhibit inefficiencies in proton efflux to the extracellular environment, leading to a hypoxic environment that disrupts the regulation of glycolysis, adenosine triphosphate (ATP) generation, and lactate production. At the molecular-level, these variations and alterations in the tumor's architectural profile differentiate them from normal cells. Tumor cells exhibit remarkable efficiency in mass-producing a range of factors, such as growth factors, transferrin, interleukins, cytokines, chemokines, proteases, and sugar moieties that play crucial roles in tumor progression. Over the past three decades, numerous successful strategies have emerged for the treatment and management of tumors. These strategies are developed on a deep understanding of the processes involved in tumor genesis and the complex interplay with the tumor microenvironment. The development and formulation of efficient drug delivery systems, including polymeric nanocarriers, vesicular systems, and inorganic nanoparticles, have demonstrated their effectiveness as targeted mechanisms for delivering therapeutics into intracellular organelles. These systems undergo successful functionalization and surface modification, facilitating recognition by tumor cell receptors. These biocompatible and biodegradable nanoengineered systems enable precise release of therapeutics at cancerous sites and have found extensive applications in diagnosis and treatment. Vesicular systems have proven to be efficient vehicles for delivering natural antioxidants and phytochemicals due to their antiproliferative- and apoptosis-inducing properties. In addition, solid lipid nanoparticles are preferred due to their high payload efficiency and stability, even at elevated body temperatures, making them suitable for delivering therapeutics to treat brain tumors. Furthermore, researchers have extensively explored repetitive branched structured dendrimers for the treatment of inoperable liver cancers. A significant percentage of systemically delivered therapeutics relies on transvascular processes for permeating malignant solid tumors, although this process is very slow and requires a high concentration gradient for successful penetration. Consequently, only a small fraction of the drug reaches the target site, resulting in poor bioavailability. It is important to consider that increasing the dosage may lead to potential toxicity. Several biological barriers exist that restrict the transportation of chemotherapeutics at systemic, organ, and cellular levels.

2. Biological barriers influencing tumor-targeted drug delivery systems

The anatomy and physiology of both tumor and host cells present inherent biological barriers that restrict the entry of drug delivery systems. Therefore, to achieve effective therapeutic results at the target site, it is imperative to design drug delivery systems that are tailored to overcome the obstacles.

2.1. Systemic barriers

Biodistribution and clearance represent two prominent systemic barriers that pose challenges to nano-based drug delivery approaches, particularly in achieving efficient delivery to the target site. These barriers encompass a range of structural and chemical processes that shield ingested foreign substances from adverse pH conditions and the immune system's responses. The immune system, including macrophages, plays a critical role as a barrier to active drug-loaded particles, swiftly removing them from surrounding tissues and the circulatory system[4]. Similarly, first-pass metabolism can affect the therapeutic window of drug delivery systems, particularly when targeting lung cancer. Factors within the circulatory system, mucosal lining, basal membrane, and the intercellular gaps between endothelial cells all play roles in determining the selective localization of size-dependent drug delivery systems[5]. For instance, nanoparticles tend to accumulate more within the larger gaps between endothelial cells and in areas with a discontinuous basal membrane in blood vessels,

such as bone spaces. On the other hand, in regions with a continuous basal membrane, which includes endocrine glands, nanoparticles may have poorer localization[6].

2.2. Organ-level barriers

One of the critical barriers at the organ level is the blood-brain barrier, which is of utmost concern for effectively delivering therapeutic agents and nutrients across the blood-brain membrane. The brain capillaries that line the brain exhibit a high degree of polarization and consist of different luminal and abluminal membranes with different functional roles[7]. In addition, the presence of tight junctions in the endothelial cells of brain capillaries restricts the diffusion of small hydrophilic molecules, resulting in a low rate of transcytosis (poor movement of solutes through transcellular pathways). Several factors related to nanocarriers influence their ability to transverse the blood-brain barrier, including lipid solubility, surface area, size, polarity, and concentration gradients[8].

2.3. Cellular-level barriers

The internalization of nanocarriers, achieved through processes such as phagocytosis, pinocytosis, or receptor-mediated endocytosis, represents cellular-level barriers. Cellular endocytosis is a common occurrence in tumor cells, although it may vary from cell to cell and can be affected by extracellular conditions. The functionalization of nanocarriers with ligands plays a crucial role in enhancing internalization, cellular uptake, and achieving precise targeting with tumors[9]. In addition, the size of nanocarriers has an impact on cellular uptake and the internalization process. Smaller particles (<200 nm) can be internalized through a clathrin-mediated process, while larger particles (>200 nm) are taken up via caveolin-mediated pathways[10]. The presence of surface charges on tumor-targeted nanocarriers is also significant, as they influence cell binding, signaling, and cell responses. These surface charges determine the extent and type of protein interactions, thus governing cell adhesion.

3. Molecular principles in tumor-targeted drug delivery systems

At present, three approaches are employed in targeted drug delivery systems for the management of tumors at the molecular level. These approaches include passive targeting based on tumor vasculature, active targeting through molecular binding, and cell-mediated targeting[11].

3.1. Passive targeting

Passive targeting involves the targeting of structural features associated with the newly formed blood vessels that supply nutrition and metabolic support to the tumor site. During the initial stages of tumor growth, there is a significant release of pro-angiogenic factors that contribute to the formation of convoluted, disorganized, and immature vessels with indistinct arterioles, venules, and capillaries. These developed tumor vessels exhibit aberrant cellular organization and contain numerous factors, including vascular endothelial factor, tumor-infiltrating leucocytes, protein factor, and tumor necrosis factor. In addition, reactive ions such as reactive oxygen, carbon monoxide, nitric oxide, and hydrogen peroxide are present, along with various processes associated with hemoxigenase, matrix metalloproteinase, and inflammation[12]. All of these factors play a role in regulating vascular permeability within tumor vessels, as well as in processes related to inflammation, intravasation, and the distribution of tumor cells[13].

Tumor-targeted therapeutics aim to accumulate around the tumor and induce an enhanced permeation and retention effect (EPR), facilitating the increased accumulation of bioactive agents at the target site. The disorganized architecture of tumors, along with leaky vasculature and impaired lymphatic drainage, enables enhanced EPR efficiency. A schematic illustration of passive targeting is depicted in Figure 1. Several drug delivery approaches, such as liposomes, nanoparticles, micelles, polymeric nanoparticles, and dendrimers, achieve enhanced EPR through passive targeting, gradually releasing active ingredients within the tumor mass. Numerous passively targeted drug delivery systems from different countries have been successfully employed in clinical use. Examples of such nanocarriers include Doxil™, DaunoXome™, Marqibo™, Onivyde™ (USA), Mepact™, Myocet™ (Europe), SMANCS™ (Japan), and Genexol-PM™ (Korea).

3.2. Active targeting

Active targeting, also referred to as receptor-mediated targeting, capitalizes on the distinctive overexpression of specific receptors, such as vascular epithelial growth factors, transferrin receptors, and human epidermal growth factors within tumor masses. These receptors serve as recognition for target ligands, including tethered antibodies, linked peptides or proteins, aptamers, affisomes, and small molecules. The presence of leaky vasculature, a disrupted lymphatic system, and a hypoxic or acidic environment within tumors further facilitate the covalent or non-covalent binding between receptors and ligands, essential for the successful execution of active targeting[14]. Figure 2 illustrates the fundamental concept behind the internalization of a tumor-targeted drug delivery system through active targeting. The epidermal growth factor receptors (EGFRs) family is incessantly involved

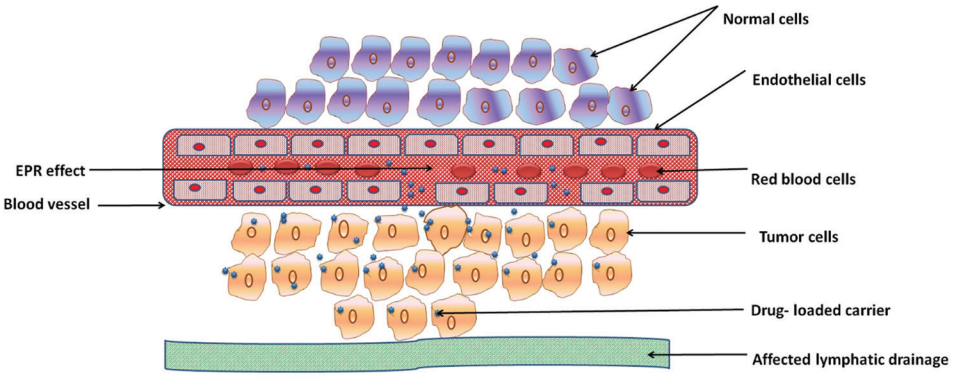

Figure 1. Schematic illustration of tumor targeting using drug-loaded nanocarriers through passive targeting approach.
Abbreviation: EPR: Enhanced permeability and retention.

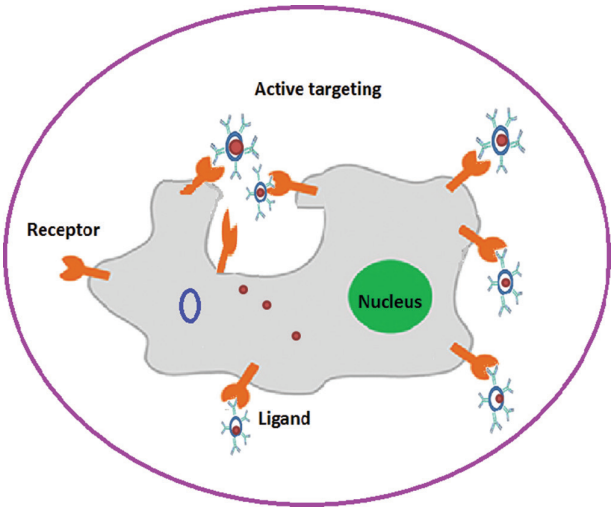

Figure 2. Ligand-bound receptor-mediated or active targeting of tumor cells.

in tumor cell metabolism and targeting suitability. The overexpression of EGRF is associated with the development of various cancers, including those affecting the breast, stomach, and lungs. Consequently, EGRF becomes the preferred active targeting site for the efficient delivery of anticancerous agents[15]. In addition, folate receptors are highly expressed on the cell surface in epithelial, cervical, ovarian, brain, lung, and colorectal cancer regions. Furthermore, myriad disorders and cancers, including the pancreas, prostate, testicles, lymphomas, and sarcomas, exhibit elevated levels of folate receptors. Hence, folate receptors are the preferred choice for active targeting using various inorganic nanoparticles.

Furthermore, tumor progression is closely associated with the angiogenesis process, which is physiologically regulated through the overexpression of vascular EGFRs and integrins found in endothelial cells[16]. This overexpression has been linked to the development of prostate cancer, leukemia, and melanoma. Both of these target sites are preferred for active targeting, as they not only restrict the supply of nutrients but also mediate the disruption of tumor cells[17]. Potential targets containing specific proteins include B-cell maturation antigen and lymphocyte antigens (relevant to hematological tumors), G-protein coupled receptors (such as lysophosphatidic acid, melanocortin, estrogen, angiotensin, vasopressin, and gastrin-releasing peptides), cluster differentiation proteins, interleukin receptors (associated with gliomas), and prostate-specific membrane antigens[18,19]. Current tumor-targeted drug delivery systems are designed to improve blood perfusion, promote internalization, and facilitate tissue infiltration by activating antitumor responses.

3.3. Cell-mediated targeting

The cell-mediated targeting approach is a highly recommended strategy for anticancer drug delivery owing to its distinct virtues, including the precise direction of drugs to the target site, prolonged retention, and controlled drug release, all while minimizing immunogenicity and cytotoxicity. This approach involves drug interactions with cell-mediated substrates, which encompass cytokines (macrophage colony-stimulating factor), chemokines (monocyte chemotactic proteins), and cellular growth factors (EGFR and vascular endothelial growth factor)[20]. Drug carriers loaded with low molecular compounds, genetic materials, proteins, and oncolytic viruses activate T-lymphocytes, neutrophils, monocytes, macrophages, and mesenchymal stem cells, all working together to target tumor cells[21]. Figure 3 depicts the process of cell-mediated antitumor activity.

Various factors, including cell adhesion molecules and regulatory T cells, amplify cancer-associated responses, while cytotoxic T cells and natural killer (NK) cells

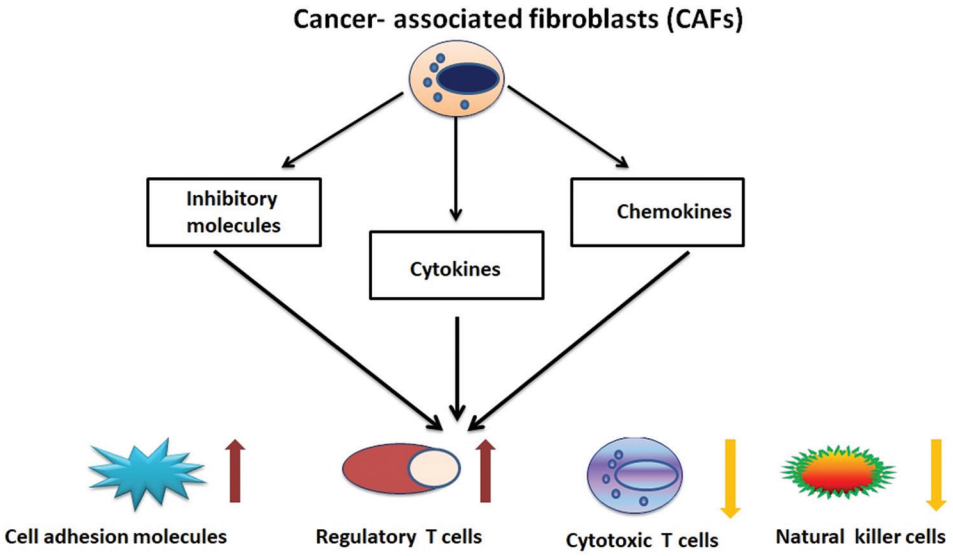

Figure 3. Stimulation of cell-mediated responses by cancerous cells.

restrict cancer progression[21]. T cells combat cancer cells through both direct and indirect mechanisms. In the context of lymphoma and bone marrow cancers, these cells themselves become cancerous. NK cells are capable of directly destroying cancerous cells through perforin- or granzyme-based mechanisms. Similarly, cytotoxic CD8+ cells are highly desirable for targeting cancer and are potent effectors often employed in chemotherapy. New-generation genetically modified cytotoxic T cells are currently being explored in clinical trials for potential cancer treatment.

4. Types of tumor-targeted drug delivery systems

4.1. Microscale tumor-targeted drug delivery system

Highly proliferative tumor cells exhibit distinct genetic and functional differences compared to normal cells, necessitating cell-specific drug treatments. Conventional approaches not only fail to deliver drugs to the target sites (abnormal cells) but also lead to severe side effects. Microspheres offer the potential to target tumor-affected cells with minimal side effects. These free-flowing colloidal microspheres (an approximate size of 200 μm) are composed of drug-entrapped biodegradable polymers capable of controlled drug release at the target organ vessels. Microspheres have found widespread application in drug delivery, particularly in contexts such as organ transplantation, surgery, and radiation treatments associated with hepatic metastases[22]. For instance, Sangi *et al.* discussed a microsphere-based chemotherapeutic system designed for lung targeting, involving the development of 5-fluorouracil-loaded gelatin microspheres with an average size of 9.6 μm[23]. After I/V (intravenous injection), the half-life of the drug significantly improved that extended from 1.23 to 18.3 h, and remained prolonged in circulatory system. These microspheres exhibited a shriveled shape, microsized (5–15 μm), biodegradability, biocompatibility, and stability under both ambient and refrigerated storage conditions. Histopathological studies revealed no changes in the stained lung tissue. In another study, Fan *et al.* explored dual drug release from nanofibrous microspheres for the targeted treatment of colon cancer[24]. They prepared polymeric nanofibrous microspheres containing docetaxel and curcumin without the use of surfactants. They utilized pluronic, a water-soluble biocompatible polymer, which exhibited an affinity for the intestinal surface and contributed to the improved solubility and stability of poor water-soluble therapeutics. This developed system demonstrated biodegradability and provided slow and controlled drug release due to its fibrous surface. In vivo studies demonstrated synergistic antitumor efficacy against colon carcinoma (CT 26) through the use of dual drugs (docetaxel and curcumin) within nanofibrous microspheres. In addition, the system held promise for the treatment of abdominal metastasis of colon cancer.

Shell *et al.* demonstrated the bright luminescence of europium chelate microspheres, which were affixed with multiple copies of cetuximab[25]. This system enabled the selective imaging of overexpressive EGRFs in A431 tumor cells. The microspheres were intravenously injected into athymic mice that had previously been treated for A431 flank tumors. The outcomes, gathered using enzyme-linked

immunoassay and fluorescence microscopy, revealed the selective accumulation of cetuximab microspheres at the targeted tumor site. Conjugated europium antibody microspheres have the potential for efficient tumor site imaging and accumulation within the tumor *in vivo*.

Another micronized delivery system, microemulsions (0.1 μm), serves as adaptable carriers that exhibit enhanced bioavailability of poorly soluble actives, improved absorption, and high permeation due to their small size distribution and low surface tension[26]. Table 1 compiles a few microscale tumor-targeted delivery approaches and their applications. These systems are thermodynamically stable and can effectively deliver both hydrophobic and hydrophilic actives across the skin[27].

4.2. Nanoscale tumor-targeted drug delivery systems

4.2.1. Polymeric nanocarriers

Polymeric nanocarriers are considered a promising approach for drug delivery to alleviate various disorders, including tumors. Their remarkable pharmacokinetic properties, namely, solubility, stability, significant distribution, and accumulation at tumor cells, have garnered attention for developing new chemotherapy regimens[36]. Polymers utilized include polyethylene glycols, polysaccharides, and polyvinyl alcohol, which not only enhance solubility but also extend the circulation half-life of the active drug and bypass the opsonization process. Improved stability, prolonged retention time, and reduced clearance of polymeric nanoparticles offer notable applications in oncology. These cargos are actively taken up by the cell-mediated active transport system[37]. Moreover, these systems are protected from the unfavorable environment of the gastrointestinal tract and bypass first-pass metabolism, resulting in increased bioavailability and reduced metabolic clearance. Furthermore, the polymeric integrity enables a high payload and controlled release of the actives at the target site[38]. Polymeric nanocarriers entail the use of polymeric nanoparticles, polymeric micelles, dendrimers, and polyplexes for specific drug delivery at the tumor target site, as illustrated in Figure 4, and they are further elaborated as follows:

(a) Polymeric nanoparticles

Nanodimensional particles serve as excellent carriers for site-specific drug release and effective antitumor management by virtue of their biocompatibility and prolonged circulation efficiency. Numerous nanocarriers (below 1000 nm), including liposomes, polymeric

Table 1. Microscale tumor-targeted delivery systems and their applications

Therapeutic agent and formulation	Targeted site	Research Objective	Application	References
Yttrium-90 microspheres	Liver	Development of microspheres to provide prolonged patient survival through precisely nourishing vasculature related to hepatic tumors	Local radiotherapy for liver tumors	[28]
MDHJ (Methyl dihydrojasmonate) containing microemulsion	Breast	Phytochemical MDHJ microemulsion has the capability to reduce tumor volume and necrotic effects in MCF-7 cell lines	Targeting solid tumor (transdermally)	[29]
Magnetic iron oxide bovine serum albumin microspheres	Skin	Prolonged delivery of sulforaphane through iron oxide magnetic microspheres	Promising drug carrier for anticancer drug	[30]
Mitoxantrone (MXN)-albumin microspheres	Breast	Preparation of MXN microspheres to reduced toxicity and improved moderate survival in murine mammary adenocarcinoma	Localized breast cancer chemotherapy	[31]
5-fluorouracil microspheres	Brain	Formulation of biodegradable microspheres for sustain release of 5-fluorouracil and impressive management of neoplastic cells present in brain tissues	Prolonged local delivery of 5-fluorouracil in malignant brain tumor	[32]
CA125-poly(lactic-co-glycolic acid) (PLGA) microspheres	Ovary	Preparation of antigen CA125-loaded PLGA microspheres for induction of T lymphocytes	Immunotherapy of ovarian cancer	[33]
Pancreatin microspheres	Pancreas	Development of enteric-coated pancreatin microspheres for the direct release in the pancreatic duct	Unresectable pancreatic cancer	[34]
Paclitaxel microspheres	Urinary bladder	Development of bioadhesive paclitaxel microspheres for the controlled release at the urothelium	Intracavitary treatment for superficial carcinoma of the urinary bladder	[35]

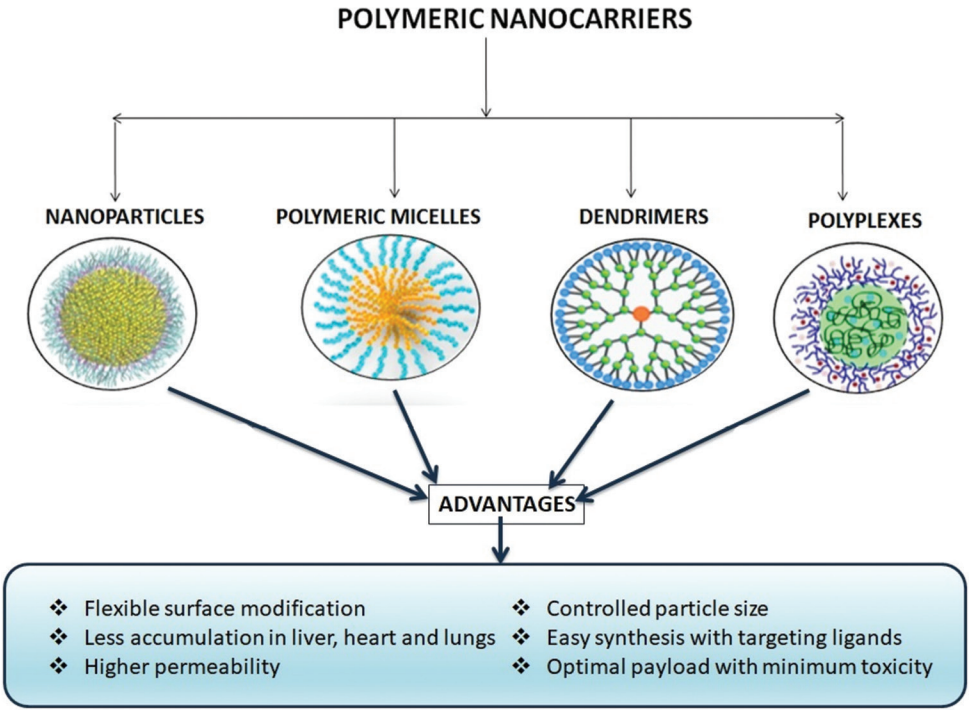

Figure 4. Polymeric nanocarriers involved in tumor management.

nanoparticles, solid lipid nanoparticles, dendrimers, and inorganic nanoparticles, have been reported for their effectiveness in the treatment of various types of tumors[39]. Their unique size, shape, and surface architecture allow for active targeting (binding to specific cell receptors), passive targeting (enhanced EPR and dysfunctional lymph vessels), and cell-mediated targeting (stimulated cytokines and chemokines). The size of nanoparticles significantly influences various factors, including circulation time, biodistribution, accumulation, penetration, and cellular uptake within tumor cells or tissues. Circulation time and particle size serve as pivotal determinants of the drug delivery system's efficacy. Notably, particle size greatly affects clearance through the mononuclear phagocytic system (MPS), with smaller nanodimensional particles undergoing reduced uptake by this system. In addition, nanoparticle size plays a critical role in biodistribution, renal filtration, and vascular infusion within the liver. The literature describes that nanoparticles below 50 nm can easily penetrate endothelial cells and infiltrate liver cells, while smaller particle sizes (approximately 5 nm) are excreted through renal filtration. The variable pore size (ranging from 200 nm to 1.2 μm) is influenced by leaky vasculature and the rapid growth of tumor cells[40].

However, larger particles are inefficient at entering tumor cells; they are retained in the surrounding of tumor cells but struggle to penetrate dense tumor cells[41]. In contrast, smaller particles (below the pore diameter of tumor cells) can easily penetrate tumor cells and exhibit passive targeting but are swiftly pushed back into the circulatory system due to the high interstitial pressure within tumor cells[42]. Therefore, optimizing particle size can enhance intratumor distribution, cell penetration, retention, and, consequently, the effectiveness of antitumor treatment. Yu *et al.* have demonstrated an intelligent, size-tunable approach for proficient antitumor action[43]. The size-tunable approach overcomes the limitations associated with nanoparticles, as their sizes can be adjusted (shrunk or enlarged) in response to physiological stimuli. This adjustment significantly improves the retention and penetration of the tuned particles within tumor cells. Both internal (pH, enzyme, and redox reactions) and external stimuli (temperature and light) modulate the morphology (shape and size) of nanoparticles through the processes such as protonation, π-π stacking, and hydrogen bonding. As a result, sized-tuned particle drug delivery systems are utilized for efficient therapy, diagnostics, and bioimaging of cancers. Figure 4 illustrates smart polymeric nanocarriers that exhibit a controlled release of actives within tumor cells, thereby boosting drug efficiency by modifying the tumor microenvironment[44]. Table 2 compiles certain polymeric nanoparticles and their applications for the management of various tumor cells.

Table 2. Polymers employed in the development of tumor-targeted drug delivery systems

Polymers	Approaches	Research highlights	References
Polyethylene glycol (PEG)-functionalized poly(lactic-co-glycolic) acid	CD133 aptamer-decorated salinomycin nanoparticles (AP-SAL-NP)	The nanocarrier AP-SAL-NP exhibited comparative specific and selective cytotoxicity for CD133(+) osteosarcoma cancer stem cells than bare SAL-NP.	[45]
Hyaluronic acid, nonsulfated glycosaminoglycan	Hyaluronan-paclitaxel bioconjugate (ONCOFID-P) for ovarian cancer	After intraperitoneal administration, the developed polymeric conjugate ONCOFID-P interacted with CD44 via an active transport mechanism and exhibited a higher therapeutic concentration at target sites, that is, human ovarian cancer, when compared to paclitaxel.	[46]
Polyethylene glycol	Utilizing gelatinase nanoparticles for the delivery of miR200c-docetaxel in augmented elimination of cancer stem cells	The developed miR-200c/DOC nanoparticles significantly suppressed the growth of the tumor. Furthermore, these polymeric nanocarriers demonstrate a promising approach for nucleic acid delivery in the management of tumor disorders.	[47]
Biodegradable polylactic acid	Docetaxel-loaded polylactic acid nanoparticles for anti-metastatic remedy	Developed nano-cargos were effective against lung cancer stem-like cells (CSLCs) and proved an effective strategy for lung cancer metastatic treatment.	[48]
Chitosan	Cisplatin-encapsulated chitosan (CS) nanoparticles for improved cellular cytotoxicity in tumor cells	PEG-epidermal growth factor peptide-grafted cisplatin-encapsulated CS nanoparticles were effective against lung cancer cells.	[49]

(b) Polymeric micelles

Polymeric micelles are colloidal particulate systems with particle size approximately 5–100 nm. FDA-approved Genexol-PM (an advanced form of paclitaxel) has found application in the management of breast cancer. These systems have the potential to incorporate ligands (such as antibodies) and form chelate complexes for site-specific drug delivery[50]. Polymeric micelles have demonstrated their competence in delivering hydrophobic drugs effectively, thanks to their exclusive self-assembled morphology that enhances solubility and bioavailability. Amphiphilic di- and tri-block copolymers can self-assemble to create spherical micelles with a hydrophobic core (for the encapsulation of bioactive agent) and a hydrophilic shell (for the provision of stealth properties to the system). This exclusive morphology of polymeric micelles extends circulation time and reduces the likelihood of clearance by the reticuloendothelial system. These particles ensure enhanced permeability across tumor cells and higher drug accumulation. These systems are more efficacious and possess superior stability at lower concentrations compared to micelles derived from surfactants. Recent clinical studies have suggested the potential applications of polymeric micelles in oncotherapy. In addition, the block polymers in polymeric micelles are stimuli-sensitive, responding to factors such as pH, ultrasound, light, heat, and more, enabling controlled delivery of bioactive agents on activation, whether by active or passive means[51].

Kanamala *et al*. discussed the chemical design and vital applications of pH-sensitive polymeric micelles for tumor-targeted drug delivery[52]. Among various stimuli, pH-triggered systems are particularly significant due to their direct influence on the extracellular and intracellular microenvironment of solid tumors. Various mechanisms, including protonation, the breakdown of chemical bonds, and charge reversal, facilitate cellular uptake and drug delivery from polymeric micelles. Optimized stimuli-responsive polymeric micelle assemblies can undergo alterations or rearrange their chemical structure into unimers when exposed to different stimuli. These polymeric micelles effectively recognize the abnormal microenvironment of tumor cells (weak acidity, hypoxic conditions, abnormal temperatures, elevation of metabolites, and overexpression of receptors), enabling active targeting. Table 3 compiles various polymeric micelles that have been investigated for their antitumor efficacy. On cellular uptake, these nanocarriers enhance therapeutic efficacy, imaging sensitivity, and the delivery of antineoplastic agents under various extracellular and intracellular stimuli, including reductive or oxidative microenvironments, anomalous bioactive substances, and the presence of enzymes such as beta-glucuronidase and matrix metalloproteinase[53].

(c) Dendrimers

Nanosized globular dendrimers consist of three distinct sites: A central core, a branched mantle, and a corona adorned with peripheral functional groups. The unique architecture and characteristic features of dendrimers enable high payload capacity and site-specific drug delivery.

Table 3. Polymeric micelles and their antitumor importance

Components	Purpose	Outcomes	References
Thioridazine (THZ), doxorubicin (DOX), urea-functionalized diblock copolymers of polycarbonate and polyethylene glycol	Co-delivery of THZ-DOX using polymeric micelles for the management of breast cancer	Nanodimensional THZ- and DOX-embedded polymeric micelles (100 nm) exhibited synergistic action via inhibiting cancer stem cells. Developed micelles were efficient in lowering the side population of sorted cancer stem cells.	[54]
Curcumin,N-isopropylacryamide, N-vinyl-2-pyrrolidone, polyethylene glycol monoacrylate	Nanocurcumin polymeric micelles for cancer therapy	Developed nanocurcumin micelles (50 nm) were efficient against pancreatic cancer. Readily dispersed nanocurcumin exposed to advanced physicochemical parameters. Moreover, induced cellular apoptosis, inhibition of nuclear factor kappa B, and associated cytokines/interleukins stepped toward remarked control of tumor growth.	[55]
Amphiphilic block polymer N-octyl-O-sulphate chitosan and paclitaxel	Paclitaxel-embedded polymeric micelles for treatment of multidrug-resistant cancer	Formulated micelles (PTX-M) showed two-fold higher cellular uptake and lesser paclitaxel efflux compared to bare paclitaxel. The outcomes suggested efficient activity (75%) both for hepatocellular carcinoma and multidrug-resistant HepG2 cells.	[56]
Phenformin, diblock polymers (PEG-urea functionalized polycarbonate and acid functionalized polycarbonate)	Phenformin polymeric micelles for prevention of metastasis associated with lung carcinoma	Phenformin, an antidiabetic drug, has the efficiency to kill cancerous cells. Phenformin-diblock polymers composed of micelles (102 nm) were stable and compatible with non-cancerous cells. More than 90% of the drug was delivered for 96 h, predicted its prolonged efficacy. *In vivo*, results on H460 human lung carcinoma exhibited superior antitumor action in affected tissues.	[57]
Pluronic P123/F127 and curcumin	Ultrasound triggered pluronic-curcumin micelles for improved chemotherapy	Developed curcumin-loaded pluronic P123/F127 polymeric micelles can be readily permeabilized and well uptaken through cellular mode on ultrasound stimulation. After intratumoral injection, polymeric micelles exhibited prolonged circulation time and exhibited spatial-temporal delivery of curcumin.	[58]

The periphery of these nanocarriers supports the conjugation of targeting ligands, imaging agents, and bioactive substances, while the inner core facilitates the incorporation of inorganic metal nanoparticles, commonly employed in a myriad of biomedical applications[58]. Dendrimers (measuring 10–20 nm in size) easily extravasate and selectively accumulate within tumor cells through the EPR effect, a form of passive targeting. This accumulation results in a high concentration of actives within the tumor. Moreover, these nanocarriers bind to high molecular weight plasma proteins, facilitating prolonged circulation time and reduced renal clearance. However, passive targeting encounters certain anatomical and pathophysiological barriers that can impede drug delivery to the target site and potentially lead to multidrug-resistant tumors. In contrast, active targeting facilitates selective conjugation between overexpressed receptors and ligand-functionalized dendrimers. The peripheral structure of dendrimers is enriched with reactive functional moieties, enabling successful binding to various ligands, including antibodies, genes, amino acids, biotin, aptamers, and folic acid. This characteristic allows for efficient targeting of tumor tissues[59].

Several classes of dendrimers, such as polyamidoamine (PAMAM), poly-L-lysine (PLL), polypropyleneimine (PPI), polyethylene glycol (PEG), citric acid-polyethylene glycol-citric acid (CPEGC), and carbohydrate-based dendrimer (glycodendrimer), are extensively utilized in chemotherapy[60,61]. Among these, clinically proven PAMAM dendrimers, which consist of an ethylenediamine core and methyl acrylate-linked ethylenediamine branches, have been extensively explored for antitumor drug delivery. They are valued for their hydrophilicity, biocompatibility, and non-immunogenicity. The permeation efficacy of PAMAM dendrimers depends on their generation, which determines their morphology[62]. Higher-generation dendrimers are spherical and compact, offering a larger surface area than their smaller-generation counterparts[63]. However, the presence of terminal cationic groups in PAMAM dendrimers may interact with negatively charged healthy cells, causing the disruption of cell membranes and leading to cell death. Therefore, surface modification with shielding moieties is employed to control cytotoxicity and enhance cellular uptake within tumor-specific cells. Table 4 summarizes a selection of dendrimers and their applications in antitumor therapies. Liu *et al.* designed phospholipid-decorated PAMAM (PL-dendriplexes) to encapsulate siMDR1 for mitigating multidrug resistance in breast cancer cells (MCF-7/

Table 4. Types of dendrimers and their associated ligands formulated for antitumor applications

Dendrimers type	Generation	Ligand/therapeutic agent	Application	References
Poly(amidoamine) dendrimers with polyethylene glycol and lactobionic acid (PAMAM-PEG-Gal)	-	Astrocyte elevated gene-1 (AEG-1) and all-trans-retinoic acid (ATRA)	Hepatocellular carcinoma	[68]
Poly(amidoamine) dendrimers (PAMAM)	Fifth-generation	siRNA, cisplatin, and selenium	Lung cancer	[69]
	Fourth-generation	Gallic acid	Breast cancer	[70]
	Third-generation	Methotrexate	Folic receptor-expressing tumor cells	[71]
	Second-, third-, and fourth-generations	Arginine	Suppress TEL/AML1 protein in gene therapy	[72]
Polypropylene imine (PPI)	Fifth-generation	Retinoic acid, dexamethasone, ATRA	Breast cancer	[73]
	Fourth-generation	Melphalan	Folic receptor-expressing tumor cells	[74]
	Fluorinated third-, fourth-, and fifth-generations	Lipofectamine 2000	Human embryonic kidney cells and HeLa cells	[75]
Poly-L-lysine (PLL)	Sixth-generation	Doxorubicin	Chemotherapy	[76]
	Fifth-generation	Doxorubicin	Lung metastases	[77]
	Third-generation	Porphyrin	Gene transfection	[78]
	First-, second-, and third-generations	Fluorescein isothiocyanate and 5-fluorouracil	Multidrug-resistant tumors	[79]

ADR cells)[62]. The developed polymeric nanocarriers demonstrated superior gene silencing efficacy and reduced p-glycoprotein (p-gp) expression. Furthermore, PL-dendriplexes exhibited a synergistic effect with paclitaxel, enhancing apoptosis, regulating the cell cycle, and effectively managing multidrug-resistant cancers. In a study by Jiang *et al.*, a nanodimensional miR-150 encapsulated dendriplex containing FLT3L-G7 PAMAM was developed for the treatment of acute myeloid leukemia (AML). These dendriplexes were designed to target the tumor suppressor through the overexpressed FMS-like tyrosine kinase 3 (FLT3 receptors). The FLT3L-grafted miR-170 nanocarriers selectively targeted overexpressed receptors in AML cells, promoting apoptosis[63]. These designed dendriplexes tend to accumulate in the bone marrow, inhibiting the progression of FLT3 without disrupting normal hematopoiesis. In addition, maltose-derived polypropylene imine glycodendrimers (PPI-mOS, 4th generation) have been explored for anticancer therapy. These cationic nanocarriers efficiently interact with negatively charged nucleoside analogs (cytarabine), overcoming their metabolic limitations (inefficient cellular uptake and drug resistance). The studies conducted on leukemic cell lines (1301 and HL-60) revealed significant cytotoxicity and apoptosis due to the augmented cellular uptake. Furthermore, the system demonstrated the ability to inhibit the human equilibrative nucleoside transporter (hENT1), which plays an important role in the oncogenesis of leukemia[64]. Another advanced carbosilane dendrimer has been successfully employed for nucleic acid delivery. Their termination sites are rendered with anionic or cationic functional groups, which participate in electrostatic interactions between cell membrane and phosphate groups of nucleic acids. These dendrimers exhibit distinct morphologies based on their generation number and display excellent biocompatibility[65]. Similarly, positively charged phosphorous dendrimers have been explored as carriers for anticancer applications. Their functionalization with triethylammonium and cyclic ammonium groups has shown potential for transporting therapeutics to target sites for the management of several fatal disorders, including bovine spongiform encephalopathy (BSE), Alzheimer's disease, and Prion disease[66].

The development of polycationic phosphorous dendrimers (G1–G3) for the transportation of DNA plasmids in tumor management has been reported. These designed dendrimers were functionalized with piperidine-derived moieties and complexed with negatively charged plasmid DNA (pDNA), encoding p53 and enhanced green fluorescence protein. Viability assay using the CCK-8 method exhibited a 50% cell viability rate for human cervical carcinoma (HeLa cells) at an N/P ratio (the molar ratio of the positive charge of the dendrimers to phosphates

in the pDNA backbone) of 20. Furthermore, cell viability was found to decrease in a dose-dependent manner. The results revealed that fabricated polyplexes (composed of polycationic phosphorous dendrimers and plasmid) had reduced positive charge in the system, resulting in minimal cytotoxicity. These outcomes suggested that the fabricated phosphorus dendrimers hold promise as an effective carrier system for gene delivery in cancer treatment[67].

(d) Polyplexes

These polymeric nanocarriers are formulated by conjugating siRNA/DNA or genes via electrostatic interactions between cationic polymers and anionic nucleic acid components. These systems serve the dual proposes of protecting sensitive genes from enzyme degradation and facilitating controlled release at the tumor site. Polycationic polyplexes show great promise as a drug delivery approach for the specific delivery of anticancer agents due to their ability to enhance transfection efficiency. DNA polyplexes (polymeric-based) and DNA lipoplexes (lipid-based) are systemic gene delivery systems necessary for cases of tumor metastases, where cancerous cells spread throughout the organism. Polyethyleneimine polyplexes, functionalized with PEG, have been developed and conjugated with transferrin or epidermal growth factor to facilitate effective DNA (or gene) transfer within tumor cells. This modification masks the surface charge of polyplexes to prevent interactions with systemically present circulatory components, including erythrocytes, plasma, and the reticuloendothelial system[80]. Table 5 enlists surface-modified cationic and anionic polyplexes designed to efficiently deliver nucleic acid in tumors.

Lee *et al.* explored the successful delivery of branched peptide (GE11) for cancer cells overexpressing EGFR. They investigated the use of low molecular weight disulfide cross-linked polyethylenimine and PEG to develop GE11-tethered polyplexes and evaluated their transfection efficiency in EGFR-overexpressed tumor cells. The formulated polyplexes demonstrated efficient gene condensing capacity, improved transfection efficiency, and specific targeting capabilities[81]. Polyplexes are generally designed for receptor-mediated gene delivery through systemic routes, facilitating efficient internalization due to their augmented transfection efficiency. In this context, Taschauer *et al.* evaluated the significance of the overexpression of CD49f in both benign and malignant tumors[82]. CD49f molecules are associated with the phosphatidylinositol 3-kinase and the serine/threonine protein kinase (Akt signaling pathway), which play a crucial role in the regulation and development of bone mesenchymal stem cells and contribute to tumor metastasis in solid cancers such as hemangioma, breast cancer, prostate cancer, and gastric cancer. A nanodimensional molecular conjugate (200 nm) consisting of the CD49f peptide (CYESIKVAVS) and linear polyethyleneimine (LPEI) was synthesized for the purpose of targeting breast tumor lesions. The fabricated polyplexes could be aerosolized without particle aggregation. When delivered through intratracheal aerosolization, the system was well-tolerated and demonstrated measurable transgene efficacy. Hattori compiled various cationic and anionic polyplexes with genes to enable their delivery to tumor-targeted sites without aggregation with blood components[83]. Surface modification of cationic polyplexes with anionic polymers led to the development of a stable drug delivery approach that effectively delivered pDNA and siRNA to the target site[84].

4.2.2. Lipid carriers

Lipid-based nanosystems are extensively utilized for targeting and regulating the tumor microenvironment

Table 5. Surface-modified polyplexes and their conjugates for nucleic acid delivery in tumor management

Polyplexes	Nucleic acid	Conjugate	References
Cationic polymers			
Lipofectamine 2000	Plasmid DNA	Hyaluronic acid (HA)	[84]
Chitosan	Plasmid DNA	Hyaluronic acid	[85]
Polyamidoamine	Plasmid DNA	Hyaluronic acid	[86]
Protamine	Antisense DNA	HA-antisense DNA	[87]
Dendrigraft poly-L-lysine	Plasmid DNA	Chondroitin sulfate	[88]
Anionic polymers			
Poly-ɣ-glutamic acid	Plasmid DNA	Chitosan	[89]
Poly-ɣ-glutamic acid	siRNA	Dendrigraft poly-L-lysine	[90]
Heparin	Plasmid DNA	Cationic glycopolymer (Tr4)	[91]
Poly-ɣ-glutamic acid	siRNA	Polyethylenimine	[92]

in solid tumors. Through the use of lipid carriers, chemical modification, solubility enhancement, pH responsiveness, and ligand (antibody) targeting can be effectively achieved. These systems not only shield the therapeutic agents from the immune system (gangliosides) but also facilitate drug delivery in the acidic and hypoxic environments of tumor cells. Among various nanoparticle delivery systems such as polymeric nanoparticles, micelles, dendrimers, and liposomes, lipid carriers are considered the least toxic and are widely utilized for gene, DNA, and RNA delivery at the target sites[93]. Lipid carriers, such as solid lipid nanoparticles (SLNs) and nanostructured lipid carriers (NLCs), are capable of transporting both hydrophilic and hydrophobic agents. They prolong the retention time of these agents (by increasing their half-lives) and provide controlled release of therapeutic agents from the delivery depot[94]. Moreover, lipid-based systems can effectively deliver dual drugs, enhancing the outcomes of chemotherapy (Figure 5). Despite their shared lipid-based formulations, there are distinct features that set SLNs and NLCs apart: (i) SLNs have lower drug encapsulation efficiency compared to NLCs; (ii) polymeric transitions occur during the preparation of SLNs, leading to a shorter storage shelf-life compared to NLCs; and (iii) SLNs, being crystalline, exhibit a slower release of therapeutics.

Lipid carriers employed for tumor management are further elaborated as follows:

(a) Solid lipid nanoparticles

SLNs or lipospheres have emerged as a rapid and promising approach for the safe and effective delivery of drugs to the target sites. This first-generation lipid-based sub-micron colloidal carrier contains dispersed lipids in an aqueous surfactant solution. SLNs offer several advantages, including ease of preparation, stability, biocompatibility, controlled release, the feasibility of incorporating both hydrophilic and hydrophobic drugs, lyophilization capability, non-toxicity, high payload capacity, cost-effectiveness, and the potential for site-specific drug release. These attributes make them a particularly appealing choice for designing systems aimed at delivering drugs specifically to tumor sites[95]. Various types of lipids, such as triglycerides esters of hydrogenated fatty acids (Lubritab™, Dynasan™, cutina™, and sterotex™) and waxes (cetyl palmitate), in combination with biocompatible surfactants and emulsifiers, are utilized to prepare SLNs through various methods[96,97].

SLNs excel in bolstering membrane stability, extending residence time at the target site, and minimizing issues associated with drug leaching, polymer degradation, and toxicity, as seen in conventional approaches. Cholesterol, a major component of SLNs, is also highly demanded

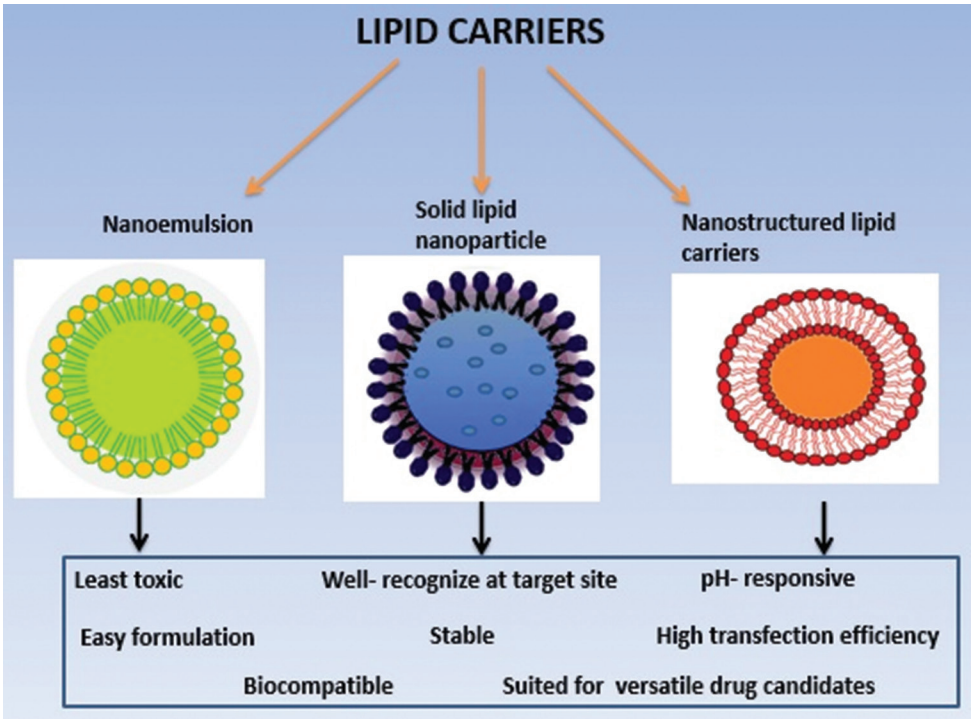

Figure 5. Lipid carriers employed for tumor management.

by tumor cells. Therefore, these lipid nanocarriers show promise for both therapeutic applications and tumor monitoring through modified uptake of low-density lipoproteins.

Bhagwat *et al*. developed transferrin-decorated SLNs containing tamoxifen citrate for improved breast tumor targeting with minimal toxicity[98]. Tamoxifen citrate, a selective estrogen receptor modulator, blocks the passage of estrogen to breast tissues, inhibiting tumor cell growth. However, the associated uterine toxicity associated with tamoxifen limits its broader application in solid tumor management. The developed transferrin-modified tamoxifen citrate-conjugated SLNs exhibited preferential accumulation at the target site (in MCF-7 cells), were qualitatively taken up at the M2 level of the cell cycle, and significantly alleviated human breast cancer in a concentration-dependent manner. The solubility and bioavailability of the poorly water-soluble candidate efavirenz can be modified through the use of SLNs. Efavirenz, a non-nucleoside reverse transcriptase inhibitor, is widely used to treat HIV-positive patients and for antineoplastic management.

Metastasis represents a critical stage in the progression of malignant tumors, such as breast cancer, and is associated with high mortality rates. To address this challenge, docetaxel-loaded SLNs (SLN-DTX) were prepared using Compritol 888 ATO. These SLN-DTX nanoparticles exhibited remarkable stability with a nanodimensional size of 128 nm, resulting in enhanced entrapment efficiency (86%) and controlled *in vitro* release of docetaxel. Notably, the developed SLN-DTX demonstrated significantly greater cellular uptake and accumulation in the G2–M phase (73%) when compared to the free drug (23%), ultimately leading to the induction of apoptosis in tumor cells. Histological investigations confirmed the antitumor activity of SLN-DTX and its potential for spontaneously preventing metastasis in a murine mammary cancer model (4T1)[99,100]. Table 6 summarizes a comprehensive overview of various SLNs and their chemopreventive potential.

(b) Nanostructured lipid carriers

Biocompatible NLCs are second-generation lipid-based drug carriers that effectively shield drugs from degradation, extending their stability and bioavailability. NLCs offer compelling advantages over traditional lipid carriers, including increased storage permanency, improved solubility, enhanced permeability, and minimal adverse effects on associated cells. These formulations are biocompatible and hold great promise for targeted cancer

Table 6. Developed solid lipid nanoparticles and their associated antitumor usages

Drug candidate	Purpose	Research highlights	Application	References
5-fluorouracil (5-FU)	Develop a biocompatible and therapeutically effective 5-FU/SLNs.	Developed 5-FU/SLNs that exhibited a 3.6-fold area under the curve, demonstrating superior inhibition of tumor cells compared to bare 5-FU. In addition, the extent of HER2 receptors and HCT116 cells was markedly reduced in liver and kidney tissues	Colorectal cancer	[101]
Alpha(v)beta(3) integrin cyclic arginyl-glycyl-aspartic acid (RGD)	Preparation of novel receptor targeting (overexpressive alpha(v) beta(3) integrin receptors) and near-infrared light-emitting SLNs for enhanced biodistribution and accumulation.	Developed RGD-SLNs exhibited active tumor targeting on intravenous administration in mice bearing xenograft human breast tumor. The system was specifically distributed in the liver, spleen, and tumor blood vessels	Chemotherapy and chemoimaging	[102]
Camptothecin (CPT)	Development of pH-sensitive SLN system for prolonged accumulation in different tumor sites.	CPT-embedded PEGylated SLNs were spherical, small (53 nm), and exhibited excellent entrapment efficiency (99%). The *in vitro* drug release profile displayed a pH-dependent pattern of drug release. Developed CPT–PEG–SLNs were effective against diverse carcinoma, including lungs (CRL5802, NCL-H358, and CL1-5), colon (HCT-116), and liver (HCC36).	Chemotherapy	[103]
Resveratrol	Inhibition of breast tumor proliferation through resveratrol-SLNs	The developed system was spherical, negatively charged, and smaller compared to bare resveratrol. Western blot analysis suggested superior inhibition efficiency against the proliferation of MDA-MB-231 cells and minimized expression of cyclin D1/c-Myc that explored potential usage for the management of breast tumors	Breast cancer treatment	[104]

therapy. Surface modification or functionalization is recommended to combat drug resistance in chemotherapy.

Thus, augmented drug performance becomes apparent at the delivery site. These novel systems are composed of both solid and liquid lipids, offering increased capacity for hydrophobic antineoplastic drug candidates. Their unordered surface lends itself to straightforward functionalization or modification with various functional moieties (stealthy polymers and ligands) to enhance transfection efficiency at the tumor site. The nanodimensional particles can readily transform into aqueous solutions, resulting in improved pharmaceutical and pharmacokinetic properties, including enhanced solubility, absorption, and bioavailability[105].

Varshosaz *et al*. have developed a lipid-based spherical nanosystem (20–100 nm) containing efavirenz. This system shows great promise for oral administration due to its high solubility, entrapment efficiency, and improved bioavailability[106]. *Ex vivo* investigations conducted on rat intestines revealed enhanced gut permeation of the developed efavirenz NLCs when compared to the efavirenz suspension. This suggests that oral administration of efavirenz through NLCs could be a viable strategy.

NLCs have garnered significant attention in the pharmaceutical and cosmeceutical sectors due to their ease of preparation, biocompatibility, high transfection efficiency, scalability, and the potential for site-specific drug delivery through various administration routes[103]. Multidrug resistance is a prominent issue with antitumor drugs (paclitaxel and doxorubicin), and NLCs offer a promising avenue for mitigation. In the formulation of NLCs, monostearin and oleic acid were utilized as the solid and liquid lipid matrix, respectively, employing the solvent diffusion method. Furthermore, drug-loaded NLCs were functionalized with a folate conjugate containing stearic acid to enhance sensitivity at the target site. Cytotoxicity and the impact on multidrug resistance were assessed for the modified NLCs in human breast cancer (MCF-7) and ovarian cancer (SKOV3) cell lines. Both NLCs, respectively, loaded with paclitaxel and doxorubicin, exhibited superior cytotoxicity against the selected cancerous cell lines, with a remarkable reversal activity of the loaded drugs[107]. Wang *et al*. also explored NLCs by coadministering paclitaxel and doxorubicin to achieve a synergistic effect and site-specific delivery for tumors without influencing normal cells[108]. They utilized the melt emulsification technique for NLC formulation. *In vitro* cytotoxicity studies targeting non-small cell lung carcinoma (NSCLC) and *in vivo* experiments using a mice model (NCL-H460 cells) both exhibited enhanced tumor-targeting efficiency.

The issue of drug resistance during chemotherapy has been addressed by Mussi *et al*., who developed a lipoidal carrier coloaded with docosahexaenoic acid and doxorubicin to enhance the antitumor efficacy[109]. The cellular uptake efficiency was evaluated in MCF-7 cells and MCF-7ADR cells, and the study was conducted using a monolayer model. Higher drug encapsulation and entrapment resulted in improved cellular uptake in MCF-7/ADR cells, signifying the circumvention of P-glycoprotein (P-gp) efflux. Wang *et al*. designed NLCs for the codelivery of doxorubicin and sorafenib (NLC/D-S) to effectively manage esophagus cancer[110]. Sorafenib, a multi-kinase inhibitor, plays a crucial role in regulating the tumor microenvironment, while doxorubicin is a potent inducer of immunogenic cell death. The highly stable and biocompatible NLC/D-S system exhibited an enhanced transfection and retention effect when evaluated against drug-resistant esophageal cancer cells. Therefore, combined therapy using NLC/D-S holds promise as an effective anticancer remedy, thanks to the significant roles of its component. Table 7 compiles several examples of NLCs and their significant importance in the mitigation of various types of tumors.

(c) Nanoemulsion

A nanoemulsion represents a heterogeneous colloidal dispersion system, consisting of nanoscaled droplets in a stable phase. These systems possess a notable capacity for encapsulating poorly soluble drug candidates due to their hydrophobic core. In the context of chemotherapy, researchers have extensively explored ligand-functionalized nanoemulsions designed to target specific components of tumor cells, facilitating efficient internalization within these cells and, consequently, curbing further tumor proliferation[117]. For instance, folate- and gadolinium-functionalized nanoemulsions of docetaxel were formulated using a high-shear micro-fluidization technique, showcasing impressive efficacy in testing on a human ovarian cancer cell line (SKOV3/SKOV3TR). The folate-targeted nanoemulsions (<150 nm) not only served as a theranostic system, efficiently delivering docetaxel through folate receptor-mediated endocytosis, but also outperformed the clinically approved Magnevist® (an MRI contrast agent) in diagnosing the affected tumor site. Moreover, this system demonstrated thermodynamical stability and prolonged residence time within tumor cells while sparing surrounded healthy cells[118].

Zheng *et al*. developed Vitamin E-decorated paclitaxel nanoemulsions for the treatment of human ovarian cancers[119]. The nanoemulsion system exhibited a significantly higher level of antiproliferation action compared to free drug administration of paclitaxel when

Table 7. Nanostructured lipid carriers, their purpose, and antitumor applications

Nanostructured lipid carriers (NLCs)	Purpose	Methodology	Application	References
β-lapachone (Lapa) and doxorubicin (DOX)	Facilitate the catalysis of NAD(P)H quinone oxidoreductase-1 (NQO1) enzyme and enhance intracellular uptake	Melted ultrasonic dispersion method	Overcome multidrug resistance in DOX-resistant breast cancer	[111]
Baicalein (BCL) and doxorubicin (DOX)	Hyaluronic acid (HA)-functionalized NLC for binding with HA receptors	Emulsion evaporation-solidification	Exerting cytotoxicity and synergistic effect against breast cancer, verified on DOX drug-resistant MCF-7 breast cancer cell line (MCF-7/ADR cells)	[112]
Gemcitabine (GEM) and Baicalein (BCL)	HA decorated prodrug NLC for effective binding with HA-overexpressing pancreatic receptors	Nanoprecipitation technique	Prodrug-based tumor-targeted drug delivery on pancreatic cancer	[113]
Doxorubicin (DOX), gemcitabine (GEM), and vincristine (VCR)	Combined prodrug delivery	Solvent diffusion	Stable and high drug-entrapped NLCs used as an antilymph cancer agent against B-cell lymphoma	[114]
Paclitaxel (PTX) and indocyanine green	Significantly enhanced the stability of drugs, produced sufficient local reactive oxygen species, and triggered accelerated drug release on laser irradiation, and also increased intracellular uptake of drugs and induced increased cytotoxicity in cancer cells through synergistic effects	Solvent diffusion	Chemo and photodynamic therapy	[115]
Cisplatin (DDP) plus paclitaxel (PTX)	Folate (FA) decorated nanostructured lipid carriers (NLCs) as nanocarriers for DDP and PTX delivery	Melted dispersion method	Folate-decorated NLCs for enhanced *in vitro* cytotoxicity and *in vivo* penetration efficacy against head-and-neck cancer cells (FaDu cells)	[116]

tested on the targeted cells (A2780/Taxol). Notably, there was a marked reduction in mitochondrial potential, increased intracellular accumulation, and an elevation in the Bax protein level, all suggesting potential applications for nanoemulsions in addressing multi-drug resistance tumors. Ahmad *et al*. developed an oil-in-water (o/w)-based nanoemulsion that contained an omega-3 fatty acid-modified taxoid prodrug (DHA/SBT/1214) for the management of prostate cancer. The nanoemulsion system exhibited enhanced cytotoxicity against PPT2 tumor xenograft compared to the commercially available Abraxane®[120]. Furthermore, *in vivo* treatment with the developed system resulted in higher cell viability with minimal induction of floating spheroids or holoclones, in contrast to the large numbers observed with Abraxane®.

4.2.3. Vesicular carriers

Vesicular nanosystems offer a means to deliver chemotherapeutic drugs precisely to target sites while sparing normal cells from harm. These drug delivery strategies excel as carriers due to their ability to control the active release of therapeutics, enabling localized action and maintaining desirable storage stability. A diverse range of lipids and amphiphilic building blocks (surfactants) has been explored for the creation of vesicular systems, which are characterized by highly ordered, concentric layers. Due to their exclusive morphology and small dimensions, these vesicular systems disperse effectively within the affected organ. Figure 6 displays various vesicular drug carriers, such as liposomes, niosomes, phytosomes, and aquasomes, developed for chemopreventive applications. The vesicular approach not only protects drugs from degradation but also extends the circulation time of bioactive agents. These vesicles offer numerous advantages, including biocompatibility, non-toxicity, flexible preparation, non-immunogenicity, and effective cellular uptake by virtue of their significant interactions with cancerous cells. These attributes make vesicles ideal nanocarriers for addressing tumor-related issues[121]. Table 8 compiles different vesicular carriers explored for their antitumor action.

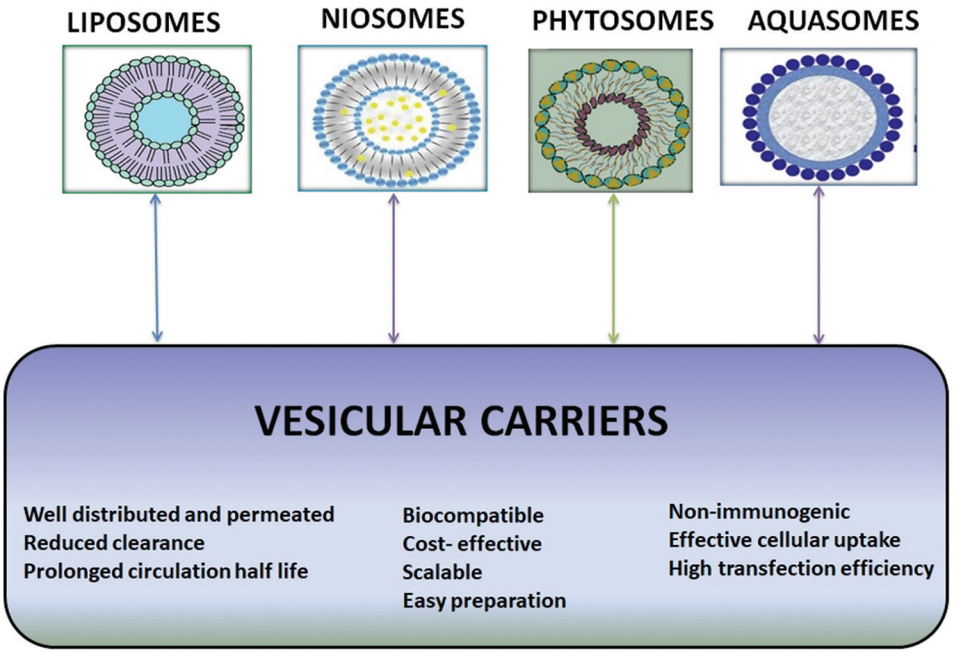

Figure 6. Types of vesicular carriers extensively employed for antitumor therapy.

Table 8. Different types of vesicular carriers for tumor management

Vesicular system	Therapeutic agent	Research highlights	Study model	Application	References
Liposomes	Mitoxantrone (MTO)	(i) Minimum MTO toxicity (ii) Improved cellular uptake (iii) Suppressed and delayed tumor growth	MDAMB-231 breast carcinoma model	Orthotopic breast carcinoma	[31]
	B16-ovalalbumin (B16-OVA), vaccine adjuvants	(i) Induced robust CD^8 T lymphocytes (ii) Impaired cell toxicity (iii) Increased programmed cell death of tumor cells (iv) Significantly improved survival rate	B16-ovalbumin (B16-OVA) solid tumor melanoma mouse model	Melanoma and immunotherapy	[135]
	anti-EGFR-9Arg-lipoplexes	(i) Remarked siRNA transfection in lung cancer cells (ii) Suppressed transcription of the targeted gene (iii) Efficiently inhibited tumor growth	LS174T-Luc cancer cells	RNA interference chemotherapy	[136]
	Thermosensitive NGRpeptide-siRNA	(i) Developed glutathione-sensitive carrier (ii) Predicted 86% encapsulation efficiency and thermal stability (iii) 3 times high *in vivo* performance of cell-penetrating peptides embedded in liposomes	HT-1080 murine model (xenograft)	Fibrosarcoma and cancer therapy	[137]
	Paclitaxel and vinorelbine	(i) High cellular uptake by both active and passive targeting mode (ii) Lessened cell toxicity compared to free drug (iii) Restricted lung metastasis	Non-small-cell lung cancer (NSCLC)-tumor-bearing C57BL/6 mice	Lung cancer	[138]

(Cont'd...)

Table 8. (*Continued*)

Vesicular system	Therapeutic agent	Research highlights	Study model	Application	References
Niosomes	Doxorubicin and curcumin	(i) Prolonged blood circulation (ii) Exhibited both active and passive targeting (iii) Improved cellular uptake due to folic acid functionalization (iv) High stability, biocompatibility, and controlled release drug delivery	MCF-7 and MDA-MB-231 cancerous cells	Breast cancer	[139]
	Paclitaxel and doxorubicin	(i) Enhanced dissolution rate of poorly soluble paclitaxel (ii) Improved antiproliferative and cell penetration action (iii) Synergistic action of both drugs to overcome drug resistance	MCF-7 and PC3-MM2 malignant cells	Multidrug resistance in chemotherapy	[140]
	Tamoxifen	(i) Distinct nanoshapherical with high entrapment efficiency (92%) (ii) 2.8-fold increase in cellular uptake (iii) Reduced tumor volume (iv) Significantly prolonged release through a diffusion process	MCF-7 cell lines	Breast cancer	[141]
	Tocotrienols T3	(i) 1.5 times higher antitumor activity compared to free drug T3 (ii) 12 times lowered tumor volume than treated with free drug T3 (iii) Significantly downregulation of genes associated with metastasis	MDA-MB-231 cells	Breast cancer	[142]
Phytosomes	Mitomycin C- soybean phosphatidylcholine conjugate	(i) Restricted rapid elimination (ii) Increased cellular uptake in HeLa cells (iii) Higher accumulation in H22 hepatoma-induced mice (iv) Enhanced cytotoxicity and advanced antitumor effect	HeLa cells and H22 hepatoma cells	Cancer management	[143]
	Icariin (flavonol glycoside)	(i) Interfered pre-G1 and G2/M phase of cell cycle (ii) Induced apoptosis and cell death (iii) Reduced mitochondrial membrane potential (iv) Enhanced icariin cell permeation and cytotoxicity	OVCAR-3 cells	Ovarian cancer cells	[144]
	Methanolic extract of Allium sativum	(i) Enriched with antioxidants (ii) Exhibited chemopreventive action due to diallyl-disulfide functional groups (iii) Presented active targeting with 100% targeting efficiency	MCF-7 cells	Cancer management	[145]

Vesicular drug carriers, including liposomes, niosomes, phytosomes, and aquasomes, are further elaborated as follows:

(a) Liposomes

Liposomes have been extensively explored for their applications in chemoprevention. The functionalization of liposomes has the potential to enhance their circulation longevity by shielding nanocarriers from phagocyte recognition (opsonization) and preventing rapid removal from blood vessels. In addition, liposomes' variability in size facilitates effective extravasation, both within the hyperpermeable microenvironment of tumors (murine colon adenocarcinoma) and within poorly permeable tumor cells (pancreatic adenocarcinoma). The presence of surface charge can facilitate passive targeting and influence

opsonization by MPS. Neutral or anionic liposomes may evade clearance mechanisms, thereby prolonging their residence time in the circulatory system. In contrast, cationic liposomes tend to form non-specific interactions with negatively charged blood components, leading to their rapid clearance through the reticuloendothelial system (RES)[122].

Eloy *et al.* developed dual drug delivery immunoliposomes for the management of human epithelial growth factor receptor 2 (HER2) carcinoma[123]. These liposomes contained both paclitaxel (an anticancer drug) and rapamycin (an mTOR inhibitor) and were surface-coated with trastuzumab, an anti-HER2 monoclonal antibody, for efficient active targeting. The developed system had a particle size of 140 nm, with a higher entrapment efficiency (56 % for paclitaxel and 69 % for rapamycin) and improved stability (−9.85 mV). The trastuzumab-decorated liposome exhibited more than 70% affinity for HER 2, indicating their potential for the targeted delivery of paclitaxel and rapamycin in breast cancer.

Prasad *et al.* developed a liposome-based nano-theranostic system to improve the image resolution of solid tumors[124]. The multifunctional liposomes loaded with doxorubicin, gold nanoparticles, and quantum dots exhibited photo-triggered antitumor efficacy. In vivo antitumor diagnostics revealed bimodal imaging capabilities and tumor suppression, facilitated by the release of heat and oxygen-reactive groups. This novel vesicular formulation has opened new avenues for targeting tumors and improving tumor imaging.

Tumor-associated macrophages are important targets for chemotherapy, as they play a crucial role in regulating tumor proliferation within the tumor microenvironment. Yin *et al.* developed a dual-target vesicular system functionalized with anti-programmed death ligand 1 (anti-PD-L1) for the co-delivery of simvastatin and gefitinib, aimed at managing brain metastasis and lung cancer[125]. These liposomes demonstrated the ability to bind with transferrin receptors, efficiently penetrate the blood-brain barrier, and minimize drug resistance by suppressing the EGFR-Akt-Erk signaling pathway.

(b) Niosomes

Niosomes are self-assembled lipoidal bilayer vesicular drug carriers consisting of non-ionic surfactants and cholesterol. These systems can accommodate a wide range of therapeutically active agents with varying solubility, making them a promising strategy for multidrug applications. Unlike liposomes, niosomes are preferentially chosen for designing nanoscaled chemotherapeutic carriers due to their cost-effectiveness, scalability, stability (they are non-leakage vesicles), lack of special storage requirements, and resistance to degradation through hydrolysis and oxidation processes[126]. Mohamad Saimi *et al.* designed and optimized an aerosol delivery system for the treatment of lung cancer. They sonicated gemcitabine and cisplatin in sodium chloride solution and amalgamated them into niosomes composed of Tween 65 and Span 60 (at a 1:2 ratio) and cholesterol[127]. The optimized dual drug embedded niosomes were nanoscale (approximately 166 nm in size), had a low polydispersity index of 0.16, a zeta potential of around 15 mV, and exhibited controlled drug release for 24 h. The cytotoxicity of the aerosolized niosomal system was tested against both MRC5 normal lung cells and A549 cancerous cells, demonstrating reduced toxicity to the normal cells and high toxicity to the cancerous cells after 72 h. These results suggest a novel application for aerosolized niosomes in the management of lung cancer.

Kulkarni and Rawtani developed self-assembled niosomes to customize the solubilities of tamoxifen and doxorubicin for an effective response against breast cancer[128]. These codelivery niosomes were spherical, displayed high entrapment efficiencies, and sustained drug release for 3 days. Achieving a 15-fold increase in antitumor efficacy, through the synergistic action, compared to a free drug combination, was demonstrated in MCF-7 cell lines. The developed niosomes also exhibited significantly enhanced biodistribution and improved cellular uptake, suggesting their potential for breast cancer management. Niosomes coupled with ligands are widely explored in chemotherapy due to their ability to engage receptor-mediated endocytosis[129]. Both PEG-functionalized niosomes and ligand (peptide)-coupled niosomes are actively internalized via endocytosis, with PEG functionalization providing immunoprotection and promoting drug accumulation within tumor cells. Coupling a tumor-homing peptide (tLip-1) to the niosome surface demonstrated high penetration through active targeting in human glioblastoma (U87) cells[130].

(c) Aquasomes and phytosomes

Aquasomes and phytosomes are vesicular drug carriers resembling the properties of water, with sizes typically ranging from 60–300 nm. Aquasomes are self-assembled architecture held together by ionic, van der Waals, or non-covalent bonds. These systems consist of three major components: a central ceramic core material (providing structural stability), a carbohydrate coating substance (protecting drug), and entrapped drugs (for therapeutic action). They are primarily designed to deliver acid-labile drugs (protein and peptides) in both a sustained and targeted manner. Aquasomes have found successful applications in the delivery of various substances, including antigens, enzymes, hemoglobin, and insulin[131].

Aquasomes and phytosomes exhibit distinct morphological and functional differences. Aquasomes consist of a carbohydrate coating over a ceramic core (for stability) and are often adorned with absorbed bioactives or proteins. The cores of aquasomes are typically prepared using methods such as self-precipitation, coprecipitation, and sonication. In contrast, phytosomes are complex vesicular structures that contain phospholipids and herbal extracts (curcumin and polyphenols). They are typically prepared using the solvent evaporation method.

Etoposide is used in the treatment of drug-resistant testicular cancer, small-cell lung cancer, lymphoma, and leukemia. Its utilization is hindered by limitations such as poor bioavailability, lipophilicity, and adverse effects such as hematological toxicity, hypotension, and bronchospasm. To overcome these pharmaceutical limitations, etoposide-embedded aquasomes were designed using the lyophilization technique. The formulated aquasomes were smooth and stable and exhibited a preference for targeting lung cells, the liver, the spleen, and the kidney. When compared to free drug administration, the embedded aquasomes showed a significantly higher accumulation and localization within the targeted tumor cells[132].

Another class of vesicular systems is the phytosomes or phytophospholipid drug delivery system, designed to encapsulate bioactive agents derived from plants and facilitate their delivery across cell membranes. These systems typically have a size of approximately 40 kDa (100–1200 nm). They are capable of encapsulating various plant extracts (polyphenols, flavonoids, tannins, and terpenoids) within their core. In addition, they can be conjugated with targeted proteins at the outer periphery, enabling both active and passive targeting[133,134].

4.2.4. Inorganic nanocarriers

Inorganic nanocarriers are primarily explored for their roles in tumor imaging, facilitating the tracking of drug location, release pattern, and the evaluation of therapeutic effects. In addition, these nanocarriers are employed as theranostics to address issues related to drug resistance in chemotherapy. Commonly used inorganic carriers include iron oxide nanoparticles, quantum dots, carbon-based nanoparticles, and mesoporous silica nanoparticles. These carriers are favored for their large surface area and tunable size and structure. As depicted in Figure 7, various inorganic nanocarriers are utilized for chemotherapy. They demonstrated stimuli-responsive behaviors (temperature, magnetic field, and light), enabling the targeted release of antitumor agents, including genes and DNA, in a manner often likened to a "Trojan horse" pattern of drug release[146]. Table 9 compiles a selection of inorganic-based nanocarriers and outlines their biomedical significance in tumor management.

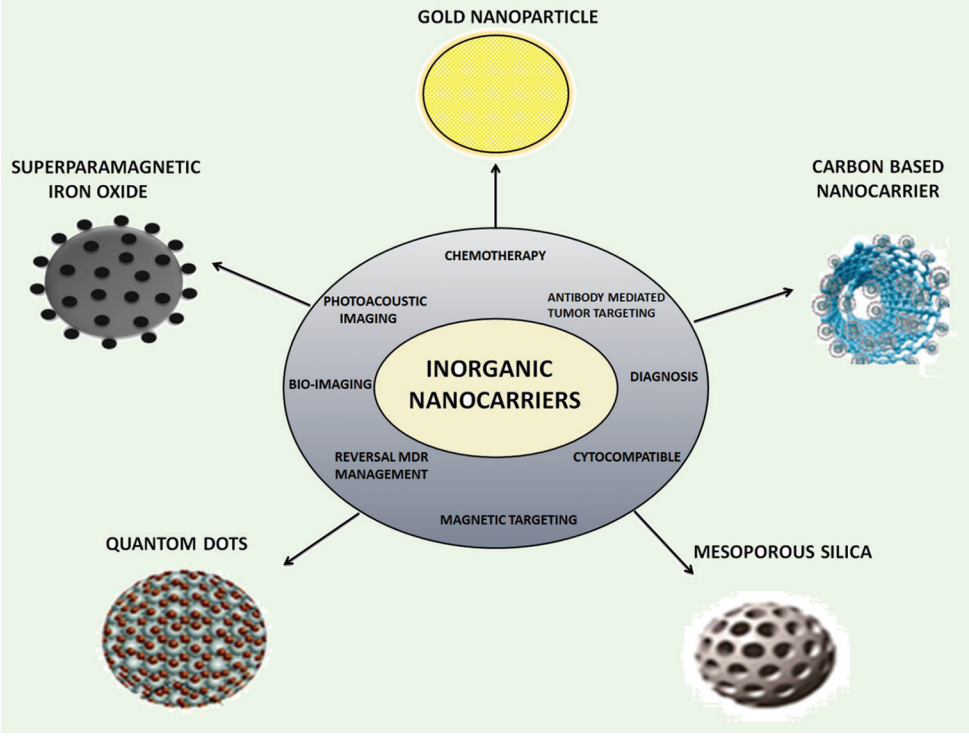

Figure 7. Various inorganic nanocarriers employed for tumor management.

Table 9. Inorganic nanocarriers utilized in tumor management

Type of nanocarrier	Inorganic compound	Research highlights	Applications	References
Inorganic nanocarriers oxide	Superparamagnetic iron oxide	Powerful noninvasive tool for bioimaging	Magnetic resonance imaging in chemotherapy	[152]
	Glutathione-induced 6-mercaptopurine and 6-thioguanine-gold nanoparticles	(i) Controlled nanomolar release of anticancer drugs at target site (ii) Effective live cell imaging technique	Monitoring and controlling Raman spectroscopic tool for tumor	[153]
	siRNA/iron oxide composite	(i) Coating of polyethyleneimine prevented the degradation of composite (ii) Reduced the expression of P-glycoprotein through siRNA transfection	MCF-7/ADR breast cancer	[154]
	Monodisperse gold-loaded iron oxide (GdIO)	Synergized enhancement of T1 and T2 contrast agents	Liver tumor diagnosis	[155]
	Doxorubicin-embedded polymeric gold nanoparticles	(i) Required a smaller dose of doxorubicin (ii) Greatly reduced tumor rate/growth (iii) Provided high therapeutic efficacy and less toxicity	Chemophotothermal therapy	[156]
	Superparamagnetic iron oxide	(i) Controlled clustering structure (ii) Internalized within mesenchymal stem cells (MSCs)	Mesenchymal stem cell (MSC) tracking and magnetic resonance imaging	[157]
	Daunorubicin and 5-bromotetrandrine-loaded iron oxide nanoparticles	(i) Increased tumor temperature (ii) Reduced p-gp and BCL-2 expression (iii) Increased caspase-3 and Bax expression	Reversal of multiple drug resistance (MDR) in leukemia	[158]
Quantum dots (QD)	Beta-cyclodextrin functionalized (CdSe/ZnSe) QDs for co-delivery of doxorubicin and siRNA	(i) Down-regulation of P-gp and mdr1 mRNA (ii) Enabled tracking through laser confocal microscopy	Real-time tracking and chemotherapeutic agent	[159]
	Dual receptor (EGRF and integrin αvβ3) targeted QD/AS-ODN/GE11-c(RGDfK)	(i) Enhanced gene silencing efficiency (ii) Augmented cellular uptake	Non-viral gene carrier for tumor management	[160]
	Manganese doped-zinc selenide quantum dots	(i) High gene transfection efficiency (ii) Biocompatible, and stable	Delivery of siRNA to pancreatic cancer	[161]
Carbon-based nanocarriers	Paclitaxel-C6 ceramide	(i) No toxicity in cell viability (ii) Improved aqueous solubility of paclitaxel (iii) Required 100 times less drug	MDR-pancreatic cancer	[162]
	Single-walled and multiwalled carbon nanotubes (SWNTs and MWNTs)	(i) Enhanced tissue penetration (ii) Provided spatial resolution (iii) Served as T2 contrast agent	Imaging probes (photoacoustic imaging)	[163]
	PEGylated MWNTs	(i) Promped drug efflux in MDR cells (ii) Stimulated ATPase activity of p-gp	Drug conjugate carrier for chemotherapy	[164]
Mesoporous silica	Trimethylammonium mesoporous silica	(i) High-efficient optical imaging of organs (ii) Stable composite within a wide range of pH	*In vivo* optical imaging	[165]
	Doxorubicin-loaded hollow mesoporous silica	(i) Displayed pore size-dependent antitumor activity (ii) Enhanced intracellular action with high MDR reversal effect	MDR reversion	[166]
	TPGS (D-tocopheryl poly ethylene glycol 1000 succinate) modified DOX- MSN	(i) Internalization through clathrin-mediated endocytosis (ii) 10-fold higher killing potency	Reversal MDR in tumor management	[167]
	Magnetic silica nanospheres	Efficient cellular uptake	Magnetic resonance imaging	[168]

The exploration of paramagnetic iron oxide and mesoporous silica nanoparticles loaded with doxorubicin and conjugated with human serum albumin has resulted in a specific focus on targeting and retention. The developed system exhibits biocompatibility and sustained release characteristics, especially in the hypoxic and acidic microenvironment of glioma tumor cells[147]. These nanocarriers have been investigated as versatile tools for encapsulating drugs, genes, and contrast agents, facilitating not only therapeutic actions but also serving as multifunctional probes for imaging tumor cells[148]. For instance, Tang *et al*. designed a magnetic targeting strategy that utilizes an antitumor nanoplatform that efficiently synergizes transfection action with magnetic guidance. Similarly, Reczyńska *et al*. modified superparamagnetic iron oxide nanoparticles (SPIONs) with a combination of non-porous and mesoporous silica coating (@SiO2@mSiO2) and non-porous silica coating (@SiO2), significantly altering the surface properties and sustaining iron release[149]. These modified systems displayed cytocompatibility and exhibited antiproliferative effects against lung cancer cells (A549 cells). Another widely employed nanocarrier, mesoporous silica, has attracted attention due to its theranostic application, attributed to its high pore volume, specific surface area, and well-structured surface properties.

Iron oxide nanoparticles and SPIONs have been explored for a myriad of biomedical applications, including the biosensing of tumor-influenced regions. These nanoparticles efficiently reduced tissue T2 relaxation time, promoting better internalization through the endocytosis pathway[150]. They are versatile carriers capable of loading a range of candidates, such as nucleic acids, antineoplastic agents, and chemical inhibitors. SPIONs that are conjugated with transferrin, aptamers, peptides, antibodies, or hyaluronic acid serve as efficient tumor-targeted drug delivery systems. They are easily recognized by overexpressed receptors and feature bioimaging capabilities while minimizing off-target effects[151]. Moreover, these nanoparticles hold the potential to reverse multidrug resistance effects in chemotherapy and are ideal candidates for diagnostic purposes to monitor therapeutic performances.

Semiconductor quantum dots represent a novel class of fluorescent molecular imaging agents known for their exclusive photophysical properties, including dual imaging capabilities, enhanced signal brightness, size-dependent light emission, and the ability to excite various fluorescent colors simultaneously. Moreover, these agents can effectively bind metal ions to their surfaces due to their high sensitivity and selectivity for metal ions. Over the past two decades, these fluorescent particles have found applications in diagnosis and drug delivery at tumor-targeted sites[169]. For instance, Nifontova *et al*. investigated the cytotoxicity of quantum dots-loaded microcapsules that were functionalized with trastuzumab, a monoclonal antibody[170]. This system specifically targeted the overexpressed HER2 in breast cancer, demonstrating sensitive and promising antibody-mediated tumor targeting with quantum dots. AbdElhamid *et al*. formulated highly fluorescent theranostic nanocapsules based on mercaptopropionic acid-coated cadmium telluride quantum dots, incorporating dual drugs — honokiol and celecoxib[171]. These nanocapsules were further modified with anionic chondroitin sulfate (for CD44 targeting) and cationic lactoferrin (low-density lipoprotein targeting). These multifunctional theranostics exhibited efficient internalization and were easily traceable due to their fluorescence behavior. Furthermore, they demonstrated enhanced cytotoxicity and improved antitumor efficacy against breast cancer cells.

Gold nanoparticles have been intensively engineered as nanocarriers for managing tumor-associated issues due to their biocompatibility, colloidal stability, size tunability, feasible surface modification, and enhanced tissue permeability. These nanocarriers find applications in bioimaging and photoacoustic imaging, due to their high electron density, enhanced optical scattering performance, and non-bleaching fluorescence in tumor cell imaging[172]. Albertini *et al*. developed peptide (arginine-glycine-aspartic acid)-decorated gold nanoparticles for the treatment and diagnosis of tumors[173]. They reported approximately a 4-fold increase in accumulation following subcutaneous administration and a 1.5-fold increase through the intracranial route in mice tumors.

5. Conclusion

This review summarizes a wide range of nanotechnology-based targeted drug delivery strategies that are commonly employed in tumor management. These drug delivery approaches exhibit cell specificity and selectivity while minimizing systemic toxicity. Advancements in nanotechnology have enabled the precise recognition of tumor sites, offering hope for successful drug delivery to tumor sites. Various versatile nanocarriers, including polymeric nanoparticles, lipid-based carriers, vesicular systems, and inorganic nanocarriers, have undergone extensive investigation for tumor management. These systems not only facilitate precise target site identification but also demonstrate a high capacity for tissue internalization. Targeting tumor sites through the application of magnetic fields and ultrasound radiation represents an emerging

concept with significant potential for the precise recognition of molecular addresses, bioimaging, and disease tracking at the tumor sites. These exclusive attributes have enabled researchers to develop novel approaches, including monotherapy and combination therapy (through ligand conjugation), aimed at improving tumor management. Polymeric-targeted approaches exhibit the efficiency to specifically enter the tumor vasculature without affecting neighbor cells and tissues. While these nanosystems offer promising alternatives for tumor management, they are not without challenges. These challenges include addressing the altered tumor microenvironment, improving uptake and internalization, overcoming the narrow therapeutic window for therapeutics, and navigating the regulatory processes required for approval. Moreover, achieving a vehicle with an extended biological half-life and enhanced targeting efficiency is crucial for site-specific actions. Current targeted approaches primarily emphasize safety and efficiency at the cancerous site. However, they also require careful consideration of potential long-term side effects, the determination of optimal dosage strength, and the establishment of suitable conditions. Recent advancements have introduced precise treatment methods, such as siRNA delivery, stem cell therapy, immune-based treatments, gene therapies, and ablation therapies. These approaches hold promise as alternatives to surgical procedures. Furthermore, newly introduced fields such as pathomics and radiomics are highly favored for collecting extensive clinical data and designing novel strategies to predict well-defined responses and advancements in cancer management.

Acknowledgments

The authors sincerely acknowledge the School of Pharmaceutical Sciences, Chhatrapati Shahu Ji Maharaj University, Kanpur, for providing all working facilities that contributed to the completion of this review article. Our thanks are also extended to the Faculty of Pharmacy, Uttar Pradesh University of Medical Sciences, Saifai, Etawah, for their valuable assistance in collecting the data presented in this manuscript.

Funding

None.

Conflict of interest

The authors declare no conflict of interest.

Author contributions

Conceptualization: Kamla Pathak
Writing – original draft: Shashi Kiran Misra
Writing – review and editing: Kamla Pathak

Ethics approval and consent to participate

Not applicable.

Consent for publication

Not applicable.

Availability of data

Not applicable.

References

1. Rankin EB, Giaccia AJ, 2016, Hypoxic control of metastasis. *Science*, 352: 175–180.

   https://doi.org/10.1126/science.aaf4405

2. Abolhassani H, Wang Y, Hammarström L, *et al.*, 2021, Hallmarks of cancers: Primary antibody deficiency *Versus* other inborn errors of immunity. *Front Immunol*, 12: 720025.

   https://doi.org/10.3389/fimmu.2021.720025

3. Mi Y, Mu L, Huang K, *et al.*, 2020, Hypoxic colorectal cancer cells promote metastasis of normoxic cancer cells depending on IL-8/p65 signaling pathway. *Cell Death Dis*, 11(7): 610.

   https://doi.org/10.1038/s41419-020-02797-z

4. Date AA, Hanes J, Ensign LM, 2016, Nanoparticles for oral delivery: Design, evaluation and state-of-the-art. *J Control Release*, 240: 504–526.

   https://doi.org/10.1016/j.jconrel.2016.06.016

5. Wang AZ, Langer R, Farokhzad OC, 2012, Nanoparticle delivery of cancer drugs. *Annu Rev Med*, 63: 185–198.

   https://doi.org/10.1146/annurev-med-040210-162544

6. Gustafson HH, Holt-Casper D, Grainger DW, *et al.*, 2015, Nanoparticle uptake: The phagocyte problem. *Nano Today*, 10: 487–510.

   https://doi.org/10.1016/j.nantod.2015.06.006

7. Andreone BJ, Chow BW, Tata A, *et al.*, 2017, Blood-brain barrier permeability is regulated by lipid transport-dependent suppression of caveolae-mediated transcytosis. *Neuron*, 94: 581–594.e5.

   https://doi.org/10.1016/j.neuron.2017.03.043

8. Sanchez-Covarrubias L, Slosky LM, Thompson BJ, *et al.*, 2014, Transporters at CNS barrier sites: Obstacles or opportunities for drug delivery. *Curr Pharm Des*, 20: 1 422–1449.

   https://doi.org/10.2174/13816128113199990463

9. Wang Y, Cai R, Chen C, 2019, The nano-bio interactions of nanomedicines: Understanding the biochemical driving forces and redox reactions. *Acc Chem Res*, 52(6): 1507–1518.

   https://doi.org/10.1021/acs.accounts.9b00126

10. Sun B, Sun YY, Li XP, *et al.*, 2019, Particle and bacteria

uptake by Japanese flounder (*Paralichthys olivaceus*) red blood cells: Size dependence and pathway specificity. *Tissue Cell*, 61: 79–88.

https://doi.org/10.1016/j.tice.2019.09.002

11. Kutova OM, Guryev EL, Sokolova EA, *et al.*, 2019, Targeted delivery to tumors: Multidirectional strategies to improve treatment efficiency. *Cancers* (*Basel*), 11: 68.

https://doi.org/10.3390/cancers11010068

12. Gu YT, Xue YX, Wang YF, *et al.*, 2012, Role of ROS/RhoA/PI3K/PKB signaling in NS1619-mediated blood-tumor barrier permeability increase. *J Mol Neurosci*, 48: 302–312.

https://doi.org/10.1007/s12031-012-9789-2

13. Deryugina EI, 2016, Chorioallantoic membrane microtumor model to study the mechanisms of tumor angiogenesis, vascular permeability, and tumor cell intravasation. *Methods Mol Biol*, 1430: 283–298.

https://doi.org/10.1007/978-1-4939-3628-1_19

14. Uhlen M, Zhang C, Lee S, *et al.*, 2017, A pathology atlas of the human cancer transcriptome. *Science*, 357: eaan2507.

https://doi.org/10.1126/science.aan2507

15. Naik H, Sonju JJ, Singh S, *et al.*, 2021, Lipidated peptidomimetic ligand-functionalized HER2 targeted liposome as nano-carrier designed for doxorubicin delivery in cancer therapy. P*harmaceuticals (Basel)*, 14: 221.

https://doi.org/10.3390/ph14030221

16. Dvorak HF, 2015, Tumor stroma, tumor blood vessels, and antiangiogenesis therapy. *Cancer J*, 21: 237–243.

https://doi.org/10.1097/PPO.0000000000000124

17. Goel S, Chen F, Hong H, *et al.*, 2014, $VEGF_{121}$-conjugated mesoporous silica nanoparticle: A tumor targeted drug delivery system. *ACS Appl Mater Interfaces*, 6: 21677–21685.

https://doi.org/10.1021/am506849p

18. Prager GW, Poettler M, Unseld M, *et al.*, 2012, Angiogenesis in cancer: Anti-VEGF escape mechanisms. *Transl Lung Cancer Res*, 1: 14–25.

https://doi.org/10.3978/j.issn.2218-6751.2011.11.02

19. Ma X, Xiong Y, Lee LTO, 2018, Application of nanoparticles for targeting G protein-coupled receptors. *Int J Mol Sci*, 19: 2006.

https://doi.org/10.3390/ijms19072006

20. Huang B, Abraham WD, Zheng Y, *et al.*, 2015, Active targeting of chemotherapy to disseminated tumors using nanoparticle-carrying T cells. *Sci Transl Med*, 7: 291ra94.

https://doi.org/10.1126/scitranslmed.aaa5447

21. Roger M, Clavreul A, Venier-Julienne MC, *et al.*, 2011, The potential of combinations of drug-loaded nanoparticle systems and adult stem cells for glioma therapy. *Biomaterials*, 32: 2106–2116.

https://doi.org/10.1016/j.biomaterials.2010.11.056

22. Townsend AR, Chong LC, Karapetis C, *et al.*, 2016, Selective internal radiation therapy for liver metastases from colorectal cancer. *Cancer Treat Rev*, 50: 148–154.

https://doi.org/10.1016/j.ctrv.2016.09.007

23. Sangi S, Sree HN, Bawadekji A, *et al.*, 2018, Chemotherapeutic drug targeting to lungs by way of microspheres after intravenous administration. *Drug Des Devel Ther*, 12: 3051–3060.

https://doi.org/10.2147/DDDT.S173485

24. Fan R, Li X, Deng J, *et al.*, 2016. Dual drug loaded biodegradable nanofibrous microspheres for improving anti-colon cancer activity. *Sci Rep*, 6: 28373.

25. Shell JR, Gendron LN, LaRochelle EP, *et al.*, 2019, Tumor Targeting Cetuximab Conjugated Europium Microspheres for Cherenkov Excited Luminescence Scanned Imaging (Conference Presentation). In: Proceedings of Molecular-Guided Surgery: Molecules, Devices, and Applications. Vol. 10862. p. 1086217.

https://doi.org/10.1117/12.2515383

26. Shukla T, Upmanyu N, Agrawal M, *et al.*, 2018, Biomedical applications of microemulsion through dermal and transdermal route. *Biomed Pharmacother*, 108: 1477–1494.

https://doi.org/10.1016/j.biopha.2018.10.021

27. Naves LB, Almeida L, Marques MJ, *et al.*, 2017, Emulsions stabilization for topical application. *Biomater Med Appl,* 1: 1.

28. Murthy R, Habbul A, 2006, Trans-arterial hepatic radioembolisation of yttrium-90 microspheres. *Biomed Imag Interven J*, 2: e43.

https://doi.org/10.2349/biij.2.3.e43

29. Yehia R, Hathout RM, Attia DA, *et al.*, 2017, Anti-tumor efficacy of an integrated methyl dihydrojasmonate transdermal microemulsion system targeting breast cancer cells: *In vitro* and *in vivo* studies. *Colloids Surf B Biointerfaces*, 1: 512–521.

https://doi.org/10.1016/j.colsurfb.2017.04.031

30. Enriquez GG, Rizvi SA, D'Souza MJ, *et al.*, 2013, Formulation and evaluation of drug-loaded targeted magnetic microspheres for cancer therapy. *Int J Nanomed*, 8: 1393–1402.

https://doi.org/10.2147/IJN.S43479

31. Cordeiro Pedrosa LR, van Tellingen O, Soullié T, *et al.*, 2015, Plasma membrane targeting by short chain sphingolipids inserted in liposomes improves anti-tumor activity of mitoxantrone in an orthotopic breast carcinoma xenograft model. *Eur J Pharm Biopharm*, 94: 207–219.

https://doi.org/10.1016/j.ejpb.2015.05.003

32. Han R, Yang YM, Dietrich J, *et al.*, 2008, Systemic 5-fluorouracil treatment causes a syndrome of delayed myelin destruction in the central nervous system. *J Biol*, 7: 12.

https://doi.org/10.1186/jbiol69

33. Bardos AP, editor, 2005, Treatment of Ovarian Cancer. New York: Nova Science Publishers Inc., p79–86.

34. Woo SM, Joo J, Kim SY, *et al.*, 2016, Efficacy of pancreatic exocrine replacement therapy for patients with unresectable pancreatic cancer in a randomized trial. *Pancreatology*, 16(6): 1099–1105.

https://doi.org/10.1016/j.pan.2016.09.001

35. Tamura K, Kikuchi E, Konno T, *et al.*, 2015, Therapeutic effect of intravesical administration of paclitaxel solubilized with poly(2-methacryloyloxyethyl phosphorylcholine-co-n-butyl methacrylate) in an orthotopic bladder cancer model. *BMC Cancer*, 15: 317.

https://doi.org/10.1186/s12885-015-1338-2

36. Kapoor DN, Bhatia A, Kaur R, *et al.*, 2015, PLGA: A unique polymer for drug delivery. *Ther Deliv*, 6: 41–58.

https://doi.org/10.4155/tde.14.91

37. Florence AT, 2005, Nanoparticle uptake by the oral route: Fulfilling its potential? *Drug Discov Today Technol*, 2: 75–81.

https://doi.org/10.1016/j.ddtec.2005.05.019

38. Mittal G, Sahana DK, Bhardwaj V, *et al.*, 2007, Estradiol loaded PLGA nanoparticles for oral administration: Effect of polymer molecular weight and copolymer composition on release behavior *in vitro* and *in vivo*. *J Control Release*, 119: 77–85.

https://doi.org/10.1016/j.jconrel.2007.01.016

39. Jana S, Maiti S, Jana S, editors, 2017, Biopolymer-Based Composites. United Kingdom: Woodhead Publishing. p221–267.

40. He C, Hu Y, Yin L, *et al.*, 2010, Effects of particle size and surface charge on cellular uptake and biodistribution of polymeric nanoparticles. *Biomaterials*, 31: 3657–3666.

https://doi.org/10.1016/j.biomaterials.2010.01.065

41. Wang R, Shen Q, Li X, *et al.*, 2018, Efficacy of inverso isomer of CendR peptide on tumor tissue penetration. *Acta Pharm Sin B*, 8: 825–832.

https://doi.org/10.1016/j.apsb.2018.06.006

42. Maman S, Witz IP, 2018, A history of exploring cancer in context. *Nat Rev Cancer*, 18: 359–376.

https://doi.org/10.1038/s41568-018-0006-7

43. Yu W, Liu R, Zhou Y, *et al.*, 2020, Size-tunable strategies for a tumor targeted drug delivery system. *ACS Cent Sci*, 6: 100–116.

44. Begines B, Ortiz T, Pérez-Aranda M, *et al.*, 2020. Polymeric nanoparticles for drug delivery: Recent developments and future prospects. *Nanomaterials* (*Basel*), 10: 1403.

https://doi.org/10.3390/nano10071403

45. Ni M, Xiong M, Zhang X, *et al.*, 2015, Poly(lactic-co-glycolic acid) nanoparticles conjugated with CD133 aptamers for targeted salinomycin delivery to CD133+ osteosarcoma cancer stem cells. *Int J Nanomed*, 31: 2537–2554.

https://doi.org/10.2147/IJN.S78498

46. Banzato A, Bobisse S, Rondina M, *et al.*, 2008, A paclitaxel-hyaluronan bioconjugate targeting ovarian cancer affords a potent *in vivo* therapeutic activity. *Clin Cancer Res*, 14: 3598–3606.

https://doi.org/10.1158/1078-0432.CCR-07-2019

47. Liu Q, Li RT, Qian HQ, *et al.*, 2013, Targeted delivery of miR-200c/DOC to inhibit cancer stem cells and cancer cells by the gelatinases-stimuli nanoparticles. *Biomaterials*, 34: 7191–7203.

https://doi.org/10.1016/j.biomaterials.2013.06.004

48. Yang N, Jiang Y, Zhang H, *et al.*, 2015, Active targeting docetaxel-PLA nanoparticles eradicate circulating lung cancer stem-like cells and inhibit liver metastasis. *Mol Pharm*, 12: 232–239.

https://doi.org/10.1021/mp500568z

49. Nascimento AV, Singh A, Bousbaa H, *et al.*, 2015, Combinatorial-designed epidermal growth factor receptor-targeted chitosan nanoparticles for encapsulation and delivery of lipid-modified platinum derivatives in wild-type and resistant non-small-cell lung cancer cells. *Mol Pharm*, 12: 4466–4477.

https://doi.org/10.1021/acs.molpharmaceut.5b00642

50. Majumder N, Das NG, Das SK, 2020, Polymeric micelles for anticancer drug delivery. *Ther Deliv*, 11(10): 613–635.

https://doi.org/10.4155/tde-2020-0008

51. Keskin D, Tezcaner A, 2017, Micelles as delivery system for cancer treatment. *Curr Pharm Des*, 23(35): 5230–5241.

https://doi.org/10.2174/1381612823666170526102757

52. Kanamala M, Wilson WR, Yang M, *et al.*, 2016, Mechanisms and biomaterials in pH-responsive tumour targeted drug delivery: A review. *Biomaterials*, 85: 152–167.

https://doi.org/10.1016/j.biomaterials.2016.01.061

53. Ge Z, Liu S, 2013, Functional block copolymer assemblies responsive to tumor and intracellular microenvironments for site-specific drug delivery and enhanced imaging performance. *Chem Soc Rev*, 42: 7289–7325.

54. Ke XY, Lin NVW, Gao SJ, *et al.*, 2014, Co-delivery of thioridazine and doxorubicin using polymeric micelles for targeting both cancer cells and cancer stem cells.

Biomaterials, 35: 1096–1108.

https://doi.org/10.1016/j.biomaterials.2013.10.049

55. Bisht S, Feldmann G, Soni S, *et al.*, 2007, Polymeric nanoparticle-encapsulated curcumin ("nanocurcumin"): A novel strategy for human cancer therapy. *J Nanobiotechnology*, 5: 3.

https://doi.org/10.1186/1477-3155-5-3

56. Jin X, Mo R, Ding Y, *et al.*, 2014, Paclitaxel-loaded N-octyl-O-sulfate chitosan micelles for superior cancer therapeutic efficacy and overcoming drug resistance. *Mol Pharm*, 11: 145–157.

https://doi.org/10.1021/mp400340k

57. Krishnamurthy S, Ng VW, Gao S, *et al.*, 2014, Phenformin-loaded polymeric micelles for targeting both cancer cells and cancer stem cells *in vitro* and *in vivo*. *Biomaterials*, 35: 9177–9186.

https://doi.org/10.1016/j.biomaterials.2014.07.018

58. Wu P, Jia Y, Qu F, *et al.*, 2017, Ultrasound-responsive polymeric micelles for sonoporation-assisted site-specific therapeutic action. *ACS Appl Mater Interfaces*, 9: 25706–25716.

https://doi.org/10.1021/acsami.7b05469

59. Huang R, Wang Y, editors, 2020, New Nanomaterials and Techniques for Tumor-targeted Systems. Berlin: Springer. p337–369.

60. Kesharwani P, Iyer AK, 2015, Recent advances in dendrimer-based nanovectors for tumor-targeted drug and gene delivery. *Drug Discov Today*, 20: 536–547.

https://doi.org/10.1016/j.drudis.2014.12.012

61. Palmerston ML, Pan J, Torchilin VP, 2017, Dendrimers as nanocarriers for nucleic acid and drug delivery in cancer therapy. *Molecules*, 22: 1401.

https://doi.org/10.3390/molecules22091401

62. Liu J, Li J, Liu N, *et al.*, 2017, *In vitro* studies of phospholipid-modified PAMAM-siMDR1 complexes for the reversal of multidrug resistance in human breast cancer cells. *Int J Pharm*, 530: 291–299.

https://doi.org/10.1016/j.ijpharm.2017.06.026

63. Jiang X, Bugno J, Hu C, *et al.*, 2016, Eradication of acute myeloid leukemia with FLT3 ligand-targeted miR-150 nanoparticles. *Cancer Res*, 76: 4470–4480.

https://doi.org/10.1158/0008-5472.CAN-15-2949

64. Szulc A, Pulaski, L, Appelhans D, *et al.*, 2016, Sugar-modified poly (propylene imine) dendrimers as drug delivery agents for cytarabine to overcome drug resistance. *Int J Pharm*, 513: 572–583.

https://doi.org/10.1016/j.ijpharm.2016.09.063

65. Sheveleva NN, Dolgushev M, Lähderanta E, *et al.*, 2022, Mechanical relaxation of functionalized carbosilane dendrimer melts. *Phys Chem Chem Phys*, 24: 13049–13056.

66. Caminade AM, 2020, Phosphorus dendrimers as nanotools against cancers. *Molecules*, 25: 3333.

https://doi.org/10.3390/molecules25153333

67. Chen L, Li J, Fan Y, *et al.*, 2020, Revisiting cationic phosphorus dendrimers as a nonviral vector for optimized gene delivery toward cancer therapy applications. *Biomacromolecules*, 21: 2502–2511.

https://doi.org/10.1021/acs.biomac.0c00458

68. Rajasekaran D, Srivastava J, Ebeid K, *et al.*, 2015, Combination of nanoparticle-delivered siRNA for astrocyte elevated gene-1 (AEG-1) and all-trans retinoic acid (ATRA): An effective therapeutic strategy for hepatocellular carcinoma (HCC). *Bioconjug Chem*, 26: 1651–1661.

https://doi.org/10.1021/acs.bioconjchem.5b00254

69. Zheng W, Cao C, Liu Y, *et al.*, 2015, Multifunctional polyamidoamine-modified selenium nanoparticles dual-delivering siRNA and cisplatin to A549/DDP cells for reversal multidrug resistance. *Acta Biomater*, 11: 368–380.

https://doi.org/10.1016/j.actbio.2014.08.035

70. Sharma A, Gautam SP, Gupta AK, 2011, Surface modified dendrimers: Synthesis and characterization for cancer targeted drug delivery. *Bioorg Med Chem*, 19: 3341–3346.

https://doi.org/10.1016/j.bmc.2011.04.046

71. Zhang Y, Thomas TP, Lee KH, *et al.*, 2011, Polyvalent saccharide-functionalized generation 3 poly(amidoamine) dendrimer-methotrexate conjugate as a potential anticancer agent. *Bioorg Med Chem*, 19: 2557–2564.

https://doi.org/10.1016/j.bmc.2011.03.019

72. Nam HY, Hahn HJ, Nam K, *et al.*, 2008, Evaluation of generations 2, 3 and 4 arginine modified PAMAM dendrimers for gene delivery. *Int J Pharm*, 363: 199–205.

https://doi.org/10.1016/j.ijpharm.2008.07.021

73. Dhakad RS, Tekade RK, Jain NK, 2013, Cancer targeting potential of folate targeted nanocarrier under comparative influence of tretinoin and dexamethasone. *Curr Drug Deliv*, 10: 477–491.

https://doi.org/10.2174/1567201811310040012

74. Kesharwani P, Tekade RK, Jain NK, 2014, Formulation development and *in vitro-in vivo* assessment of the fourth-generation PPI dendrimer as a cancer-targeting vector. *Nanomedicine* (*Lond*), 9: 2291–2308.

https://doi.org/10.2217/nnm.13.210

75. Liu H, Wang Y, Wang M, *et al.*, 2014, Fluorinated poly(propylenimine) dendrimers as gene vectors. *Biomaterials*, 35: 5407–5413.

https://doi.org/10.1016/j.biomaterials.2014.03.040

76. Niidome T, Yamauchi H, Takahashi K, *et al.*, 2014, Hydrophobic cavity formed by oligopeptide for doxorubicin delivery based on dendritic poly(L-lysine). *J Biomater Sci Polym Ed*, 25: 1362–1373.

https://doi.org/10.1080/09205063.2014.938979

77. Kaminskas LM, McLeod VM, Ryan GM, *et al.*, 2014, Pulmonary administration of a doxorubicin-conjugated dendrimer enhances drug exposure to lung metastases and improves cancer therapy. *J Control Release*, 183: 18–26.

https://doi.org/10.1016/j.jconrel.2014.03.012

78. Ma D, Zhao Y, Zhou XY, *et al.*, 2013, Photoenhanced gene transfection by a star-shaped polymer consisting of a porphyrin core and poly(L-lysine) dendron arms. *Macromol Biosci*, 13: 1221–1227.

https://doi.org/10.1002/mabi.201300139

79. Zhao J, Zhou R, Fu X, *et al.*, 2014, Cell-penetrable lysine dendrimers for anti-cancer drug delivery: synthesis and preliminary biological evaluation. *Arch Pharm* (*Weinheim*), 347: 469–477.

80. Ogris M, Wagner E, 2002, Tumor-targeted gene transfer with DNA polyplexes. *Somat Cell Mol Genet*, 27: 85–95.

https://doi.org/10.1023/a:1022988008131

81. Lee D, Lee YM, Kim J, *et al.*, 2015, Enhanced tumor-targeted gene delivery by bioreducible polyethylenimine tethering EGFR divalent ligands. *Biomater Sci*, 3: 1096–1104.

https://doi.org/10.1039/c5bm00004a

82. Taschauer A, Polzer W, Alioglu F, *et al.*, 2019, Peptide-targeted polyplexes for aerosol-mediated gene delivery to CD49f-overexpressing tumor lesions in lung. *Mol Ther Nucleic Acids*, 18: 774–786.

https://doi.org/10.1016/j.omtn.2019.10.009

83. Hattori Y, 2017, Progress in the development of lipoplex and polyplex modified with anionic polymer for efficient gene delivery. *J Genet Med Gene Ther*, 1: 3–18.

84. Chen M, Zeng Z, Qu X, *et al.*, 2015, Biocompatible anionic polyelectrolyte for improved liposome based gene transfection. *Int J Pharm*, 490: 173–179.

https://doi.org/10.1016/j.ijpharm.2015.05.046

85. Ito T, Koyama Y, Otsuka M, 2014, Preparation of calcium phosphate nanocapsule including deoxyribonucleic acid-polyethyleneimine-hyaluronic acid ternary complex for durable gene delivery. *J Pharm Sci*, 103: 179–184.

86. Gu J, Chen X, Ren X, *et al.*, 2016, CD44-Targeted hyaluronic acid-coated redox- responsive hyperbranched poly (amido amine)/plasmid DNA ternary nanoassemblies for efficient gene delivery. *Bioconjug Chem*, 27: 1723–1736.

https://doi.org/10.1021/acs.bioconjchem.6b00240

87. Mok H, Park JW, Park TG, 2007, Antisense oligodeoxynucleotide-conjugated hyaluronic acid/protamine nanocomplexes for intracellular gene inhibition. *Bioconjug Chem*, 18: 1483–1489.

https://doi.org/10.1021/bc070111o

88. Iwanaga M, Kodama Y, Muro T, *et al.*, 2017, Biocompatible complex coated with glycosaminoglycan for gene delivery. *J Drug Target*, 25: 370–378.

https://doi.org/10.1080/1061186X.2016.1274996

89. Liao ZX, Peng SF, Ho YC, *et al.*, 2012, Mechanistic study of transfection of chitosan/DNA complexes coated by anionic poly (gamma-glutamic acid). *Biomaterials*, 33: 3306–3315.

https://doi.org/10.1016/j.biomaterials.2012.01.013

90. Kodama Y, Kuramoto H, Mieda Y, *et al.*, 2017, Application of biodegradable dendrigraft poly-l-lysine to a small interfering RNA delivery system. *J Drug Target*, 25: 49–57.

https://doi.org/10.1080/1061186X.2016.1184670

91. Boyle WS, Senger K, Tolar J, *et al.*, 2017, Heparin enhances transfection in concert with a trehalose-based polycation with challenging cell types. *Biomacromol*, 18: 56–67.

https://doi.org/10.1021/acs.biomac.6b01297

92. Tan GK, Tabata Y, 2014, Chondroitin-6-sulfate attenuates inflammatory responses in murine macrophages via suppression of NF-kappaB nuclear translocation. *Acta Biomater*, 10: 2684–2692.

https://doi.org/10.1016/j.actbio.2014.02.025

93. García-Pinel B, Porras-Alcalá C, Ortega-Rodríguez A, *et al.*, 2019, Lipid-based nanoparticles: Application and recent advances in cancer treatment. *Nanomaterials* (*Basel*), 9: 638.

https://doi.org/10.3390/nano9040638

94. Ozpolat B, Sood AK, Lopez-Berestein G, 2014, Liposomal siRNA nanocarriers for cancer therapy. *Adv Drug Deliv Rev*, 66: 110–116.

https://doi.org/10.1016/j.addr.2013.12.008

95. Mukherjee S, Ray S, Thakur RS, 2009, Solid lipid nanoparticles: A modern formulation approach in drug delivery system. *Indian J Pharm Sci*, 71: 349–358.

https://doi.org/10.4103/0250-474X.57282

96. Iqbal MA, Shadab Md, Sahni JK, *et al.*, 2012, Nanostructured lipid carriers system: Recent advances in drug delivery. *J Drug Target*, 20: 813–830.

https://doi.org/10.3109/1061186X.2012.716845

97. Yang R, Gao R, Li F, *et al.*, 2011, The influence of lipid characteristics on the formation, *in vitro* release, and *in vivo* absorption of protein-loaded SLN prepared by the double emulsion process. *Drug Dev Ind Pharm*, 37: 139–148.

https://doi.org/10.3109/03639045.2010.497151

98. Bhagwat GS, Athawale RB, Gude RP, *et al.*, 2020,

Formulation and development of transferrin targeted solid lipid nanoparticles for breast cancer therapy. *Front Pharmacol*, 11: 614290.

https://doi.org/10.3389/fphar.2020.614290

99. da Rocha MCO, da Silva PB, Radicchi MA, *et al.*, 2020, Docetaxel-loaded solid lipid nanoparticles prevent tumor growth and lung metastasis of 4T1 murine mammary carcinoma cells. *J Nanobiotechnology*, 18: 43.

https://doi.org/10.1186/s12951-020-00604-7

100. Smith T, Affram K, Nottingham EL, *et al.*, 2020, Application of smart solid lipid nanoparticles to enhance the efficacy of 5-fluorouracil in the treatment of colorectal cancer. *Sci Rep*, 10: 16989.

https://doi.org/10.1038/s41598-020-73218-6

101. Shuhendler AJ, Prasad P, Leung M, *et al.*, 2012, A novel solid lipid nanoparticle formulation for active targeting to tumor α (v) β(3) integrin receptors reveals cyclic RGD as a double-edged sword. *Adv Healthc Mater*, 1: 600–608.

https://doi.org/10.1002/adhm.201200006

102. Chuang CH, Wu PC, Tsai TH, *et al.*, 2017, Development of pH-sensitive cationic PEGylated solid lipid nanoparticles for selective cancer-targeted therapy. *J Biomed Nanotechnol*, 13: 192–203.

https://doi.org/10.1166/jbn.2017.2338

103. Wang W, Zhang L, Chen T, *et al.*, 2017, Anticancer effects of resveratrol-loaded solid lipid nanoparticles on human breast cancer cells. Molecules, 22: 1814.

https://doi.org/10.3390/molecules22111814

104. Miao J, Du Y, Yuan H, *et al.*, 2015, Improved cytotoxicity of paclitaxel loaded in nanosized lipid carriers by intracellular delivery. *J Nanopart Res*, 17: 10.

105. Khosa A, Reddi S, Saha RN, 2018, Nanostructured lipid carriers for site-specific drug delivery. *Biomed Pharmacother*, 103: 598–613.

https://doi.org/10.1016/j.biopha.2018.04.055

106. Varshosaz J, Taymouri S, Jahanian-Najafabadi A, *et al.*, 2018, Efavirenz oral delivery via lipid nanocapsules: Formulation, optimisation, and *ex-vivo* gut permeation study. *IET Nanobiotechnol*, 12: 795–806.

https://doi.org/10.1049/iet-nbt.2018.0006

107. Zhang XG, Miao J, Dai YQ, *et al.*, 2008, Reversal activity of nanostructured lipid carriers loading cytotoxic drug in multi-drug resistant cancer cells. *Int J Pharm*, 361: 239–244.

https://doi.org/10.1016/j.ijpharm.2008.06.002

108. Wang Y, Zhang H, Hao J, *et al.*, 2016, Lung cancer combination therapy: Co-delivery of paclitaxel and doxorubicin by nanostructured lipid carriers for synergistic effect. *Drug Deliv*, 23: 1398–1403.

https://doi.org/10.3109/10717544.2015.1055619

109. Mussi SV, Sawant R, Perche F, *et al.*, 2014, Novel nanostructured lipid carrier co-loaded with doxorubicin and docosahexaenoic acid demonstrates enhanced *in vitro* activity and overcomes drug resistance in MCF-7/Adr cells. *Pharm Res*, 31: 1882–1892.

https://doi.org/10.1007/s11095-013-1290-2

110. Wang JY, Song YQ, Peng J, *et al.*, 2020, Nanostructured lipid carriers delivering sorafenib to enhance immunotherapy induced by doxorubicin for effective esophagus cancer therapy. *ACS Omega*, 5: 22840–22846.

https://doi.org/10.1021/acsomega.0c02072

111. Li X, Jia X, Niu H, 2018, Nanostructured lipid carriers co-delivering lapachone and doxorubicin for overcoming multidrug resistance in breast cancer therapy. *Int J Nanomedicine*, 13: 4107–4119.

https://doi.org/10.2147/IJN.S163929

112. Liu Q, Li J, Pu G, *et al.*, 2016, Co-delivery of baicalein and doxorubicin by hyaluronic acid decorated nanostructured lipid carriers for breast cancer therapy. *Drug Deliv*, 23: 1364–1368.

https://doi.org/10.3109/10717544.2015.1031295

113. Li Z, Zou X, Zhu H, *et al.*, 2018, Inhibitory effect of baicalein combined with gemcitabine in human pancreatic cancer cell lines. *Oncol Lett*, 15: 5459–5464.

https://doi.org/10.3892/ol.2018.8043

114. Ni S, Qiu L, Zhang G, *et al.*, 2017, Lymph cancer chemotherapy: Delivery of doxorubicin-gemcitabine prodrug and vincristine by nanostructured lipid carriers. *Int J Nanomedicine*, 12: 1565–1576.

https://doi.org/10.2147/IJN.S120685

115. Ding X, Xu X, Zhao Y, *et al.*, 2017, Tumor targeted nanostructured lipid carrier co-delivering paclitaxel and indocyanine green for laser triggered synergetic therapy of cancer. *RSC Adv, 7:* 35086–35095.

116. Yang J, Ju Z, Dong S, 2016, Cisplatin and paclitaxel co-delivered by folate-decorated lipid carriers for the treatment of head and neck cancer. *Drug Deliv*, 24: 792–799.

https://doi.org/10.1080/10717544.2016.1236849

117. Sánchez-López E, Guerra M, Dias-Ferreira J, *et al.*, 2019, Current applications of nanoemulsions in cancer therapeutics. *Nanomaterials* (*Basel*), 9: 821.

https://doi.org/10.3390/nano9060821

118. Ganta S, Singh A, Rawal Y, *et al.*, 2016, Formulation development of a novel targeted theranostic nanoemulsion of docetaxel to overcome multidrug resistance in ovarian cancer. *Drug Deliv*, 23: 968–980.

https://doi.org/10.3109/10717544.2014.923068

119. Zheng N, Gao Y, Ji H, *et al.*, 2016, Vitamin E derivative-based multifunctional nanoemulsions for overcoming multidrug resistance in cancer. *J Drug Target*, 24: 663–669.

https://doi.org/10.3109/1061186X.2015.1135335

120. Ahmad G, El-Sadda R, Botchkina G, *et al.*, 2017, Nanoemulsion formulation of a novel taxoid DHA-SBT-1214 inhibits prostate cancer stem cell-induced tumor growth. *Cancer Lett*, 406: 71–80.

https://doi.org/10.1016/j.canlet.2017.08.004

121. Bozzuto G, Molinari A, 2015, Liposomes as nanomedical devices. *Int J Nanomedicine*, 10: 975–999.

https://doi.org/10.2147/IJN.S68861

122. Gonda A, Zhao N, Shah J, *et al.*, 2019, Engineering tumor-targeting nanoparticles as vehicles for precision nanomedicine. *Med One*, 4: e190021.

https://doi.org/10.20900/mo.20190021

123. Eloy JO, Petrilli R, Chesca DL, *et al.*, 2017, Anti-HER2 immunoliposomes for co-delivery of paclitaxel and rapamycin for breast cancer therapy. *Eur J Pharm Biopharm*, 115: 159–167.

https://doi.org/10.1016/j.ejpb.2017.02.020

124. Prasad R, Jain NK, Yadav AS, *et al.*, 2020, Liposomal nanotheranostics for multimode targeted *in vivo* bioimaging and near-infrared light mediated cancer therapy. *Commun Biol*, 3: 284.

https://doi.org/10.1038/s42003-020-1016-z

125. Yin W, Zhao Y, Kang X, *et al.*, 2020, BBB-penetrating codelivery liposomes treat brain metastasis of non-small cell lung cancer with $EGFR^{T790M}$ mutation. *Theranostics*, 10: 6122–6135.

https://doi.org/10.7150/thno.42234

126. Gharbavi M, Amani J, Kheiri-Manjili H, *et al.*, 2018, Niosome: A promising nanocarrier for natural drug delivery through blood-brain barrier. *Adv Pharmacol Sci*, 2018: 6847971.

127. Mohamad Saimi NI, Salim N, Ahmad N, *et al.*, 2021, Aerosolized niosome formulation containing gemcitabine and cisplatin for lung cancer treatment: Optimization, characterization and *in vitro* evaluation. *Pharmaceutics*, 13: 59.

https://doi.org/10.3390/pharmaceutics13010059

128. Kulkarni P, Rawtani D, 2019, Application of box-behnken design in the preparation, optimization, and *in vitro* evaluation of self-assembly-based tamoxifen- and doxorubicin-loaded and dual drug-loaded niosomes for combinatorial breast cancer treatment. *J Pharm Sci*, 108: 2643–2653.

https://doi.org/10.1016/j.xphs.2019.03.020

129. Seleci DA, Seleci M, Walter JG, *et al.*, 2016, Niosomes as nanoparticular drug carriers. *J Nanomaterials*, 2016: 7372306.

130. Ruoslahti E, 2012, Peptides as targeting elements and tissue penetration devices for nanoparticles. *Adv Mater*, 24: 3747–3756.

https://doi.org/10.1002/adma.201200454

131. Dahir L, Kajol Kaur A, Manocha A, *et al.*, 2020, Aquasomes: Water like bodies vesicular system for therapeutics molecules as robust system for delivery. *EJMCM*, 7: 2585–2607.

132. Gaikwad SS, Morade YY, Kothule AM, *et al.*, 2023, Overview of phytosomes in treating cancer: Advancement, challenges, and future outlook. *Heliyon*, 9: e16561.

https://doi.org/10.1016/j.heliyon.2023.e16561

133. Azeez NA, Deepa VS, Sivapriya V, 2018, Phytosomes: Emergent promising nano vesicular drug delivery system for targeted tumor therapy. *Adv Nat Sci Nanosci Nanotechnol,* 9: 033001.

134. Dancey JE, 2005, Inhibitors of the mammalian target of rapamycin. *Expert Opin Investig Drugs*, 14: 313–328.

https://doi.org/10.1517/13543784.14.3.313

135. Stark FC, Weeratna RD, Deschatelets L, *et al.*, 2017, An archaeosome-adjuvanted vaccine and checkpoint inhibitor therapy combination significantly enhances protection from murine melanoma. *Vaccines* (*Basel*), 5: 38.

https://doi.org/10.3390/vaccines5040038

136. Lee YK, Lee TS, Song IH, *et al.*, 2015, Inhibition of pulmonary cancer progression by epidermal growth factor receptor-targeted transfection with Bcl-2 and survivin siRNAs. *Cancer Gene Ther*, 22: 335–343.

https://doi.org/10.1038/cgt.2015.18

137. Yang Y, Yang Y, Xie X, *et al.*, 2016, Dual stimulus of hyperthermia and intracellular redox environment triggered release of siRNA for tumor-specific therapy. *Int J Pharm*, 506: 158–173.

https://doi.org/10.1016/j.ijpharm.2016.04.035

138. Karpuz M, Silindir-Gunay M, Ozer AY, *et al.*, 2021, Diagnostic and therapeutic evaluation of folate-targeted paclitaxel and vinorelbine encapsulating theranostic liposomes for non-small cell lung cancer. *Eur J Pharm Sci*, 56: 105576.

https://doi.org/10.1016/j.ejps.2020.105576

139. Tavano L, Mauro L, Naimo GD, *et al.*, 2016, Further evolution of multifunctional niosomes based on pluronic surfactant: Dual active targeting and drug combination properties. *Langmuir*, 32: 8926–8933.

https://doi.org/10.1021/acs.langmuir.6b02063

140. Khan DH, Bashir S, Correia A, *et al.*, 2019, Utilization of

green formulation technique and efficacy estimation on cell line studies for dual anticancer drug therapy with niosomes. *Int J Pharm*, 572: 118764.

https://doi.org/10.1016/j.ijpharm.2019.118764

141. Shaker DS, Shaker MA, Hanafy MS, 2015, Cellular uptake, cytotoxicity and *in-vivo* evaluation of Tamoxifen citrate loaded niosomes. *Int J Pharm*, 493: 285–294.

https://doi.org/10.1016/j.ijpharm.2015.07.041

142. Tan DMY, Fu JY, Wong FS, *et al.*, 2017, Tumor regression and modulation of gene expression via tumor-targeted tocotrienol niosomes. *Nanomedicine* (*Lond*), 20: 2487–2502.

https://doi.org/10.2217/nnm-2017-0182

143. Li Y, Wu H, Jia M, *et al.*, 2014, Therapeutic effect of folate-targeted and PEGylated phytosomes loaded with a mitomycin C-soybean phosphatidyhlcholine complex. *Mol Pharm*, 11: 3017–3026.

https://doi.org/10.1021/mp5001873

144. Alhakamy NA, Badr-Eldin SM, Fahmy UA, *et al.*, 2020, Thymoquinone-loaded soy-phospholipid-based phytosomes exhibit anticancer potential against human lung cancer cells. Pharmaceutics, 2: 761.

https://doi.org/10.3390/pharmaceutics12080761

145. Nazeer AA, Veeraiyan S, Vijaykumar SD, 2017, Anti-cancer potency and sustained release of phytosomal diallyl disulfide containing methanolic allium sativum extract against breast cancer. *Int Res J Pharm*, 8: 34–40.

146. Pasqua L, Leggio A, Sisci D, *et al.*, 2016, Mesoporous silica nanoparticles in cancer therapy: Relevance of the targeting function. *Mini Rev Med Chem*, 16: 743–753.

https://doi.org/10.2174/1389557516666160321113620

147. Tang XL, Jing F, Lin BL, *et al.*, 2018, pH-responsive magnetic mesoporous silica-based nanoplatform for synergistic photodynamic therapy/chemotherapy. *ACS Appl Mater Interfaces*, 10: 15001–15011.

https://doi.org/10.1021/acsami.7b19797

148. Lin G, Mi P, Chu C, *et al.*, 2016, Inorganic nanocarriers overcoming multidrug resistance for cancer theranostics. *Adv Sci* (*Weinh*), 3: 1600134.

https://doi.org/10.1002/advs.201600134

149. Reczyńska K, Marszałek M, Zarzycki A, *et al.*, 2020, Superparamagnetic iron oxide nanoparticles modified with silica layers as potential agents for lung cancer treatment. *Nanomaterials* (*Basel*), 10: 1076.

https://doi.org/10.3390/nano10061076

150. Zhi D, Yang T, Yang J, *et al.*, 2020, Targeting strategies for superparamagnetic iron oxide nanoparticles in cancer therapy. *Acta Biomater*, 102: 13–34.

https://doi.org/10.1016/j.actbio.2019.11.027

151. Wang X, Zhou Z, Wang Z, *et al.*, 2013, Gadolinium embedded iron oxide nanoclusters as T1-T2 dual-modal MRI-visible vectors for safe and efficient siRNA delivery. *Nanoscale*, 5: 8098–8104.

https://doi.org/10.1039/c3nr02797j

152. Jin R, Lin B, Li D, *et al.*, 2014, Superparamagnetic iron oxide nanoparticles for MR imaging and therapy: Design considerations and clinical applications. *Curr Opin Pharmacol*, 18: 18–27.

https://doi.org/10.1016/j.coph.2014.08.002

153. Ock K, Jeon WI, Ganbold EO, *et al.*, 2012, Real-time monitoring of glutathione-triggered thiopurine anticancer drug release in live cells investigated by surface-enhanced Raman scattering. *Anal Chem*, 84: 2172–2178.

https://doi.org/10.1021/ac2024188

154. Lin G, Zhu W, Yang L, *et al.*, 2014, Delivery of siRNA by MRI-visible nanovehicles to overcome drug resistance in MCF-7/ADR human breast cancer cells. *Biomaterials*, 35: 9495–9507.

https://doi.org/10.1016/j.biomaterials.2014.07.049

155. Zhou Z, Huang D, Bao J, *et al.*, 2012, A synergistically enhanced T (1) -T(2) dual-modal contrast agent. *Adv Mater*, 24: 6223–6228.

156. Lee SM, Kim HJ, Kim SY, *et al.*, 2014, Drug-loaded gold plasmonic nanoparticles for treatment of multidrug resistance in cancer. *Biomaterials*, 35: 2272–2282.

https://doi.org/10.1016/j.biomaterials.2013.11.068

157. Liu G, Wang Z, Lu J, *et al.*, 2011, Low molecular weight alkyl-polycation wrapped magnetite nanoparticle clusters as MRI probes for stem cell labeling and *in vivo* imaging. *Biomaterials*, 32: 528–537.

https://doi.org/10.1016/j.biomaterials.2010.08.099

158. Ren Y, Zhang H, Chen B, *et al.*, 2012, Multifunctional magnetic Fe3O4 nanoparticles combined with chemotherapy and hyperthermia to overcome multidrug resistance. *Int J Nanomedicine*, 7: 2261–2269.

https://doi.org/10.2147/IJN.S29357

159. Li JM, Wang YY, Zhao MX, *et al.*, 2011, Multifunctional QD-based co-delivery of siRNA and doxorubicin to HeLa cells for reversal of multidrug resistance and real-time tracking. *Biomaterials*, 33: 2780–2790.

https://doi.org/10.1016/j.biomaterials.2011.12.035

160. Zhang MZ, Li C, Fang BY, *et al.*, 2014, High transfection efficiency of quantum dot-antisense oligonucleotide nanoparticles in cancer cells through dual-receptor synergistic targeting. *Nanotechnology*, 25: 255102.

https://doi.org/10.1088/0957-4484/25/25/255102

161. Wang Y, Yang C, Hu R, *et al.*, 2015, Assembling Mn: ZnSe

quantum dots-siRNA nanoplexes for gene silencing in tumor cells. *Biomater Sci*, 3: 192–202.

162. Wu CH, Cao C, Kim JH, *et al.*, 2012, Trojan-horse nanotube on-command intracellular drug delivery. *Nano Lett*, 12: 5475–5480.

https://doi.org/10.1021/nl301865c

163. Gong H, Peng R, Liu Z, 2013, Carbon nanotubes for biomedical imaging: The recent advances. *Adv Drug Deliv Rev*, 65: 1951–1963.

https://doi.org/10.1016/j.addr.2013.10.002

164. Cheng J, Meziani MJ, Sun YP, *et al.*, 2011, Poly (ethylene glycol)-conjugated multi-walled carbon nanotubes as an efficient drug carrier for overcoming multidrug resistance. *Toxicol Appl Pharmacol*, 250: 184–193.

https://doi.org/10.1016/j.taap.2010.10.012

165. Lee CH, Cheng SH, Wang YJ, *et al.*, 2009, Near-infrared mesoporous silica nanoparticles for optical imaging: Characterization and *in vivo* biodistribution. *Adv Funct Mater*, 19: 215–222.

166. Gao Y, Chen Y, Ji X, *et al.*, 2011, Controlled intracellular release of doxorubicin in multidrug-resistant cancer cells by tuning the shell-pore sizes of mesoporous silica nanoparticles. *ACS Nano*, 5: 9788–9798.

https://doi.org/10.1021/nn2033105

167. Zhao P, Li L, Zhou S, *et al.*, 2018, TPGS functionalized mesoporous silica nanoparticles for anticancer drug delivery to overcome multidrug resistance. *Mater Sci Eng C Mater Biol Appl*, 84: 108–117.

https://doi.org/10.1016/j.msec.2017.11.040

168. Liu J, Wang B, Hartono SB, *et al.*, 2012, Magnetic silica spheres with large nanopores for nucleic acid adsorption and cellular uptake. *Biomaterials*, 33: 970–978.

https://doi.org/10.1016/j.biomaterials.2011.10.001

169. Wu P, Zhao T, Wang S, *et al.*, 2014, Semiconductor quantum dots-based metal ion probes. *Nanoscale*, 6: 43–64.

170. Nifontova G, Ramos GF, Baryshnikova M, *et al.*, 2019, Cancer cell targeting with functionalized quantum dot-encoded polyelectrolyte microcapsules. *Front Chem*, 7: 34.

https://doi.org/10.3389/fchem.2019.00034

171. AbdElhamid AS, Zayed DG, Helmy MW, *et al.*, 2018, Lactoferrin-tagged quantum dots-based theranostic nanocapsules for combined COX-2 inhibitor/herbal therapy of breast cancer. *Nanomedicine* (*Lond*), 13: 2637–2656.

https://doi.org/10.2217/nnm-2018-0196

172. He H, Xie C, Ren J, 2008, Nonbleaching fluorescence of gold nanoparticles and its applications in cancer cell imaging. *Anal Chem*, 80: 5951–5957.

https://doi.org/10.1021/ac8005796

173. Albertini B, Mathieu V, ci N, *et al.*, 2019, Tumor targeting by peptide-decorated gold nanoparticles. *Mol Pharm*, 16: 2430–2444.

https://doi.org/10.1021/acs.molpharmaceut.9b00047

ACCSCIENCE PUBLISHING

Tumor Discovery

REVIEW ARTICLE

Surgical implantation of malignant cells: A review of evidence from 1850 to present day

Ajay Vidyarthi*, Kunal Ranjan, Pritesh Rajeev Singh, Shruti Khemka, and Vinay Venkataramu

Department of Head and Neck Oncology, Mahavir Cancer Sansthan and Research Centre, Patna, Bihar, India

Abstract

Malignant cells, due to decreased cohesion between them, are more likely to exfoliate and implant at distant sites during manipulation. This concern was first expressed by A.G. Gerster in 1885. In this review, we undertook a comprehensive search of the literature to find the evidence for or against the iatrogenic implantation of cancer cells. An exhaustive search on PubMed, Medline, Embase, Science Direct, and Google Scholar yielded 215 relevant publications. The evidence presented in these publications was extracted and synthesized to draw conclusions for this review. Diagnostic and therapeutic procedures through fine/wide bore needles have demonstrated malignant cells in the needle tract but the incidence of recurrences ranges from 0.0003% to 0.9%. There is evidence of malignant cells adhering to surgical instruments, and some reports showed that the number cells needed for successful implantation is 10^6 – 10^7 cells in porcine models. A recent prospective study on colorectal malignancies has shown that the presence of intraperitoneal cells reduced 2-year survival but was not an independent predictor of the outcome. Port site recurrences have been documented since 1978 but the current consensus is more inclined to supporting the improper manipulation of tumor, rather than the laparoscopic procedure itself, as the inducer of port site recurrences. Intraperitoneal morcellation of leiomyomas and leiomyosarcomas does cause intra-peritoneal dissemination of tumor cells. Finally, many approaches to preventing implantation have been explored but lavage of operative site with distilled water may stand as the most promising strategy.

Keywords: Iatrogenic implantation; Malignant cells; Fine needle aspiration; Port site recurrence; Morcellation; Perception and practices

***Corresponding author:**
Ajay Vidyarthi
(ajay.oncosurg@gmail.com)

Citation: Vidyarthi A, Ranjan K, Singh PR, *et al.*, 2023, Surgical implantation of malignant cells: A review of evidence from 1850 to present day. *Tumor Discov*, 2(3): 1411.
https://doi.org/10.36922/td.1411

Received: July 28, 2023
Accepted: November 13, 2023
Published Online: November 30, 2023

1. Introduction

The risk of surgical implantation of malignant cells was first mentioned by A.G. Gerster before the New York Surgical Society in February 1885[1] and first published by L.H. Lack in 1896[2]. He documented a series of 35 cases where implantation was the most probable cause of recurrence. Since then, many similar or relevant case reports have emerged, starting with the report by Jackson, Ney, and Fisher in 1959 to at least four reports on implantation metastasis in organs ranging from colon, rectum, anal canal, and thyroid in 2022. Based on other case reports, implantation metastasis in tracheotomy sites,

laparotomy scars, skin graft donor sites, and laparoscopic port sites was also reported. Implantations have also been reported in craniotomy scars of meningiomas. In light of the accumulating evidence, we aimed to review both past and present literature that supports iatrogenic implantation of malignant cells as the one of the triggers of metastasis. In this review, we considered 109 case reports and may have missed a few others which were published in non-indexed journals. In our clinical practice, we have received complaints for invoking metastasis in these cases due to our careless technique, which prompted us to carry out a search of the literature for evidence on this phenomenon.

2. Methods

A comprehensive search on PubMed, Medline, Embase, Science Direct, and Google Scholar was conducted. The MeSH terms used included "cancer cell implantation," "implantation of malignant cells," "iatrogenic implantation tumor cells," "cancer seeding instruments," "residual tumor cells wash water," "residual tumor cells surgical instruments," "residual tumor cells wounds," and "skin/cutaneous recurrence." Publications published from 1885 to 2022 were targeted in this literature search.

All results were examined for relevance by briefly checking the title of publications. The publications were sorted according to type and year of publication. All relevant publications were selected from the list after a quick review of the abstracts by two authors. Finally, evidence was extracted from the text and synthesized by two other authors. The final manuscript was edited by two authors. This review is prepared and written as per the PRISMA statement for reporting systematic reviews and meta-analyses[3].

3. Results

The search yielded 53,087 results of which 175 seemed relevant. When sorted by date of publication, another 14 were found irrelevant, leaving behind 161 relevant studies. Out of the filtered publications, there were 94 case reports/case series, 22 animal experiment studies, and 13 studies on human subjects. Seven human studies were of prospective nature, seven were retrospective (a few studies included animal experiments and retrospective observation in humans), and one was cross-sectional. There were 16 reviews and one survey. No studies reporting randomized or non-randomized trials were found among the selected publications. A further search of cross-references yielded another 67 studies, of which 12 were irrelevant and one was a duplicate study, leaving behind 54 relevant studies. There were four trials, five prospective and three retrospective studies, eight cross-sectional studies, four animal experiments, two human experiments, 10 case reports/case series, 16 reviews, and two meta-analyses. Figure 1 presents a summary of the above-mentioned results, and Figure 2 summarizes the results from search of cross-references.

4. Discussion

4.1. Modes of iatrogenic implantation

A recurrent growth of cancer cells can be suspected of being iatrogenic when a tumor sharing the same histology as the original cancer occurs at a site distant from the field of intervention or outside the lymphatic basin of the primary tumor. The most probable explanation for this phenomenon is the transfer of cells through surgical supplies, lavage water, *etc.* These recurrences have been reported at sites of tracheostomy and percutaneous gastrostomy in head-and-neck cancers, at graft donor sites in sarcomas, on abdominal incision scars, and at laparoscopic and thoracoscopic port sites. They have also been reported in the needle tract of fine/wide bore needle aspiration sites.

Common modes of implantation of malignant cells in present-day scenario include:

(1) Implantation through surgical instruments and supplies.
(2) Implantation during diagnostic/therapeutic procedures using fine/wide bore needles.
(3) Intraperitoneal and port site implantation.
(4) Implantation due to intraperitoneal morcellation of tumor.

The ensuing review will discuss the history of implantation and the evidence for or against the above modes of implantation, and examine the efficacy of preventive measures.

4.2. History

Charles Ryall[4] first pointed out the danger of implantation of cancers cells and advocated changing of drapes, instruments, *etc.* Cole *et al.*[5] studied suture line recurrence in colorectal cancers after resection and noted that smears taken from the lumen outside the ligature used to isolate the resected segment of colon showed no cells as opposed to smears from inside the ligature. A retrospective study of gastric cancer patients undergoing curative surgery from 1931 to 1957 showed wound recurrence in 1.9% of 569 patients[6]. In addition, Haverback and Smith[7] proved that cancer cells can be transplanted by suture in mouse experiments while tumor cells have been demonstrated to adhere to surgical knives[8]. During this period, many animal experiments have been conducted to demonstrate the implantation of cancer cells as well as several methods of prevention have been introduced. A comprehensive review of the evidence was published by Colin Thomas Jr[9] in 1961. It was found that two to three million Ehrlich's

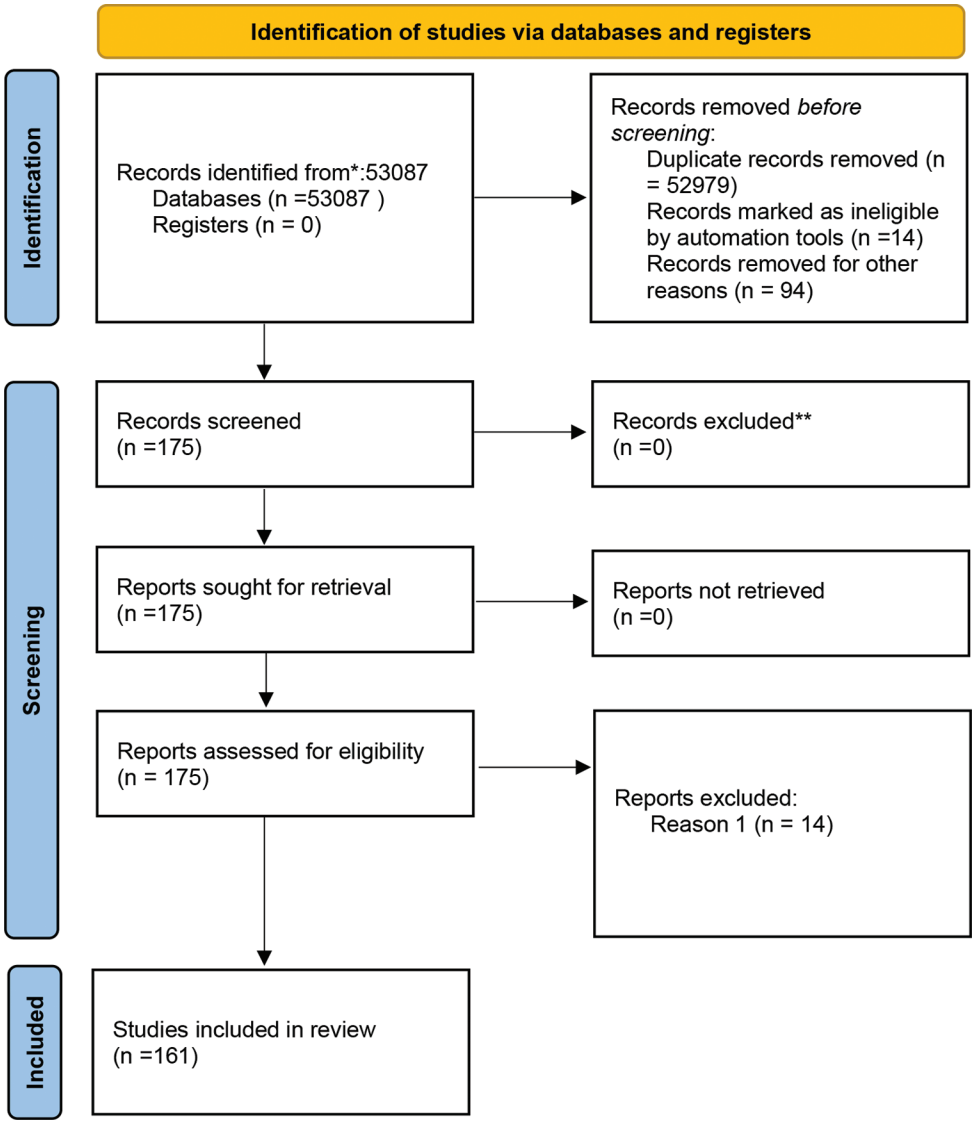

Figure 1. PRISMA flowchart showing identification of studies from database.

ascites tumor cells were needed to cause pulmonary metastasis and 300,000 to 500,000 cells were needed in the case of peritoneal metastasis. Similar findings were published by Southam and Brunshwig[10], who also found that subcutaneous nodules did not resulted following auto-transplantation with an inoculum of less than one million cells in humans.

4.3. Implantation during cytology

Clark *et al.* first reported implantation of malignant cells of the prostate at the site of fine needle aspiration in 1953[11]. This was followed by reports of implantation using Trucut, Vim-Silverman, Moonen, Turkel, 14-gauge needle, and other unspecified needles[12]. In a quantitative study on seeding of melanoma cells in patients with intraocular melanomas using the 30-gauge needle tracts, Glasgow *et al.* compared the number of cells found in needle tracts to the number needed to cause growth of tumors in animal models and found much fewer cells in the needle tracts[12]. In 1998, Mighell and High[13] examined serial sections of resected cancer specimen of six patients known to have undergone fine-needle aspiration of head-and-neck tumors. Needle tract was identified in two of six specimens, and both cases demonstrated tumor cells along the tract. Smith[14] investigated the incidence of needle tract seeding through questionnaires sent to 470 hospitals. He found an incidence of one in 16,381 biopsies, which compared favorably to the results of previous surveys of two in 11,700 biopsies and two in 66,937 biopsies. Risk of implantation during therapeutic and diagnostic procedures on primary

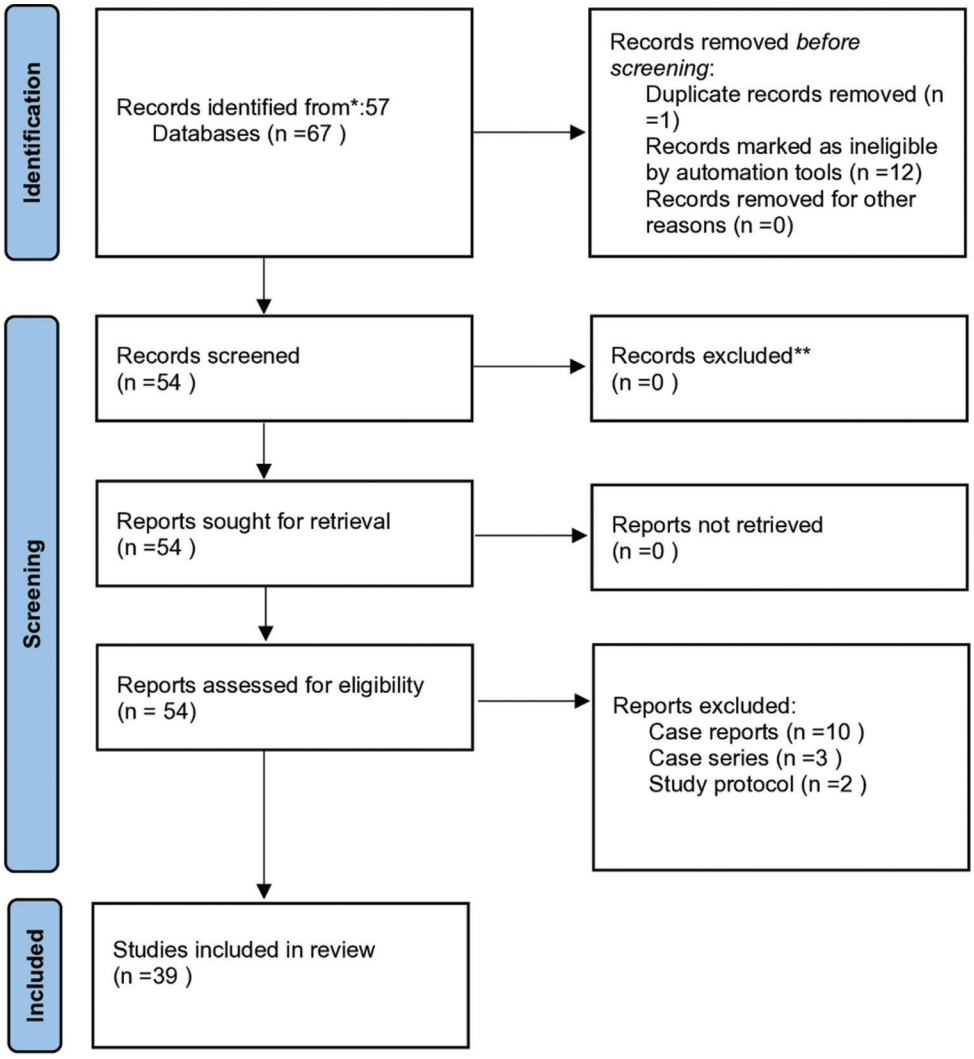

Figure 2. PRISMA flowchart showing identification of studies from cross-references.

liver cancers has been found to be about 0.9% in a large multi-center study[15]. Evidence for the same in metastatic tumors is lacking.

More evidence revolving around tumor cell seeding during needle biopsy in breast cancer is available in the literature. Loughran and Keeling[16] reviewed the evidence and found that tumor cell displacement occurred in 76 out of 352 patients undergoing large core needle biopsy. The incidence of seeding was 42% if the interval between biopsy and examination of tract was <15 days but only 15% if it was 28 days or more. The local recurrence rate in 71% of 313 patients who have been subjected to pre-operative percutaneous biopsies was 11%, but the rate dropped to 3% when radiotherapy was applied but maintained at 34% if the patients were not given radiotherapy.

4.4. Head-and-neck cancers

Smith *et al.*[17] analyzed the smears from the washing of the incision site after radical surgery for cancer in 111 patients, of which 53 had head-and-neck cancers. They investigated if any part of local failure could be explained by cancer seeding on the wound. There was a slight difference in local recurrences between positive and negative smears which did not reach statistical significance ($P \leq 0.07$). Similar studies by Harris and Smith[18] in 69 patients of head-and-neck cancers, analyzed using life-table methods, failed to detect significant differences in local recurrence rates or time to recurrence. Sako *et al.*[19] performed cytological examination of wound washings and wound drainage fluids, collected in 24-h aliquots, for 72 h postoperatively in 60 patients with head-and-neck cancers. At the end of surgery, 15% of patients with negative wound irrigation showed malignant cells in their wound drainage and two

patients developed skin recurrences in the neck during follow-up. The presence of cancer cells in washings from the surgeon's gloves and instruments has been documented by Curran *et al.*[20]. These findings and observations are clear indications that exfoliated cancer cells are present in wound washings, drainage fluid, and washings from surgical gloves and instruments and can implant in the cut surfaces and wounds, thereby causing local and cutaneous failures. However, none of the previous studies have been able to detect a statistically significant association between positive smears and local and distant failures.

Many animal experiments have been conducted to explore methods to prevent the implantation of cancer cells. In each experiment, an aggressively growing tumor strain was used, and about 10,000 – 5,000,000 cells were required for successful implantation in small animals[21-24] while 10^6 – 10^7 cells in porcine models[25]. These figures have been corroborated by different researchers[9,10]. Studies designed to enumerate the viable cells in these washings are hitherto unavailable. To quote Dr. George E. Moore[22], "… if you have a patient with far-advanced carcinoma of the stomach and inoculate him with cells from his own cancer, subcutaneously, they will grow only 10 – 15% of the time."

4.5. Abdominal and peritoneal implantation

In 1952, on the findings of 10.9% recurrence in suture lines in 55 patients of colorectal cancer, Cole[26] reasoned that (i) based on previous evidence, colorectal cancer is susceptible to proximal, rather than distal, lymphatic spread; (ii) surgeons remove about 5 centimeters of bowel proximally and distally so they do not go through the tumor; and (iii) recurrences were found only on end-to-end anastomosis and not if a proximal segment end colostomy has been performed; given these reasonings, the recurrence must have been caused by the implantation of malignant cells originating in the colonic lumen. Fortner *et al.* recorded recurrent tumors in the abdominal wall in 1.9% of gastric carcinomas[6]. The viability of these tumor cells and their ability to leak through an anastomosis and cause local recurrence has been documented in 1984[27] and 1989[24]. A study on exfoliated cells implanted on rats has shown that the cell growth occurred on damaged mucosa but the intact mucosa was completely resistant to implantation[28]. The presence of free peritoneal tumor cells[29] has a positive predictive value of 91% and specificity of 97% for tumor recurrence. A systematic review on free intraperitoneal tumor cells concluded that their presence was a negative prognostic factor in colorectal cancers[30]. Howver, results of the recent EVOCAPE 2[31] multicenter prospective study showed that although 2-year survival was significantly lower in patients with intraperitoneal cancer cells, it was not an independent predictor on multivariate analysis. Probably, the frequency at which these shed tumor cells result in perioperative metastasis is difficult to measure[32].

4.6. Port site metastasis

The first case of port site metastasis was reported in a patient of malignant ovarian ascites[33] and since then whether the laparoscopic procedure or the physical effect of the procedure triggered the metastasis has been a subject of debate. It has been reported following laparoscopic resection of gallbladder, ovarian, gastric, lung, colonic, and other malignancies but the greatest number have occurred after colonic resection (<35)[25]. Port site metastasis in colorectal cancers have been studied in much greater detail than cancers of other sites. It has been found that over a 2-year period the incidence of port site metastasis varies from 0 – 2.3% [25,34]. Two reviews[34,35] list tumor cell spillage, tumor aggressiveness (stage and grade), and pneumoperitoneum as the possible risk factors. Quantitative measurements of residual cancer cells after robotic-assisted radical cystectomy revealed that cancer cells can be found in most pelvic washes and a majority of these patients developed recurrence within 2 – 16 months[36]. A meta-analysis of 1182 subjects demonstrated that the presence of both pre-resection and post-resection tumor cells increased the odds ratio of local and overall recurrence[37]. An investigation into the effect of carbon dioxide pneumoperitoneum in T cell immune-deficient nude mice model revealed no difference in intraperitoneal implantation[38] as compared to gasless laparoscopy. In another experiment comparing pneumoperitoneum, gasless laparoscopy, and laparotomy, the authors found significant differences in total tumor load and growths at omentum and scrotal fat in mice subjected to carbon dioxide pneumoperitoneum[39]. These contradictory results point to the fact that there is no consensus on the etiology of port site recurrence.

Many other theories have been advanced to explain port site metastasis, including "chimney effect" due to leakage of gas along trocars[40], aerosolization of tumor cells, and direct contamination of trocar site by surgical instruments[41]. Often, port site recurrence is detected at the site of specimen retrieval due to tumor spillage[42]. Morcellation of the specimen can also cause intraperitoneal dissemination of cancer[43]. In their review on the etiology of port site recurrences, Whelan and Lee opined that poor surgical technique leading to traumatization of the tumor is the principal cause of the release of substantial number of cells, which is a prerequisite to port site recurrence. As the surgeon gains experience in laparoscopic surgery, his tumor handling improves, decreasing the number of exfoliated malignant cells and the incidence of port site recurrences. The rate of port site recurrences now drops

to match the incidence of abdominal scar recurrences in open colectomy[25].

4.7. Cutaneous metastasis

Cutaneous metastasis of internal malignancy is a rare event with incidence rates ranging from 1.0% to 4.6%[44]. Metastasis usually develops at the umbilicus, in surgical scars, at laparoscopic port sites, and near metastatic lymph nodes. However, the most common source of dermal metastasis in the face and neck is oral cavity cancer[45]. A retrospective study on patients who had been subjected to excision of primary tumor and neck dissection and then developed skin metastasis revealed that previous skin involvement, extracapsular extension of metastatic nodes, and indication for chemotherapy are predictors of dermal metastasis, irrespective of stage[46]. These cutaneous metastasis are painless, solitary, or multiple nodules separate from the overlying epidermis and distinct from direct skin invasion[47]. Other cutaneous metastasis can be divided into metastatic umbilical tumors or Sister Mary Joseph nodules (SJNs) and non-SJN metastasis. The non-SJN metastases are further subdivided into those occurring due to surgery, injury, or lymphadenopathy. In non-SJNs, direct implantation, hematogenous spread, and extranodal extension play a key role. Thereafter, the tumor cells hinge on the factors involved in wound healing and inflammation for proliferation[44]. An unusual case of metastasis of adenocarcinoma of the colon to the skin of the right groin, scrotum, and perineum presenting as erythema, papules, and fake blisters has been reported[48], stating that Koebner phenomena maybe involved.

4.8. Iatrogenic myoma

When uterine leiomyomas ("fibroids") are treated with laparoscopic myomectomy or sub-total hysterectomy, the tumor must be cut into pieces or morcellated to enable extraction. If a power morcellator, which cuts the tumor into cores of 1 cm diameter, is used, there will be intraperitoneal dispersal of microscopic tumor fragments. The first few cases regarding this have been reported in 2003[49] and 2005[50], documenting intraperitoneal dissemination of endometrial tissue visualized by means of post-operative histopathology. Seidman *et al.*[51] investigated 1091 instances of morcellation and found leiomyoma variants or atypical and malignant smooth muscle tumors in 1.2% cases, including endometrial stromal sarcoma, cellular leiomyoma, atypical leiomyoma, smooth muscle tumor of uncertain potential (STUMP), and leiomyosarcoma. Moreover, they documented disseminated disease in 64.3% of all tumors. Nezhat and Kho[52] reviewed reports of parasitic myomas (pedunculated myomas that have lost their attachment to the uterus and become parasitic on surrounding organs), in which eight of 15 reports had been published between 2004 and 2009. Eleven out of 16 patients had a past history of surgery, which involved electric morcellator in six cases and some unspecified form of morcellation in the other five cases. The majority of the parasitic myomas were found in the pelvis but three were located in the upper right quadrant near the liver and gallbladder. Nezhat and Kho also recorded at least five reports of leiomyomatosis peritonealis disseminata (LPD) occurring in association with laparoscopic myomectomy and the use of morcellators. LPD is a rare benign condition characterized by multiple smooth muscle myofibroblastic and fibroblastic nodules on the peritoneal surfaces of pelvic and abdominal cavities on the surface of the uterus, intestines and abdominal walls. Based on the findings of these reports, the parasitic myomas are christened "iatrogenic myomas." The Clinical Practice Guidelines[53] reviewed by Gynecology Guideline Management and Oversight Committees and the Executive of the Society of Gynaecologic Oncology of Canada (GOC) recommend that:

(1) Morcellation is contraindicated in established cancer, pre-cancerous lesions, or suspected cancer.
(2) Patients should be counseled about the risks (malignant and non-malignant), benefits, and alternatives as part of informed consent.
(3) Morcellation should be avoided in hereditary cancer syndromes that predispose to uterine malignancies.

4.9. Present-day beliefs and practices

Early in 1937, an editorial published in *The New England Journal of Medicine* made a mention regarding the search for tumor cells on surgical knives used for the surgery of malignant tumors[8]. This had then been reiterated by Curran *et al.* in 1996[20]. A prospective study of the gloves and instruments used in head-and-neck cancer surgeries found cells in all washings.

Yu *et al.* attempted to study each surgical supply separately in patients undergoing D2 resection for gastric cancers[54]. Surgical supplies were divided into five groups: (i) Surgical instruments; (ii) surgical gloves of the surgeon, first assistant, and second assistant; (iii) surgical gloves and gauze used by the scrub nurse; (iv) gauze used to clear operative field; and (v) stapler devices. The immersion fluid was centrifuged and the precipitate was cultured in 20% bovine fetal serum with 5% carbon dioxide. Although exfoliated cells were found in all five groups of supplies, they were most frequent in the gloves and gauze used by the scrub nurse and the gauze used to clear the operative field. Many authors have recommended that surgical instruments and drapes be changed when moving from one anatomical field to another, *for example*, from site of resection to site of harvest of flap. They also suggested that

the site of resection be thoroughly washed before moving on to reconstruction.

Berger-Richardson *et al.* investigated the beliefs and practices of surgeon regarding glove and instrument changes[55]. They conducted a mailed survey among surgeons registered with the College of Physicians and Surgeons of Ontario to investigate how surgeons handle gloves and instruments used in cancer resection, the strategies used to prevent cancer seeding, and whether they believe gloves and instruments can be vectors for cancer cell seeding. They found that 52% of the respondents had changed gloves and 40% had changed instruments. The most commonly cited reasons for such action were "gut feeling," clinical training, and clinical observation. Only 4% cited evidence as the reason for changing. Surgeons with fellowship training in general surgical oncology or breast were more likely to change gloves and instruments than surgeons trained in site-specific oncology or without training in oncology.

Caudill *et al.* investigated the increased cost stemming from practicing these precautionary measures, which is ultimately passed on to the patients[56]. The authors stated that all these precautionary measures may not be essential because most of the breast reconstruction surgeries target low-stage tumor and there is no convincing evidence that breast cancer cells can successfully circulate, seed or implant in other anatomical areas. Based on a conservative estimate, the patient is expected to bear a "precaution fee" amounting to $1231.83 per surgery.

4.10. Prevention of implantation

Can the implantation of cancer cells be prevented? Is mechanical washing using saline sufficient or is a cytotoxic/cytostatic agent needed? Among the multitude of chemicals tested on animal models were sodium hypochlorite, nitrogen mustard, ethyl alcohol, 5% formaldehyde, thiotepa, *etc.*[5,21-23]. Most authors found nitrogen mustard and formaldehyde to be effective. Nash *et al.*[57] found proflavine hemisulfate to be effective while topical oxaliplatin was also found to prevent port site metastasis[58]. More modern approaches entail the introduction of drug-loaded hydrogels[59] and dehydrated ethanol[60] into the surgical cavity, which have been proven to successfully prevent implantation of cancer cells. Electron therapy, if done within 10 – 15 days of thoracoscopy, has been found to be effective in impeding the implantation of cancer cells in patients with malignant mesothelioma after invasive thoracoscopy[61].

Ito *et al.*[62] investigated the tumoricidal effects of hypo-osmolar distilled water *in vitro* and in mice *in vivo*. The *in vitro* assay showed tumor cell lysis in 15 min and a significant decrease in intraperitoneal tumor volume in mice treated with distilled water. Therefore, the authors concluded that a water lavage, although not curative, may delay peritoneal outgrowth and prolong survival of patient.

The possible role of intraoperative rectal washout has been investigated by Terzi *et al.*[63]. Local recurrence rates were similar in rectal washout and no washout groups, and none of the patients developing local recurrence had malignant cells on the circular stapler. After reviewing the evidence regarding utility of rectal washout and types of washout, Okoshi *et al.*[64] opined that there is insufficient evidence to recommend one washout solution over another or even that a rectal washout is potent enough to decrease the risk for anastomotic recurrence. Nevertheless, a rectal wash does not appear to damage the rectum and may be used before anterior resection.

Schneider *et al.*[65] studied the prevention of port site recurrences in a porcine model and concluded that surgical technique has a major influence on recurrence. These results are in concordance with results of human studies where contamination of instruments and trocars with cancer cells was much higher than contamination of carbon dioxide. Therefore, the measures recommended by Tsivian and Sidi[66] for the prevention of port site recurrence in urologic surgery may be applied to all laparoscopic surgery and are listed below:

(1) Sufficient technical preparation
(2) Avoidance of laparoscopic surgery if ascites is present
(3) Trocar fixation with avoidance of gas leakage along the trocar
(4) Avoidance of tumor boundary violation
(5) Cautious consideration of morcellation
(6) Use of an impermeable bag if morcellation is done
(7) Use of a bag for intact specimen removal
(8) Drainage placement, if needed, before abdomen deflation
(9) Povidone-iodine irrigation of the laparoscopic instruments, trocar, and port site wounds
(10) Suturing of 10-mm trocar wounds

A retrospective study[67] on 446 patients undergoing cytoreduction for ovarian cancer, among which port site excision had been performed to prevent port site recurrence in 82 patients, found no difference in survival between those with port site excision and those without. A higher incidence of wound complications was seen in the excision group. The authors suggested that no port site resection be done in patients without microscopic evidence of port site recurrence.

5. Conclusions

Despite the evidence of cancer cells implantation from the contaminated surgical sutures and knives, successful

implantation may require up to 2 – 3 million cells. The most robust evidence of implantation of tumor cells along needle tracts is in the core biopsy needles from breast cancers, but with a measly incidence rate of implantation measuring at 0.9%. However, fine needle aspirations are considered oncologically safe procedures with very low rates of implantation and tract recurrences. Multiple studies have demonstrated the presence of malignant cells in wound washings and wound drainage fluid but these studies failed to detect a significant increase in local or cutaneous recurrences due to their presence. Although viable intraperitoneal tumor cells have been detected and found to cause intraperitoneal recurrences, the EVOCAPE 2 prospective study failed to establish it as an independent predictor of local recurrence. Laparoscopic surgery of intraperitoneal tumors is generally regarded as one of the factors contributing to port site recurrences, but poor surgical technique leading to excessive tumor handling remains the most probable cause. In addition, peritoneal implantation of benign myomas and accidental leiomyosarcoma has become a clinically known fact; therefore, appropriate precautions must be taken if intraperitoneal morcellation is involved as part of the treatment. At present, lavage of the surgery site with distilled water is the most effective method to prevent the implantation of malignant cells.

Acknowledgments

None.

Funding

None.

Conflict of interest

The authors declare that they have no conflict of interest to declare.

Author contributions

Conceptualization: Ajay Vidyarthi
Writing – original draft: Ajay Vidyarthi, Shruti Khemka, Vinay Venkataramu
Writing – review and editing: Kunal Ranjan, Pritesh Rajeev Singh

Ethics approval and consent to participate

Not applicable.

Consent for publication

Not applicable.

Availability of data

Not applicable.

References

1. Gerster AG, 1885, On the Surgical Dissemination of Cancer. New York: New York Surgical Society. p98–109.
2. Lack LH, 1896, A contribution to the operative treatment of malignant disease of the larynx,with special reference to the danger of cancerous wound infection. *Lancet*, 147: 1638–1641.
3. Moher D, Liberati A, Tetzlaff J, *et al*., 2010, Prefered reporting items for systematic reviews and meta-analyses: The PRISMA statement. *Int J Surg*, 8: 336–341.
   https://doi.org/10.1016/j.ijsu.2010.02.007
4. Ryall C, 1907, Cancer infection and cancer recurrence: A danger to avoid in cancer operations. *Lancet*, 170: 1311–1316.
5. Cole WH, Roberts S, Watne A, *et al*., 1958, The dissemination of cancer cells. *Bull New York Acad Med*, 34(3): 163–183.
6. Fortner JG, Lawrence W, 1960, Implantation of gastric cancer in abdominal wounds. *Ann Surg*, 152(5): 789–794.
   https://doi.org/10.1097/00000658-196011000-00003
7. Haverback CZ, Smith RR, 1959, Transplantation of tumour by suture thread and its prevention: An experimental study. *Cancer*, 12(5): 1029–1042.
   https://doi.org/10.1002/1097-0142(195909/10)12:5<1029::aid-cncr2820120524>3.0.co;2-q
8. The transfer of tumor cells by the surgical knife, 1937, *N Engl J Med*, 216(13): 570.
9. Thomas CGJ, 1961, Tumor cell contamination of the surgical wound: Experimental and clinical observations. *Ann Surg*, 153(5): 697–704.
   https://doi.org/10.1097/00000658-196105000-00008
10. Southam CM, Brunshwig A, 1961, Quantitative studies of autotransplantation of human cancer. *Cancer*, 14: 971–978.
11. Clarke BG, Leadbetter WF, Campbell JS, 1953, Implantation of cancer of the prostate in site of perineal needle biopsy: Report of a case. *J Urol*, 70(6): 937–939.
    https://doi.org/10.1016/S0022-5347(17)68008-X
12. Glasgow BJ, Brown HH, Zargoza AM, *et al*., 1988, Quantitation of tumor seeding from fine needle aspiration of ocular melanomas. *Am J Ophthalmol*, 105(5): 538–546.
    https://doi.org/10.1016/0002-9394(88)90248-6
13. Mighell AJ, High AS, 1998, Histological identification of carcinoma in 21 gauge needle tracks after fine needle aspiration biopsy ofhead and neck carcinoma. *J Clin Pathol*, 51: 241–243.
    https://doi.org/10.1136/jcp.51.3.241
14. Smith EH, 1991, Complications of percutaneous abdominal fine-needle biopsy. *Radiology*, 178(1): 253–258.

https://doi.org/10.1148/radiology.178.1.1984314

15. Livraghi T, Lazzaroni S, Meloni F, *et al*., 2005, Risk of tumour seeding after percutaneous radiofrequency ablation for hepatocellular carcinoma. *Br J Surg*, 92: 856–858.

https://doi.org/10.1002/bjs.4986

16. Loughran CF, Keeling CR, 2011, Seeding of tumour cells following breast biopsy: A literature review. *Br J Radiol*, 84: 869–874.

https://doi.org/10.1259/bjr/77245199

17. Smith RR, Thomas LB, Hilberg AW, 1958, Cancer cell contamination of operative wounds. *Cancer*, 11(1): 53–62.

https://doi.org/10.1002/1097-0142(195801/02)11:1<53::aid-cncr2820110113>3.0.co;2-x

18. Harris AH, Smith RR, 1960, Operative wound seeding with tumor cells: Its role in recurrences of head and neck cancer. *Ann Surg*, 151(3): 330–334.

https://doi.org/10.1097/00000658-196003000-00004

19. Sako K, Marchetta FC, Burke EM, *et al*., 1963, A study of wound drainage fluid for tumor cells as a source of recurrence. *Am J Surg*, 106(5): 797–801.

https://doi.org/10.1016/0002-9610(63)90404-5

20. Curran AJ, Smyth D, Kane B, *et al*., 1996, Exfoliated malignant cells in glove and instrument washings following head and neck surgery. *Clin Otolaryngol Allied Sci*, 21(3): 281–283.

https://doi.org/10.1111/j.1365-2273.1996.tb01742.x

21. McDonald GO, Gines SM, Cole W, 1960, Wound irrigation in cancer surgery. *AMA Arch Surg*, 80: 920–927.

22. Hatiboglu I, Moore GE, Wilkins HJ, *et al*., 1960, Effects of chemotherapeutic agents on wounds contaminated with tumor cells: An experimental study. *Ann Surg*, 152(4): 559–567.

https://doi.org/10.1097/00000658-196010000-00001

23. Thomas CG Jr., Brown BC, 1960, Studies on the prevention of surgical implantation of cancer. *Ann Surg*, 151(4): 581–588.

https://doi.org/10.1097/00000658-196004000-00020

24. O'Dwyer PJ, Martin EW Jr, 1989, Viable intraluminal tumour cells and local/regional tumour growth in experimental colon cancer. *Ann R Coll Surg Engl*, 71: 54–56.

25. Whelan RL, Lee SW, 1999, Review of investigations regarding the etiology of port site tumor recurrence. *J Laparoendosc Adv Surg Tech A*, 9(1): 1–16.

https://doi.org/10.1089/lap.1999.9.1

26. Cole WH, 1952, Recurrence in carcinoma of the colon and proximal rectum following resection for carcinoma. *Arch Surg*, 65(2): 264.

https://doi.org/10.1001/archsurg.1952.01260020277008

27. Umpleby HC, Fermor B, Symes MO, *et al*., 1984, Viability of exfoliated colorectal carcinoma cells. *Br J Surg*, 71(9): 659–663.

https://doi.org/10.1002/bjs.1800710902

28. Hubens G, Lafullarde T, Van Marck E, *et al*., 1994, Implantation of colon cancer cells on intact and damaged colon mucosa and serosa: An experimental study in the rat. *Acta Chir Belg*, 94(5): 258–262.

29. Nekarda H, Geb C, Stark M, *et al*., 1999, Immunocytochemically detected free peritoneal tumour cells (FPTC) are a strong prognostic factor in gastric carcinoma. *Br J Cancer*, 79(3–4): 611–619.

https://doi.org/10.1038/sj.bjc.6690096

30. Mohan HM, O'Connor DB, O'Riordan JM, *et al*., 2013, Prognostic significance of detection of microscopic peritoneal disease in colorectal cancer: A systematic review. *Surg Oncol*, 22(2): e1–e6.

https://doi.org/10.1016/j.suronc.2013.01.001

31. Cotte E, Peyrat P, Piaton E, *et al*., 2013, Lack of prognostic significance of conventional peritoneal cytology in colorectal and gastric cancers: Results of EVOCAPE 2 multicentre prospective study. *Eur J Surg Oncol*, 39(7): 707–714.

https://doi.org/10.1016/j.ejso.2013.03.021

32. Craig DH, Downey C, Basson MD, 2008, SiRNA-mediated reduction of α-actinin-1 inhibits pressure-induced murine tumor cell wound implantation and enhances tumor-free survival. *Neoplasia*, 10(3): 217–222.

https://doi.org/10.1593/neo.07945

33. Döbrönte Z, Wittmann T, Karácsony G, 1978, Rapid development of malignant metastases in the abdominal wall after laparoscopy. *Endoscopy*, 10(02): 127–130.

https://doi.org/10.1055/s-0028-1098280

34. Gao Q, Guo L, Wang B, 2020, The pathogenesis and prevention of port-site metastasis in gynecologic oncology. *Cancer Manag Res*, 12: 9655–9663.

https://doi.org/10.2147/CMAR.S270881

35. Lee BR, Tan BJ, Smith AD, 2005, Laparoscopic port site metastases: Incidence, risk factors, and potential preventive measures. *Urology*, 65(4): 639–644.

https://doi.org/10.1016/j.urology.2004.09.067

36. Wei L, Hussein AA, Ma Y, *et al*., 2019, Accurate quantification of residual cancer cells in pelvic washing reveals association with cancer recurrence following robot-assisted radical cystectomy. *J Urol*, 201(6): 1105–1114.

https://doi.org/10.1097/JU.0000000000000142

37. Rekhraj S, Aziz O, Prabhudesai S, *et al*., 2008, Can intra-operative intraperitoneal free cancer cell detection

techniques identify patients at higher recurrence risk following curative colorectal cancer resection: A meta-analysis. *Ann Surg Oncol*, 15(1): 60–68.

https://doi.org/10.1245/s10434-007-9591-5

38. Lécuru F, Agostini A, Camatte S, *et al*., 2002, Impact of pneumoperitoneum on tumor growth. *Surg Endosc*, 16(8): 1170–1174.

https://doi.org/10.1007/s00464-001-9226-z

39. Bouvy ND, Marquet RL, Jeekel H, *et al*., 1996, Impact of Gas(less) laparoscopy and laparotomy on peritoneal tumor growth and abdominal wall metastases. *Ann Surg*, 224(6): 694–701.

https://doi.org/10.1097/00000658-199612000-00005

40. Ramirez PT, Wolf JK, Levenback C, 2003, Laparoscopic port-site metastases: Etiology and prevention. *Gynecol Oncol*, 91(1): 179–189.

https://doi.org/10.1016/s0090-8258(03)00507-9

41. Rané A, Eng MK, Keeley FX, 2008, Port site metastases. *Curr Opin Urol*, 18(2): 185–189.

https://doi.org/10.1097/MOU.0b013e3282f4ab73

42. Paolucci V, Schaeff B, Schneider M, *et al*., 1999, Tumor seeding following laparoscopy: International survey. *World J Surg*, 23(10): 989–995.

https://doi.org/10.1007/s002689900613

43. Sooriakumaran P, Kommu SS, Anderson C, *et al*., 2009, Port-site metastasis after laparoscopic surgery: What causes them and what can be done to reduce their incidence? *BJU Int*, 103(9): 1150–1153.

https://doi.org/10.1111/j.1464-410X.2009.08363.x

44. Otsuka I, 2019, Cutaneous metastasis after surgery, injury, lymphadenopathy, and peritonitis: Possible mechanisms. *Int J Mol Sci*, 20(13): 3286.

https://doi.org/10.3390/ijms20133286

45. Brownstein MH, Helwig EB, 1972, Patterns of cutaneous metastasis. *Arch Dermatol*, 105(6): 862–868.

https://doi.org/10.1001/archderm.1972.01620090034008

46. Chaitanya SA, Kumar AA, Dalakoti P, *et al*., 2021, Dermal metastases in oral cancer after curative treatment: A single institution cohort study. *Br J Oral Maxillofac Surg*, 59(7): 814–819.

https://doi.org/10.1016/j.bjoms.2021.02.026

47. Pitman KT, Johnson JT, 1999, Skin metastases from head and neck squamous cell carcinoma: Incidence and impact. *Head Neck*, 21(6): 560–565.

https://doi.org/10.1002/(sici)1097-0347(199909)21:6<560::aid-hed10>3.0.co;2-q

48. Yang Y, Chen R, Zhang R, 2020, Cutaneous metastasis of a colon adenocarcinoma presenting as an unusual manifestation: A report of one case. *Int J Clin Exp Pathol*, 13: 1897–1901.

49. Sepilian V, 2003, Iatrogenic endometriosis caused by uterine morcellation during a supracervical hysterectomy. *Obstet Gynecol*, 102(5): 1125–1127.

https://doi.org/10.1016/s0029-7844(03)00683-5

50. LaCoursiere DY, Kennedy J, Hoffman CP, 2005, Retained fragments after total laparoscopic hysterectomy. *J Minim Invasive Gynecol*, 12(1): 67–69.

https://doi.org/10.1016/j.jmig.2004.12.021

51. Seidman MA, Oduyebo T, Muto MG, *et al*., 2012, Peritoneal dissemination complicating morcellation of uterine mesenchymal neoplasms. *PLoS One*, 7(11): e50058.

https://doi.org/10.1371/journal.pone.0050058

52. Nezhat C, Kho K, 2010, Iatrogenic myomas: New class of myomas? *J Minim Invasive Gynecol*, 17(5): 544–550.

https://doi.org/10.1016/j.jmig.2010.04.004

53. Murji A, Scott S, Singh SS, *et al*., 2019, No. 371-morcellation during gynaecologic surgery: Its uses, complications, and risks of unsuspected malignancy. *J Obstet Gynaecol Can*, 41(1): 116–126.

https://doi.org/10.1016/j.jogc.2018.07.016

54. Yu XF, Ma YY, Hu XQ, *et al*., 2014, Analysis of exfoliated gastric carcinoma cells attached on surgical supplies. *Onco Targets Ther*, 7: 1869–1873.

https://doi.org/10.2147/OTT.S66412

55. Berger-Richardson G, Xu RS, Gladdy RA, *et al*., 2018, Glove and instrument changing to prevent tumour seeding in cancer surgery: A survey of surgeons' beliefs and practices. *Curr Oncol*, 25(3): e200–e208.

https://doi.org/10.3747/co.25.3924

56. Caudill AR, Newman A, Davison SP, 2020, Precaution costs: The presumption of breast cancer seeding and its impact on surgical expenditure. *Plast Reconstr Surg Glob Open*, 8: e2903.

https://doi.org/10.1097/GOX.0000000000002903

57. Nash SC, Ketcham AS, Smith RR, 1962, Effect of local irrigation with proflavine hemisulfate on wounds seeded with tumor cells an experimental study. *Ann Surg*, 155(3): 465–471.

https://doi.org/10.1097/00000658-196203000-00023

58. Tai YS, Abente FC, Assalia A, *et al*., 2006, Topical treatment with oxaliplatin for the prevention of port-site metastases in laparoscopic surgery for colorectal cancer. *JSLS*, 10(2): 160–165.

59. Zhuang B, Chen T, Xiao Z, *et al*., 2020, Drug-loaded implantable surgical cavity-adaptive hydrogels for prevention of local tumor recurrence. *Int J Pharm*, 577: 119048.

https://doi.org/10.1016/j.ijpharm.2020.119048

60. Sun J, Zhu Y, Peng Y, *et al*., 2018, Safety and efficacy of dehydrated ethanol soaking of the operative field in the treatment of spontaneous hepatocellular carcinoma rupture. *World J Surg Oncol*, 16(1): 86.

https://doi.org/10.1186/s12957-018-1390-x

61. Boutin C, Rey F, Viallat JR, 1995, Prevention of malignant seeding after invasive diagnostic procedures in patients with pleural mesothelioma. *Chest*, 108(3): 754–758.

https://doi.org/10.1378/chest.108.3.754

62. Ito F, Camoriano M, Seshadri M, *et al*., 2011, Water: A simple solution for tumor spillage. *Ann Surg Oncol*, 18(8): 2357–2263.

https://doi.org/10.1245/s10434-011-1588-4

63. Terzi C, Ünek T, Sağol Ö, *et al*., 2006, Is rectal washout necessary in anterior resection for rectal cancer? A prospective clinical study. *World J Surg*, 30(2): 233–241.

https://doi.org/10.1007/s00268-005-0300-x

64. Okoshi K, Kono E, Tomizawa Y, *et al*., 2020, Can rectal washout reduce anastomotic recurrence after anterior resection for rectal cancer? A review of the literature. *Surg Today*, 50(7): 644–649.

https://doi.org/10.1007/s00595-019-01825-6

65. Schneider C, Jung A, Reymond MA, *et al*., 2001, Efficacy of surgical measures in preventing port-site recurrences in a porcine model. *Surg Endosc*, 15(2): 121–125.

https://doi.org/10.1007/s004640010069

66. Tsivian A, Sidi AA, 2003, Port site metastases in urological laparoscopic surgery. *J Urol*, 169(4): 1213–1218.

https://doi.org/10.1097/01.ju.0000035910.75480.4b

67. Lago V, Gimenez L, Matute L, *et al*., 2019, Port site resection after laparoscopy in advance ovarian cancer surgery: Time to abandon? *Surg Oncol*, 29: 1–6.

https://doi.org/10.1016/j.suronc.2019.01.007

ACCSCIENCE PUBLISHING

Tumor Discovery

ORIGINAL RESEARCH ARTICLE

Early results in the novel use of contrast-enhanced susceptibility-weighted imaging in the assessment of response and progression in desmoid fibromatosis: A pilot study in a specialized cancer institution

Raul F. Valenzuela[†]*, Elvis Duran Sierra[†], Mathew A. Canjirathinkal, Colleen M. Costelloe, John E. Madewell, William A. Murphy Jr., and Behrang Amini

Department of Musculoskeletal Imaging, The University of Texas MD Anderson Cancer Center, Houston, Texas 77030, USA

Abstract

Routine radiologic reporting (RRR) often considers progressive desmoid tumors to have a higher proportion of T2-hyperintense and T1-shortened-enhancing components, while responsive or mature collagenized tumors demonstrate a higher proportion of T2-hypointense-non-enhancing components. We aim to determine the utility of the novel use of contrast-enhanced susceptibility-weighted imaging (CE-SWI) in Desmoid-Tumor treatment response assessment, distinguishing between the T1-shortening-enhancing/T2-hyperintense immature components from the T2-hypointense mature collagenized components. This pilot study included 10 single-lesion extremity desmoid fibromatosis patients undergoing standard-of-care magnetic resonance imaging, including CE-SWI. Three-dimensional (3D) tumor segmentation was performed using MIM software in 48 volumes of interest. Maximum diameter, volume, and modified Choi (mChoi) measurements were computed from CE-SWI and T2-weighted image (T2-WI). Five first-order radiomic features, including mean, skewness, kurtosis, and 10th and 90th percentiles, were calculated using in-house developed software (CARPI-AF). (i) **RECIST Progression:** We observed two cases of progression according to the T2-WI-based Response Evaluation Criteria in Solid Tumors standard (RECIST). Interestingly, CE-SWI-based-volume and CE-SWI-based-mChoi predicted the same assessment 4.5 months earlier than T2-WI-based-RECIST. RRR assessed both cases as progression; (ii) **RECIST Stability:** Out of the eight patients classified as having stable disease by T2-WI-based-RECIST, four discrepant progressions were determined: three patients showed an increase greater than 25% of T2-WI-based-volume, and two patients showed an increase greater than 25% of CE-SWI-based-volume. Moreover, from the RECIST stable group, four discrepant-positive responses were predicted by CE-SWI-based-mChoi (three patients) and T2-WI-based-mChoi (four patients). RRR only assessed one patient as having progressive disease; (iii) **First-Order Radiomics:** CE-SWI detected 23% more 90th-percentile voxels than T2-WI, while T2-WI demonstrated 8.5% more 10th-percentile voxels than CE-SWI. Notably, expected first-order response/progression-related changes in 10th-percentile, 90th-percentile, mean, and skewness were present in 90% of cases. In conclusion, CE-SWI-based-volume and CE-SWI-based-mChoi measurements could

[†]*These authors contributed equally to this work.*

***Corresponding author:**
Raul F. Valenzuela
(rfvalenzuela@mdanderson.org)

Citation: Valenzuela RF, Sierra ED, Canjirathinkal MA, *et al.*, 2023, Early results in the novel use of contrast-enhanced susceptibility-weighted imaging in the assessment of response and progression in desmoid fibromatosis: A pilot study in a specialized cancer institution. *Tumor Discov*, 2(3): 1414. https://doi.org/10.36922/td.1414

Received: July 30, 2023

Accepted: October 10, 2023

Published Online: November 6, 2023

improve the prediction of response/progression in desmoid tumors, enhancing the ability in discriminating between T2*-hypointense-collagenized-mature and T1-shortened-enhancing immature components, respectively, in predominant mature responsive and immature progressive tumors, respectively. RRR is relatively insensitive to volumetric tumor changes before RECIST progression and tends to be better tuned with T2* signal and enhancement changes.

Keywords: Susceptibility weighted imaging; Desmoid fibromatosis; First order radiomics; Modified-Choi

1. Introduction

Desmoid tumors are rare mesenchymal neoplasms composed of a clonal proliferation of fibroblasts and myofibroblasts with intracellular collagen and poorly defined margins[1-4]. These tumors are locally invasive soft-tissue lesions originating in connective tissue and express the intermediate filament vimentin but lack the expression of epithelial markers such as E-cadherin[3].

Spontaneous regressions or prolonged stabilizations occur in about 66% of desmoid cases[2]. Current guidelines recommend intervention on desmoid tumors only in cases of progression, morbidity, or symptoms. There is no consensus on the best therapeutic management of these tumors[5]. Surgery should be avoided because of the difficulties of obtaining negative margins and the high risk of local recurrence[2].

In concordance with published evidence[2,6-8], subjective clinical imaging evaluations often consider progressive desmoid tumors to have a higher proportion of T2-hyperintense and T1-shortened-enhancing components, while responsive or mature collagenized tumors demonstrate a higher proportion of T2-hypointense-non-enhancing components. The increase of T2-hypointense elements is typically considered a sign of positive response irrespective of tumor size[9-13] (Figure 1). In contrast, an increase in the T2-hyperintense and T1-shortened-enhancing components is often seen as a sign of progression that can precede enlargement[10,12-14].

Contrast-enhanced susceptibility-weighted imaging (CE-SWI) is a 3D, high spatial resolution, velocity-corrected gradient echo magnetic resonance imaging (MRI) technique that uses magnitude and filtered-phase information, separately and in combination, to generate images[15-18]. The susceptibility effect from molecules that have paramagnetic (deoxyhemoglobin, ferritin, and hemosiderin), diamagnetic (bone minerals, dystrophic calcifications, and oxyhemoglobin), or ferromagnetic (iron, nickel, and cobalt) properties are demonstrated as areas of signal loss[15,17,18]. While the most common use of CE-SWI is for identifying small amounts of calcium and hemorrhage[18,19], the soft tissue contrast offered by CE-SWI can allow for the characterization of fibrous and cellular components in desmoid fibromatosis.

This study aimed to determine the utility of the novel use of CE-SWI as a single sequence capable of simultaneously characterizing the Immature T2-hyperintense and T1-shortening enhancing and the mature T2-hypointense collagenized components, using volumetric measurements and first-order radiomic features compared against conventional T2-based Response Evaluation Criteria in Solid Tumors (RECIST) version 1.1[20-22] assessments for an improved response assessment in desmoid fibromatosis.

This study provides initial evidence outlining the novel use of CE-SWI as a single MRI sequence capable of providing insight regarding the underlying biological changes of responsive and progressive desmoid tumors using 3D volumetric assessment, allowing improved separation of T2-hypointense mature collagenized tumor from T2-hyperintense, T1-shortened-enhancing, immature, and progressive tumor components.

2. Methods

An Institutional Review Board (IRB)-approved waiver of consent was obtained for this retrospective study, including an initial pilot analysis of 10 single-lesion extremity desmoid fibromatosis patients undergoing standard-of-care MRI examinations in our institution. Diagnostic biopsy and pathologic confirmation of tumor histology were obtained in all cases at diagnosis. The MRI scans included advanced imaging sequences, including diffusion-weighted imaging/apparent diffusion coefficient[23,24], perfusion-weighted imaging with dynamic contrast enhancement (PWI/DCE)[25,26], and CE-SWI, performed between March 2021 and May 2023.

CE-SWI and T2-STIR data were collected from each patient across multiple time points in their treatment. A 3D manual tumor segmentation was performed in 48 volumes of interest (VOIs) by an imaging-specialized research assistant (M.A.C.) and an experienced skeletal radiologist (R.V.) using MIM commercial software (version 7.1.4, MIM Software Inc., Cleveland, USA).

Data obtained from each VOI included maximum diameter, volume, and modified Choi (mChoi) measurements

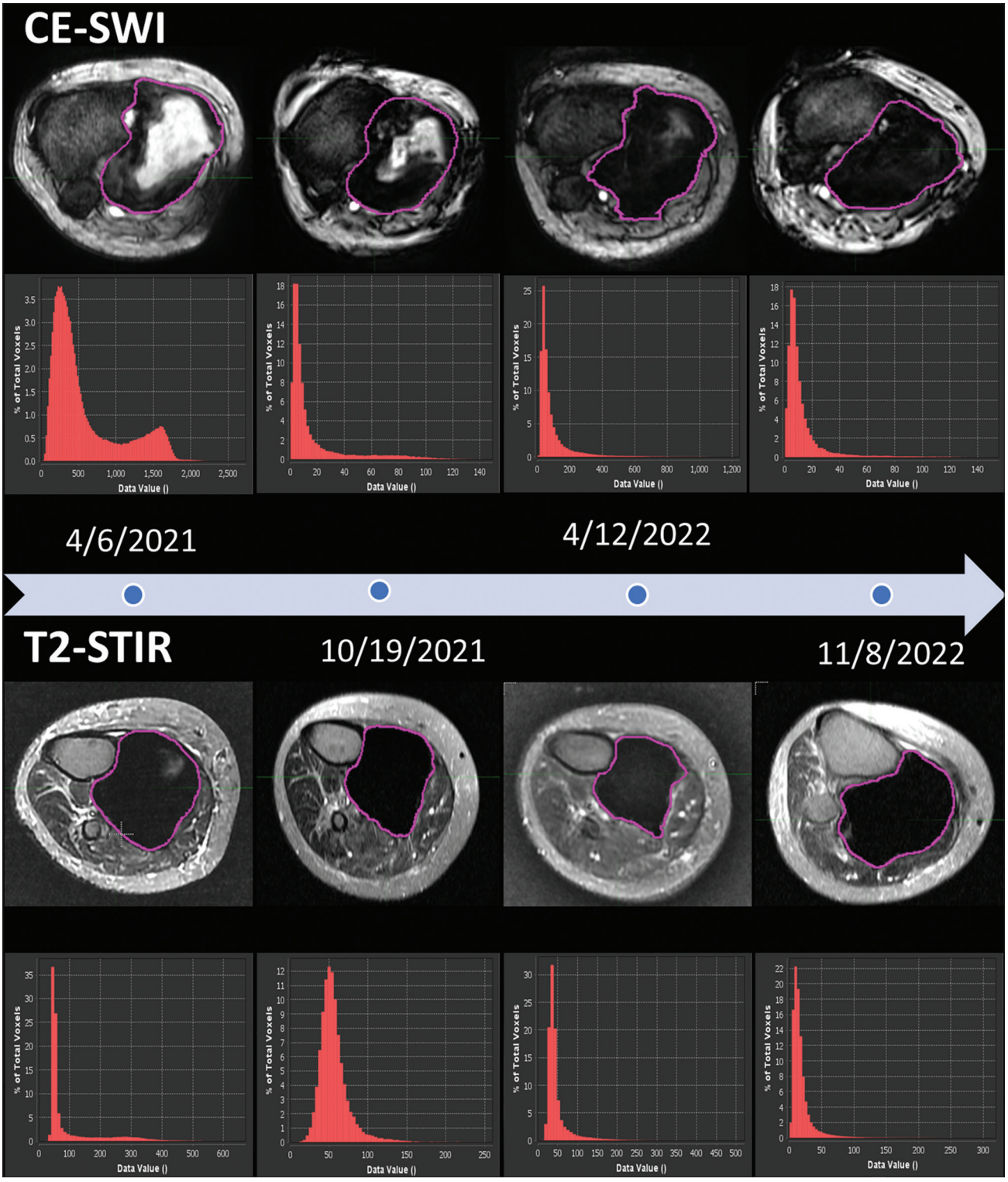

Figure 1. Comparison between contrast-enhanced susceptibility-weighted imaging (CE-SWI) (superior rows) and T2-STIR images (inferior rows) and their corresponding intensity histograms in a patient with desmoid fibromatosis undergoing treatment across 4-time points. The images from left to right demonstrate enhancement reduction and increased T2-hypointensity due to collagenization, as seen in responsive tumors. CE-SWI detected a more significant amount of voxels above the 90th percentile (right side of the histogram) relative to T2, while T2 demonstrated a higher detection of voxels below the 10th percentile (left side of the histogram) than CE-SWI.

from CE-SWI and T2-STIR sequences. mChoi values were estimated as a normalization quotient obtained by dividing an entire desmoid lesion's mean 3D intensity value by the adjacent standard muscle intensity value[6,11,27]. An IBSI-compliant[28,29] open-source in-house developed software (CARPI-AF: Cancer Radiomic and Perfusion Imaging Automated Framework) was used to automatically extract five first-order radiomic features (mean, skewness, kurtosis, 10th and 90th percentiles) from the CE-SWI and T2 images. Before radiomic feature extraction, all images were preprocessed in CARPI-AF by performing interpolation to isotropic voxel spacing of 1 mm using B-spline and discretization using a fixed histogram bin count of 50[30]. Finally, for each patient, the percentage of voxels accumulated below the 10th and above the 90th percentiles (10th and 90th percentile proportions) were computed for the 10th and 90th percentile cutoffs at the first-time point in the patient's treatment.

Patient response was assessed using conventional RECIST as a reference standard and compared against T2-STIR and CE-SWI volumetric assessment, mChoi, first-order radiomic features, and routine radiologic reporting (RRR). Thresholds for progression and response were set at 20% and 30% for unidimensional RECIST and volumetric mChoi assessments[11]. An increase of 25% and a decrease of 50% were considered thresholds for progression and response, respectively, for 3D volumetric assessment[11,31].

3. Results

This study included eight female and two male patients with an average age of 42 years (range 19 – 61 years). Five patients were treated with sorafenib, two with pazopanib, and three were undergoing active surveillance without therapy. Given the reduced pilot study sample size, we did not include an analysis of therapeutic efficacy but focused on the development of imaging biomarkers.

Of the 10 patients, two were considered true progression based on T2-based RECIST, while eight were deemed stable. No true T2-RECIST-based positive responses were included in this pilot study.

3.1. True T2-based RECIST progression

Two patients displayed true progression based on the T2-based RECIST reference standard (Figure 2, left panels). This same result was detected by CE-SWI volume and mChoi at an average of 4.5 months earlier than T2-based RECIST. According to RRR, CE-SWI volume, and mChoi, both cases were assessed as progressive. In

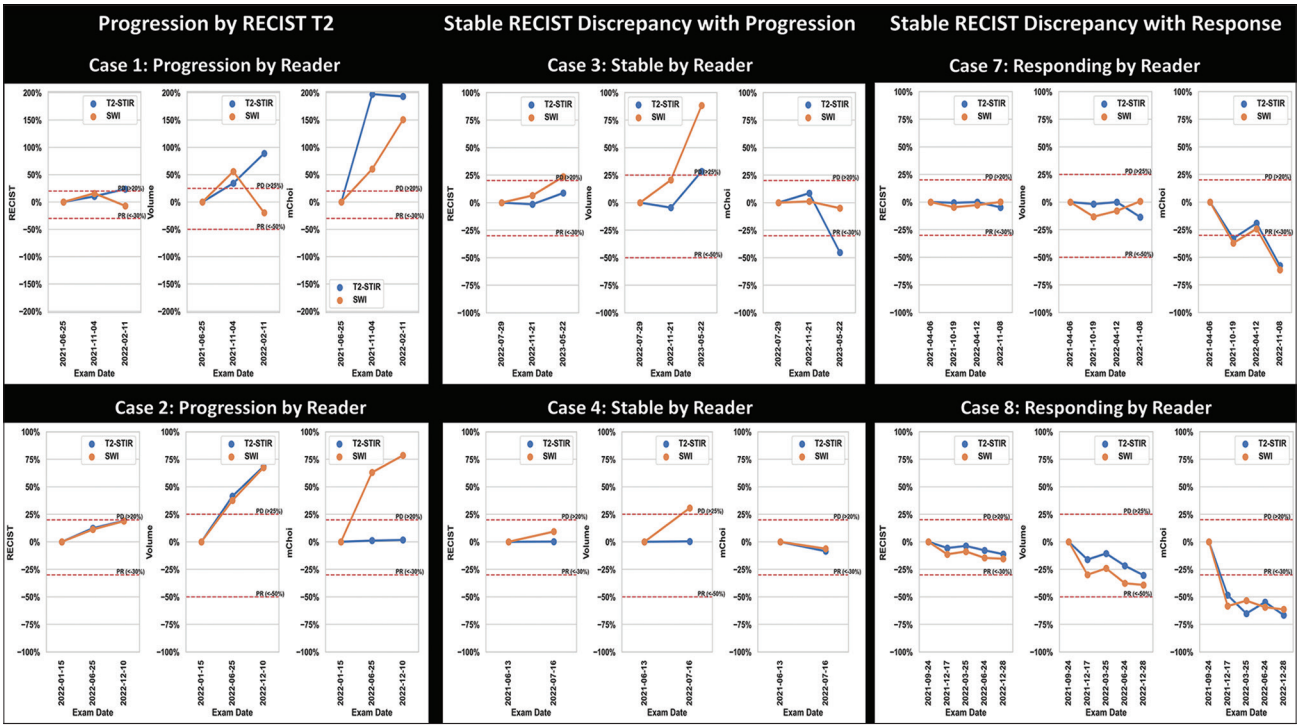

Figure 2. Left panels show true progression by T2-based Response Evaluation Criteria in Solid Tumors (RECIST), also detected by volume and mChoi with an average of 4.5 months earlier. Middle panels show stable RECIST with discrepancy assessment of progression by volume in two representative patients. Clinical radiologists (routine radiologic reporting [RRR]) are often insensitive to detect progression by volume change. Right panels show stable RECIST with discrepancy assessment of response by mChoi in two representative patients. Clinical radiologists (RRR) are very sensitive to changes in T2 signal and enhancement in correlation with the variation of mChoi values.

true progression cases, CE-SWI detected an average of 23% more voxels above the 90th percentile relative to T2, while T2 demonstrated an average of 8.5% more voxels below the 10th percentile than CE-SWI (Figure 3).

3.2. T2-based RECIST stability

3.2.1. RECIST stability with discrepant progression

Based on T2-based RECIST, four patients were determined as stable (Figure 2, middle panels). Progression was determined in these patients by an increase >25% of T2-based volume (in three patients) and CE-SWI-based volume (in two patients). Nevertheless, only one of the four progressive cases was able to be determined by RRR.

3.2.2. RECIST stability with a discrepant positive response

Four patients displayed stable T2-based RECIST with a discrepant positive response (Figure 2, right panels), as predicted by CE-SWI mChoi (in three patients) and T2 mChoi (in four patients). All cases assessed by mChoi as responding patients were also considered positive responses by RRR.

3.2.3. First-order radiomics

The expected trends associated with responding patients (Figure 4), including increasing 10th-percentile hypointense voxel proportion, decreasing 90th -percentile hyperintense voxel proportion, decreasing mean, and increasing skewness, and the opposite trends in progressive disease patients, were present in at least one of these features in 9 out of 10 (90%) patients; all four expected trends were present in 3 out of 10 (30%) patients (Figure 5 and Table 1).

4. Discussion

This pilot study suggests that RRR-based desmoid tumor assessment is relatively insensitive to volumetric tumor changes preceding RECIST progression (Figure 2, middle panels). On the other hand, they tend to be better tuned with changes in T2-hypointensity as a measure of collagenization and with changes in T1-shortening-enhancement as a measure of progressive disease, which are manifested in parallel with the mChoi values, concerning both positive mChoi responses in stable RECIST and to mChoi progression in RECIST progression.

All eight cases of T2-RECIST stability (100%) had a discrepant evaluation of either progression by volume or positive response by mChoi (Figure 2), suggestive of the insensitivity of RECIST to detect the biologic changes displayed by desmoid tumors under systemic treatment or active surveillance.

First-order radiomic trends, including a higher percentage of hyperintense voxel proportion (above the 90th percentile) and earlier detection of progression by mChoi, suggest an

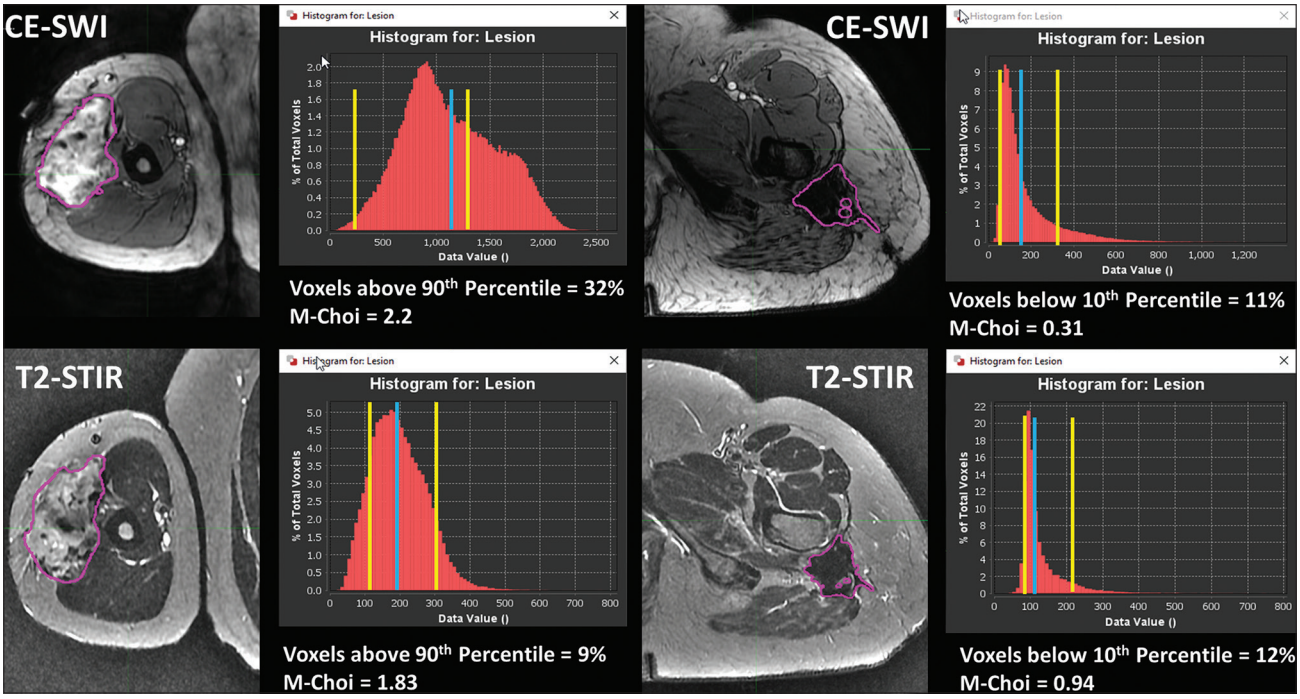

Figure 3. Left panels show a higher percentage of voxels above the 90th percentile in contrast-enhanced susceptibility-weighted imaging (CE-SWI) versus T2-STIR in an actively progressing lesion. Right panels show a higher percentage of voxels below the 10th percentile in T2 versus CE-SWI in a highly collagenized responsive tumor. On average, CE-SWI imaging captures 23% more 90th percentile voxels than T2.

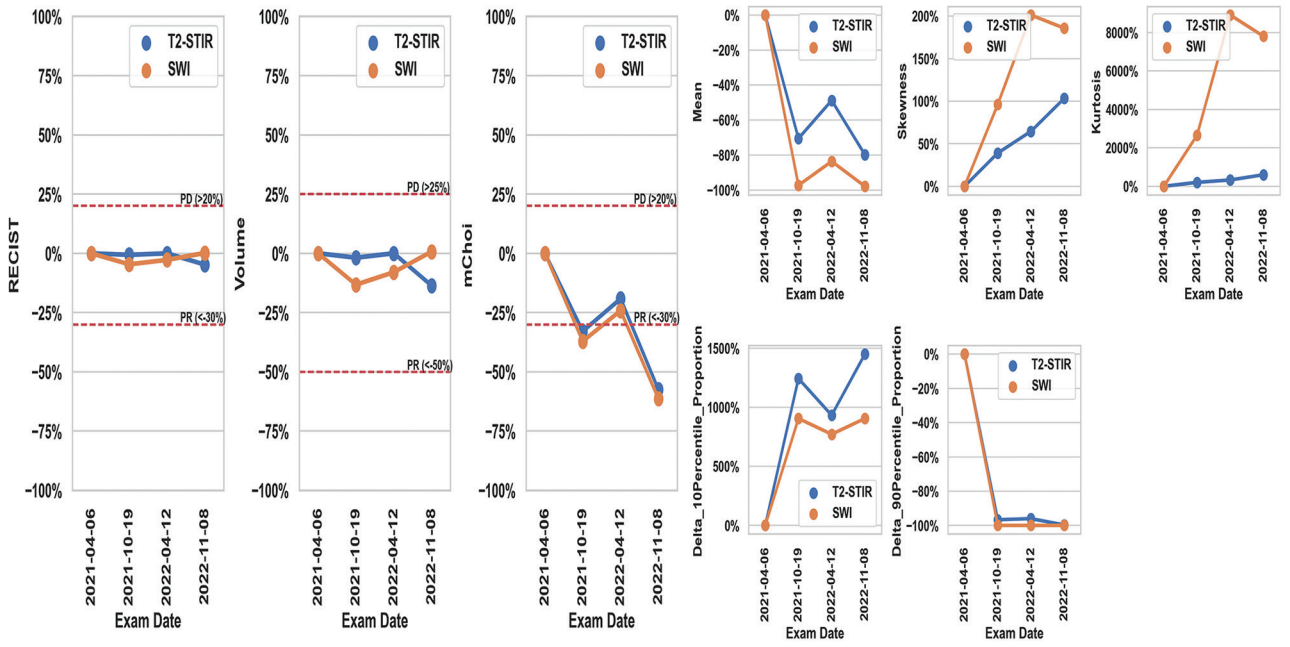

Figure 4. Plots of Response Evaluation Criteria in Solid Tumors, volume, modified Choi, and first-order radiomic features of a representative patient across treatment demonstrate expected response trends, including decreased mean, increased skewness, increased 10th percentile voxel proportion, and decreased 90th percentile voxel proportion.

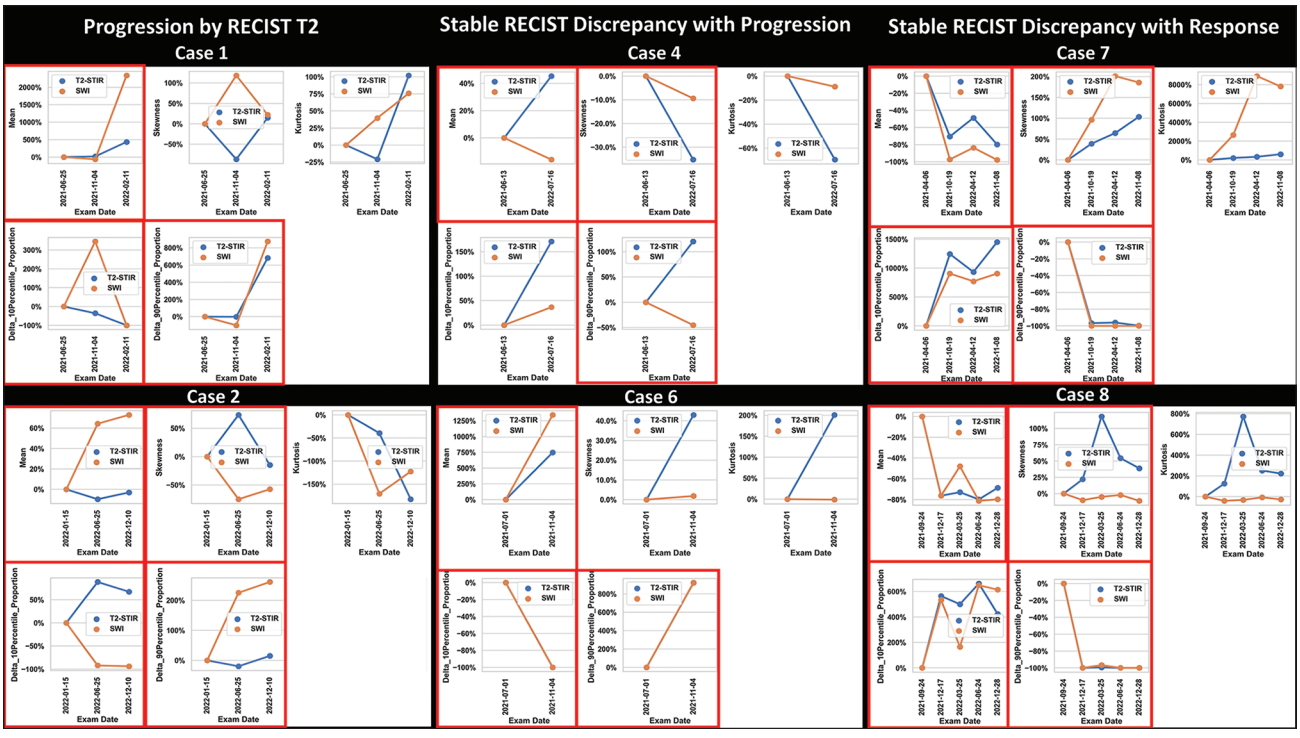

Figure 5. First-order radiomic trends in six representative patients were observed for each of the three response categories (progression by Response Evaluation Criteria in Solid Tumors [RECIST] T2, stable RECIST discrepancy with progression, and stable RECIST discrepancy with response). The red boxes highlight the trends of first-order radiomic features concordant with the expected response trends.

Table 1. Summary of trends in mean, skewness, 10th and 90th percentile proportions in CE-SWI and T2 and their concordance (Y/N) with response category for each of the 10 desmoid fibromatosis patients included in this study

Modality	Progression by RECIST T2				Stable RECIST discrepancy with progression								Stable RECIST discrepancy with response							
	Case 1		Case 2		Case 3		Case 4		Case 6		Case 10		Case 5		Case 7		Case 8		Case 9	
	SWI	T2	SWI	T2	SWI	T2	SWI	T2	SWI	T2	SWI	T2	SWI	T2	SWI	T2	SWI	T2	SWI	T2
Mean	Y	Y	Y	N	N	N	N	Y	Y	Y	N	N	N	N	Y	Y	Y	Y	N	N
Skewness	N	N	Y	Y	N	N	Y	Y	N	N	N	Y	N	N	Y	Y	N	Y	N	Y
10th percentile	Y	Y	Y	N	N	N	N	N	Y	Y	N	Y	N	Y	Y	Y	Y	Y	N	N
90th percentile	Y	Y	Y	Y	N	N	N	Y	Y	Y	N	N	N	N	Y	Y	Y	Y	N	N
Total	3	3	4	2	0	0	1	3	3	3	0	2	0	1	4	4	3	4	0	1

Notes: Y: Yes; N: No; CE-SWI: Contrast-enhanced susceptibility-weighted imaging; RECIST: Response evaluation criteria in solid tumors.

overall performance advantage of CE-SWI volumetric and mChoi assessments over conventional T2-weighted equivalents and traditional RECIST. The observed results align with the statistical power expected from a small sample size, outlining the need for a larger population analysis to extend this pilot study.

5. Conclusion

RRR is relatively insensitive to volumetric tumor changes before RECIST progression and tends to be better tuned with T2* signal and enhancement changes. Our study suggests that the novel use of CE-SWI-based volumetric and mChoi measurements could improve the prediction of response/progression in desmoid tumors by providing a better assessment by means of 3D tumor size measurements and could enhance the discrimination between the mature collagenized component and the enhancing immature components, respectively, predominant in mature responsive and immature progressive disease. In line with these encouraging early results, a larger population study that includes multifocal disease as a disease of interest, enrols RECIST-based positive response cases, and performs treatment efficacy analysis is warranted.

Acknowledgments

None.

Funding

This work was partly supported by M.R. Evelyn Hudson Foundation Endowed Professorship and the John S. Dunn, Sr. Distinguished Chair in Diagnostic Imaging.

Conflict of interest

The authors declare that they have no competing interests.

Author contributions

Conceptualization: Raul Valenzuela, Behrang Amini

Data curation: Elvis Duran Sierra, Mathew A. Canjirathinkal, Behrang Amini

Formal analysis: Raul Valenzuela, Elvis Duran Sierra, Mathew A. Canjirathinkal, Behrang Amini

Funding acquisition: John E. Madewell, William A. Murphy Jr.

Methodology: Raul Valenzuela, Elvis Duran Sierra, Mathew A. Canjirathinkal, Colleen M. Costelloe, John E. Madewell, William A. Murphy Jr.

Writing – original draft: Raul Valenzuela, Elvis Duran Sierra, Colleen M. Costelloe, John E. Madewell, William A. Murphy Jr.

Writing – review and editing: Raul Valenzuela, Elvis Duran Sierra, Colleen M. Costelloe, John E. Madewell, William A. Murphy Jr., Behrang Amini

Ethics approval and consent to participate

An approved waiver of consent was obtained for this retrospective study.

Consent for publication

An IRB granted a waiver of informed consent for this study.

Availability of data

Data can be obtained from corresponding author following formal request.

References

1. Fletcher CD, Unni K, Mertens F, 2002, World Health Organization classification of tumours. In: Pathology and Genetics of Tumours of Soft Tissue and Bone. Lyon, France: IARC press.

2. Crombé A, Kind M, Ray-Coquard I, *et al*., 2020, Progressive desmoid tumor: Radiomics compared with conventional response criteria for predicting progression during systemic therapy-a multicenter study by the French sarcoma group. *AJR Am J Roentgenol*, 215(6): 1539–1548.

https://doi.org/10.2214/AJR.19.22635

3. Wu C, Amini-Nik S, Nadesan P, *et al*., 2010, Aggressive fibromatosis (desmoid tumor) is derived from mesenchymal progenitor cells. *Cancer Res*, 70(19): 7690–7698.

https://doi.org/10.1158/0008-5472.CAN-10-1656

4. Li M, Cordon-Cardo C, Gerald WL, *et al*., 1996, Desmoid fibromatosis is a clonal process. *Hum Pathol*, 27(9): 939–943.

https://doi.org/10.1016/s0046-8177(96)90221-x

5. Cadour F, Tradi F, Bartoli A, *et al*., 2023, Diffusion weighted imaging changes in extra-abdominal desmoid tumor after cryotherapy. *Ann Med*, 55(1): 521–525.

https://doi.org/10.1080/07853890.2023.2174589

6. Sheth PJ, Del Moral S, Wilky BA, *et al*., 2016, Desmoid fibromatosis: MRI features of response to systemic therapy. *Skeletal Radiol*, 45: 1365–1373.

https://doi.org/10.1007/s00256-016-2439-y

7. Shinagare AB, Ramaiya NH, Jagannathan JP, *et al*., 2011, A to Z of desmoid tumors. *AJR Am J Roentgenol*, 197(6): W1008–W1014.

https://doi.org/10.2214/AJR.11.6657

8. Sundaram M, McGuire MH, Schajowicz F, 1987, Soft-tissue masses: Histologic basis for decreased signal (short T2) on T2-weighted MR images. *AJR Am J Roentgenol*, 148(6): 1247–1250.

https://doi.org/10.2214/ajr.148.6.1247

9. Gounder MM, Lefkowitz RA, Keohan ML, *et al*., 2011, Activity of Sorafenib against desmoid tumor/deep fibromatosis. *Clin Cancer Res*, 17(12): 4082–4090.

https://doi.org/10.1158/1078-0432.ccr-10-3322

10. Zanchetta E, Ciniselli C, Bardelli A, *et al*., 2021, Magnetic resonance imaging patterns of tumor response to chemotherapy in desmoid-type fibromatosis. *Cancer Med*, 10(13): 4356–4365.

https://doi.org/10.1002/cam4.3973

11. Subhawong TK, Feister K, Sweet K, *et al*., 2021, MRI volumetrics and image texture analysis in assessing systemic treatment response in extra-abdominal desmoid fibromatosis. *Radiol Imaging Cancer*, 3(4): e210016.

https://doi.org/10.1148/rycan.2021210016

12. Zhou MY, Bui NQ, Charville GW, *et al*., 2022, Current management and recent progress in desmoid tumors. *Cancer Treat Res Commun*, 31: 100562.

https://doi.org/10.1016/j.ctarc.2022.100562

13. Otero S, Moskovic EC, Strauss DC, *et al*., 2015, Desmoid-type fibromatosis. *Clin Radiol*, 70(9): 1038–1045.

https://doi.org/10.1016/j.crad.2015.04.015

14. Cassidy MR, Lefkowitz RA, Long N, *et al*., 2020, Association of MRI T2 signal intensity with desmoid tumor progression during active observation: A retrospective cohort study. *Ann Surg*, 271: 748–755.

https://doi.org/10.1097/SLA.0000000000003073

15. Valenzuela RF, Madewell JE, Kundra V, *et al*., 2021, Advanced imaging in musculoskeletal oncology: Moving away from RECIST and embracing advanced bone and soft tissue tumor imaging (ABASTI)-part II-novel functional imaging techniques. *Semin Ultrasound CT MR*, 42(2): 215–227.

https://doi.org/10.1053/j.sult.2020.08.013

16. Haacke EM, Reichenbach JR, 2014, Susceptibility Weighted Imaging in MRI: Basic Concepts and Clinical Applications. Hoboken: John Wiley and Sons.

17. Halefoglu AM, Yousem DM, 2018, Susceptibility weighted imaging: Clinical applications and future directions. *World J Radiol*, 10(4): 30–45.

https://doi.org/10.4329/wjr.v10.i4.30

18. Haller S, Haacke EM, Thurnher MM, *et al*., 2021, Susceptibility-weighted imaging: Technical essentials and clinical neurologic applications. *Radiology*, 299(1): 3–26.

https://doi.org/10.1148/radiol.2021203071

19. Skalski KA, Kessler AT, Bhatt AA, 2018, Hemorrhagic and non-hemorrhagic causes of signal loss on susceptibility-weighted imaging. *Emerg Radiol*, 25: 691–701.

https://doi.org/10.1007/s10140-018-1634-7

20. Eisenhauer EA, Therasse P, Bogaerts J, *et al*., 2009, New response evaluation criteria in solid tumours: Revised RECIST guideline (version 1.1). *Eur J Cancer*, 45(2): 228–247.

https://doi.org/10.1016/j.ejca.2008.10.026

21. Therasse P, Arbuck SG, Eisenhauer EA, *et al*., 2000, New guidelines to evaluate the response to treatment in solid tumors. European Organization for Research and Treatment of Cancer, National Cancer Institute of the United States, National Cancer Institute of Canada. *J Natl Cancer Inst*, 92(3): 205–216.

https://doi.org/10.1093/jnci/92.3.205

22. Ko CC, Yeh LR, Kuo YT, *et al*., 2021, Imaging biomarkers for evaluating tumor response: RECIST and beyond. *Biomarker Res*, 9(1): 52.

https://doi.org/10.1186/s40364-021-00306-8

23. Koh DM, Collins DJ, 2007, Diffusion-weighted MRI in the body: Applications and challenges in oncology. *AJR Am J Roentgenol*, 188(6): 1622–1635.

https://doi.org/10.2214/AJR.06.1403

24. Messiou C, Collins DJ, Morgan VA, *et al*., 2014, Use of apparent diffusion coefficient as a response biomarker in bone: Effect of developing sclerosis on quantified values. *Skeletal Radiol*, 43(2): 205–208.

https://doi.org/10.1007/s00256-013-1768-3

25. Jahng GH, Li KL, Ostergaard L, *et al*., 2014, Perfusion magnetic resonance imaging: A comprehensive update on principles and techniques. *Korean J Radiol*, 15(5): 554–577.

https://doi.org/10.3348/kjr.2014.15.5.554

26. Essig M, Shiroishi MS, Nguyen TB, *et al*., 2013, Perfusion MRI: The five most frequently asked technical questions. *AJR Am J Roentgenol*, 200(1): 24–34.

https://doi.org/10.2214/AJR.12.9543

27. Stacchiotti S, Collini P, Messina A, *et al*., 2009, High-grade soft-tissue sarcomas: Tumor response assessment--pilot study to assess the correlation between radiologic and pathologic response by using RECIST and Choi criteria. *Radiology*, 251(2): 447–456.

https://doi.org/10.1148/radiol.2512081403

28. Zwanenburg A, Vallières M, Abdalah MA, *et al*., 2020, The image biomarker standardization initiative: Standardized quantitative radiomics for high-throughput image-based phenotyping. *Radiology*, 295(2):328-338.

https://doi.org/10.1148/radiol.2020191145

29. Vallières M, Zwanenburg A, Badic B, *et al.,* 2018, Responsible radiomics research for faster clinical translation. *J Nucl Med*, 59(2):189-193.

https://doi.org/10.2967/jnumed.117.200501

30. Van Timmeren JE, Cester D, Tanadini-Lang S, *et al*., 2020, Radiomics in medical imaging-"how-to" guide and critical reflection. *Insights Imaging*, 11(1): 91.

https://doi.org/10.1186/s13244-020-00887-2

31. Shah GD, Kesari S, Xu R, *et al*., 2006, Comparison of linear and volumetric criteria in assessing tumor response in adult high-grade gliomas. *Neuro Oncol*, 8(1): 38–46.

https://doi.org/10.1215/S1522851705000529

ACCSCIENCE PUBLISHING

Tumor Discovery

CASE REPORT

Pleuropulmonary blastoma in a child masquerading as massive pleural effusion: A case report

Anshuman Darbari[1]*, Ishan Jhalani[1], Meenu Singh[2], Ajay Kumar[3], Khushboo Taneja[2], and Prashant Durgapal[4]

[1]Department of CTVS, AIIMS, Rishikesh, Uttarakhand, India

[2]Department of Pediatric Pulmonology, AIIMS, Rishikesh, Uttarakhand, India

[3]Department of Anaesthesia, AIIMS, Rishikesh, Uttarakhand, India

[4]Department of Pathology, AIIMS, Rishikesh, Uttarakhand, India

Abstract

Pleuropulmonary blastoma (PPB) is a rare dysembryonic lung neoplasm of childhood. Its aggressive nature is demonstrated by its large size and metastasis at the time of diagnosis. Here, we present a case of a 5-year-old male with a history of sudden dyspnea who was initially referred to the primary health-care center for emergency medical services. His initial chest radiography showed massive hydropneumothorax in the right pleural cavity, with gross mediastinal displacement. These clinical findings and rapidly decreasing peripheral saturation prompted the emergency team to insert a right-sided intercostal drainage tube. Initially, this step was able to stabilize the condition, but a subsequent computed tomography scan revealed a vast cystic-solid mass in the right hemithorax. After establishing the diagnosis of PPB by means of histopathology and immunohistochemistry, he was operated on urgently for cytoreductive purposes. Despite the initial macroscopic clearance, the mass recurrence occurred after 3 months, contributing to the ultimate fatal outcome for the patient. Due to the cystic-solid nature of type II/III PPB, it could be masquerading as hydropneumothorax in the initial chest X-ray, a misleading yet the sole initial presentation of this rare entity.

Keywords: Pleuropulmonary blastoma; Lung neoplasm; Pediatric oncology; Thoracic surgery

***Corresponding author:**
Anshuman Darbari
(darbarianshu@gmail.com)

Citation: Darbari A, Jhalani I, Singh M, *et al.*, 2023, Pleuropulmonary blastoma in a child masquerading as massive pleural effusion: A case report. *Tumor Discov*, 2(3): 1756. https://doi.org/10.36922/td.1756

Received: September 4, 2023
Accepted: November 14, 2023
Published Online: November 22, 2023

1. Background

Pleuropulmonary blastoma (PPB) is a rare dysembryonic thoracic tumor of mesenchymal origin in the childhood age group. It was first recognized by Manivel *et al.* in a study of 11 patients in 1988[1]. So far, four types of PBB have been described in the medical literature. Type I PPBs are virtuously cystic tumors that occur in young children of less than 2 years with a median age of 10 months. Type I tumor may progress to type II or III or regress to another type Ir, where "r" stands for regressing (no malignant cells are present). Type II PPBs are a mix of cystic and solid tumors usually occurring at a median

age of 35 months. Type III PPBs are solid tumors usually arising at a median age of 41 months. Type II and type III tumors are very aggressive and tend to recur or metastasize early. The common sites of metastasis are the brain, liver, lymph nodes, pancreas, kidney, and adrenal glands. Type I/Ir PPB has the best prognosis and type III has the least[2].

The clinical presentations of PPB are non-specific; hence, the chances of misdiagnosis are very high, with a poor prognosis. Surgery has been cited as the standard treatment, supplemented with chemotherapy for better curative effect. Surgical resection is usually challenging for various reasons, such as the extent and large size of the tumor, its relation with large vessels and neighboring vital structures in the thorax, and neighboring invasion. In this age group, choosing an incision for proper exposure with maximum lung preservation is also problematic. It is presumed that surveillance of *DICER1* genetic mutation may permit the earlier discovery of PPB, abrogate possible advancement to other types, and improve final outcomes[2,3].

2. Case presentation

A 5-year-old male with severe respiratory distress coupled with peripheral desaturation was referred to the emergency department, and he was initially managed with right-sided intercostal tube drain insertion as an emergency measure based on X-ray findings. After temporary stabilization, he was then referred to our institute. Contrast-enhanced computed tomography (CT) scan showed a sizeable neoplastic cystic-solid mass lesion with necrotic areas occupying the right hemithorax, compressing pericardium and great vessels, and causing the right upper and middle lobe bronchus cut-off with the pleural invasion with severe tracheal and mediastinal shift toward the left side (Figure 1). Based on CT scan findings of cystic-solid nature of the mass, PPB with extraskeletal Ewing's sarcoma, synovial sarcoma, and embryonal rhabdomyosarcoma were suggested as possible differential diagnosis. CT-guided biopsy and immunohistochemistry established the diagnosis as type II/III PPB. Microscopy indicated primitive blastema-like small cells with a high nucleocytoplasmic ratio and a poorly differentiated tumor. On immunohistochemistry, immunoreactivity for vimentin in blastemal areas with focal desmin positivity for rhabdomyoblastic cells was positive but immunonegative for epithelial membrane antigen, S100, and others. A CT scan of the brain was conducted to rule out metastasis. Screening by abdominal ultrasonography did not yield any unusual findings. The patient went into severe hypoxia and shock on the 3rd day after admission while undergoing further investigations, and urgent intubation was performed to revive him.

Due to rapid deterioration, surgical intervention was implemented for the patient after proper consents of his parents were obtained. Under general anesthesia, a clamshell incision with bilateral thoracotomy was made. The cystic-solid tumor resulted in the complete collapse of the right lung due to compression. The tumor abutted the pericardium and large vessels (both vena cavae and azygos vein), and anteriorly crossed the retrosternal space to the opposite side. There was no invasion of the pericardial or left pleural cavity. The left lung was normal. We could dissect the tumor almost to its entire extent after gentle dissection and freeing it from large vessels and the anterior surface of the pericardium. After tumor removal with right lower lobe excision, the upper and middle lobes of the right lung were preserved with complete macroscopic clearance of the thoracic cavity (Figure 2). The excised tumor was around 650 g in weight and approximately 15 × 10 × 9 cm in dimensions (Figure 3). The incision was closed in layers with bilateral intercostal drainage tubes. The excised tumor mass was again sent for detailed histopathological examination using immunohistochemical approach. The histopathology images showed that tumor has primitive blastema-like small cells with hyperchromatic nuclei, high nuclear to cytoplasmic ratio, spindled and ovoid cells, rhabdomyoblastic cells, and nodules of immature chondroid elements along with clusters of large anaplastic cells with pleomorphic nuclei. Areas of necrosis were seen in the myxoid and fibrous stroma in the tumor (Figure 4). The patient was extubated the 2nd day after operation. The

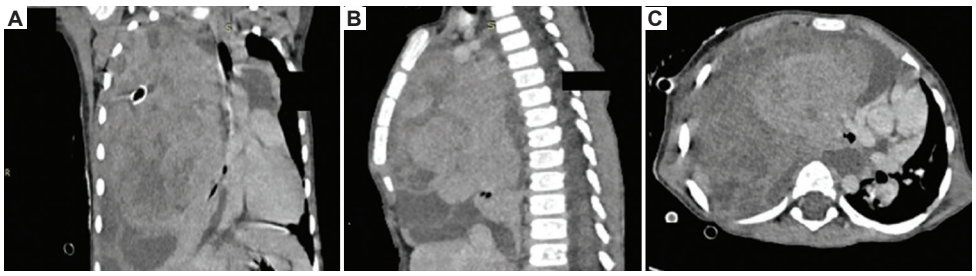

Figure 1. Computed tomography scan of the chest. (A) Coronal view showing right-sided intercostal tube in tumor mass with gross mediastinal shift. (B) Sagittal view showing the right hemithorax cystic-solid tumor. (C) Axial view showing right hemithorax cystic-solid tumor, mediastinal shift with compressed left lung.

left-sided chest tube was removed on the 4th post-operative day, while the right-sided chest tube was removed on the 6th day after expansion of the right lung, and no drainage was performed. Post-operative chest X-ray showed complete expansion of a previously collapsed right lung. A repeat chest CT scan showed clear bilateral lung zones with no evidence of recurrence or metastasis (Figure 4A). The clamshell incision wound was well healed, and the patient was healthy at discharge on the 9th post-operative day. He had been planned for doxorubicin-based chemotherapy treatment and genetic testing of *DICER1*, but his parents and family members were unwilling to send the patient for further testing, intervention, and treatment. After 87 days of surgery, he was sent back to the hospital due to severe respiratory distress with a recurrence of gross mediastinal mass (Figure 4B). In the hospital, we worked with the medical oncology team to stabilize the patient's condition at the time, but to no avail, he succumbed within 2 days of admission.

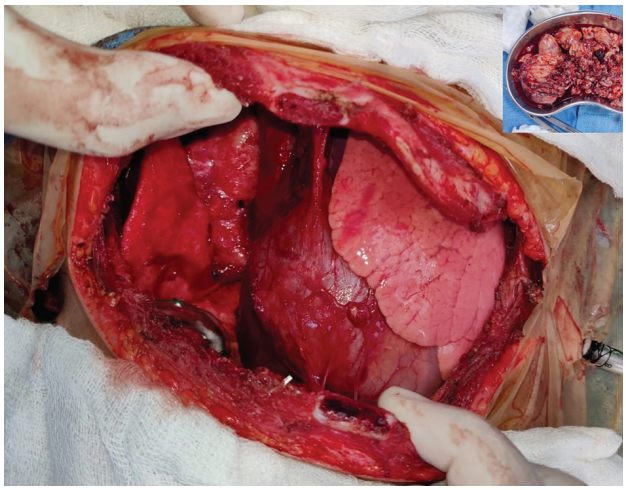

Figure 2. Intraoperative picture showing a healthy left lung, intact pericardium, and compressed right-sided lung upper and middle lobes after tumor removal. The inset shows the resected tumor mass.

3. Discussion

PPB is a rare embryonal thoracic tumor. It is highly aggressive by nature, arising from both lung and pleura, and accounting for 0.5% of all primary malignant lung tumors in the pediatric population. Three types of PBBs have been described in the literature. Type I PBB is purely cystic; type II comprises cystic and solid elements; and type III is exclusively solid. It is solely confined to the pediatric age group, specifically restricted to children under 7 years of age according to most reports[2]. In 2009, a heterozygous germline mutation in *DICER1* was identified as the first identified genetic cause in the majority of documented PPB cases. The *DICER1* gene located on human chromosome 14 instructs cells to make a protein called DICER1, which processes molecules to make microRNA. This germline mutation in *DICER1* can lead to a unique hereditary cancer predisposition syndrome, which is accompanied by PPB, cystic nephroma, ovarian Sertoli-Leydig cell tumors, ciliary body medulloepithelioma, nodular hyperplasia, pituitary blastoma, pineoblastoma, nasal chondromesenchymal hamartoma, and differentiated carcinoma of the thyroid gland. However, a review of 350 confirmed PPB cases by Messinger *et al.* confirmed that there were no clinical differences in terms of germline *DICER1* mutation and thus no distinct prognostic value[3].

Type I tumors (median age at diagnosis: 8 months) have minimal malignant components and are mostly benign. They may change to type II or type III tumors.

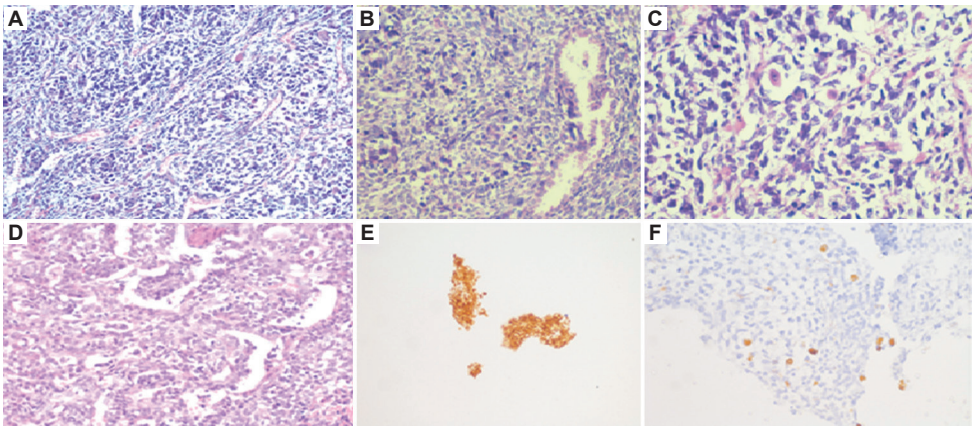

Figure 3. Histopathological findings. (A) Blastemal and sarcomatous cells (hematoxylin-eosin staining, ×400 magnification). (B) Pleomorphic anaplastic cells in sarcomatous areas (hematoxylin-eosin staining, ×400). (C) Rhabdomyoblasts in the blastemal areas (hematoxylin-eosin staining, ×400). (D) Low-grade fetal adenocarcinoma component (hematoxylin-eosin staining, ×400). (E) Tumor cells showing cytoplasmic immunoreactivity for vimentin in blastemal areas (vimentin staining, ×400). (F) Rhabdomyoblasts in tumor cells showing desmin immunoreactivity (desmin staining, ×400).

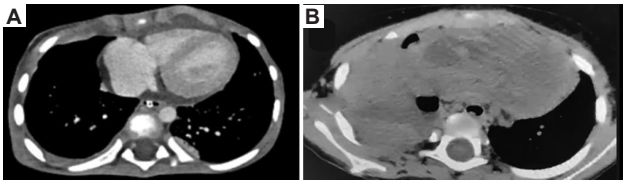

Figure 4. (A) Immediate post-operative computed tomography scan of the chest shows clear bilateral lung fields without residual macroscopic lesion. (B) A computed tomography scan of the chest shows gross local recurrence of mass in the right hemithorax with mediastinal shift at the time of readmission.

Type I (median age at diagnosis 46.5 months) is a subtype that lacks primitive cell components. In the documented registry, most cases of type I and Ir cysts are unilateral (74%), with only 55% larger than 5 cm in size. Type II tumors have cystic and solid areas of blastomatous or sarcomatous components with anaplasia in up to 60% of these cases, with the median age during diagnosis at 35 months, and distant metastases happen in 7% of patients at the time of diagnosis. Type III tumors consist of purely solid components (blastomatous and sarcomatous), with anaplasia occurring in 70% of these cases. The median age at diagnosis of type III tumor is 41 months, and distant metastases reportedly happen in 10% of patients at the time of diagnosis[3,4]. Type II and type III tumors are more metastasizable at early stage and can metastasize to the brain, lungs, and bone, with the brain being the most common site of metastasis[5]. Therefore, pre-operative staging using magnetic resonance imaging or CT scan of the brain, chest, abdomen, and sometimes, a bone scan, is strongly recommended[6]. A study by Priest *et al.* documented an overall survival rate of 45% at 5 years with an event-free survival rate of 49% at 2 years among PBB patients[7]. Type II and type III PPBs manifest aggressive behavior, with 2-year and 5-year overall survival rates of 62% and 42%, respectively, despite multimodal therapy.

Due to gross enlargement, these masses usually cause compression of vital structures in the mediastinum. In some patients with severe respiratory distress, a needle decompression can be performed or a chest tube can be inserted as a lifesaving procedure. However, chest tube placement is not favored due to possible contamination of the pleura, which might result in tumor upstaging and increase the risk for *en bloc* resection[8]. Although three treatment modalities (surgery, chemotherapy, and radiotherapy) have been tested for their efficacy in treating PBB, no clear consensus can be drawn due to the rarity, peculiarity and late presentation of the tumor.

Complete surgical resection is cited as the standard management strategy for type I tumors because it delivers good patient outcomes. For type II and type III, surgery is favored for debulking and macroscopic clearance. This technique is usually narrowed down to non-anatomical or wedge resection, lobectomy or pneumonectomy, and removal of infiltrated structures such as pericardium, diaphragm, or parietal pleura. In general speaking, gross surgical resection of the tumors may improve survival of the patients. Aggressive mediastinal dissection should be weighed against surgical morbidity and mortality[9,10]. In type II and type III PPBs, chemotherapy is mandatory for maximizing the chance of curing the patients. If metastatic disease is present, neoadjuvant chemotherapy should always be included in the treatment regimen, and doxorubicin is an important agent for type II and type III PPB. Multidrug regimens for rhabdomyosarcoma, such as ifosfamide-vincristine, actinomycin D (IVA), and IVA with doxorubicin (IVADo) or cyclophosphamide for replacing ifosfamide, can been considered for treatment, but curative evidence and optimal duration of chemotherapy have not been established. Radiotherapy has a minimal impact on this tumor. The significant international effort promoted by the EXPeRT/PARTNER group proposed possible overall strategies to treat patients with PBB. However, more corroborative evidence is needed to answer some open questions.

Prognosis is determined mainly based on the type of tumor, resection margin, metastasis, and post-operative adjuvant chemotherapy[11]. A recent report by Duc *et al.* showed that despite tumoral resection and chemotherapy, local recurrence and spinal metastasis still occurred in a 2-year-old girl with type III PPB after 5 months of treatment[12], indicating the challenges in the treatment and control of PBB. It is recommended that treatment plan should be personalized according to the specific conditions of each patient after multidisciplinary tumor board discussion since the standard consensus and guidelines surrounding the treatment of PBB are evolving[13].

4. Conclusion

The initial chest X-ray findings may misconstrue type II and type III PPB as hydropneumothorax due to the cystic-solid nature of these subtypes, and this may be the sole initial presentation of this rare entity as in our case. Further, after establishing the diagnosis, cytoreductive surgery was performed with the primary goal of complete removal of all macroscopic disease, but the patient succumbed to death due to the rapid local recurrence within a short duration, possibly caused by the lack of chemotherapy not administered in this case. Hence, multimodality treatment should always be considered for more prolonged survival in advanced cases of PPB.

Acknowledgments

None.

Funding

None.

Conflict of interest

The authors declare that they have no conflict of interest and no competing interests.

Author contributions

Conceptualization: Anshuman Darbari, Ishan Jhalani, Meenu Singh
Investigation: Khushboo Taneja
Writing – original draft: Ishan Jhalani
Writing – review & editing: Anshuman Darbari, Ajay Kumar, Prashant Durgapal,

Ethics approval and consent to participate

This case report study has been approved by the institute Ethical Committee (IEC) of All India Institute of Medical Sciences, Rishikesh, India (DHR Regn no.-EC/NEW/Inst./2022/UA/0180, Letter no.: AIIMS/IEC/23/251).

Consent for publication

Written informed consent was obtained from the patient's guardian (father) for this report publication.

Availability of data

Data can be obtained from the corresponding author upon reasonable request.

References

1. Manivel JC, Priest JR, Watterson J, *et al*., 1988, Pleuropulmonary blastoma. The socalled pulmonary blastoma of childhood. *Cancer*, 62: 1516–1526.

   https://doi.org/10.1002/1097-0142(19881015)62:8<1516::AID-CNCR2820620812>3.0.CO;2-3

2. PDQ Pediatric Treatment Editorial Board, 2002, Childhood pleuropulmonary blastoma treatment (PDQ®): Health professional version. In: PDQ Cancer Information Summaries. Bethesda, MD: National Cancer Institute US.

3. Messinger YH, Stewart DR, Priest JR, *et al*., 2015, Pleuropulmonary blastoma: A report on 350 central pathology-confirmed pleuropulmonary blastoma cases by the international pleuropulmonary blastoma registry. *Cancer*, 121: 276–285.

   https://doi.org/10.1002/cncr.29032

4. Zhang N, Zeng Q, Ma X, *et al*., 2020, Diagnosis and treatment of pleuropulmonary blastoma in children: A single-center report of 41 cases. *J Pediatr Surg*, 55: 1351–1355.

   https://doi.org/10.1016/j.jpedsurg.2019.06.009

5. Nakano Y, Gatell SP, Schultz KA, *et al*., 2019, Successful treatment of metastatic cerebral recurrence of pleuropulmonary blastoma. *Pediatr Blood Cancer*, 66: e27628.

   https://doi.org/10.1002/pbc.27628

6. Gbande P, Abukeshek T, Bensari F, *et al*., 2021, Pleuropulmonary blastoma, a rare entity in childhood. *BJR Case Rep*, 7: 20200206.

   https://doi.org/10.1259/bjrcr.20200206

7. Priest JR, McDermott MB, Bhatia S, *et al*., 1997, Pleuropulmonary blastoma: A clinicopathologic study of 50 cases. *Cancer*, 80: 147–161.

8. Zamora AK, Zobel MJ, Ourshalimian S, *et al*., 2020, The effect of gross total resection on patients with pleuropulmonary blastoma. *J Surg Res*, 253: 115–120.

   https://doi.org/10.1016/j.jss.2020.03.019

9. Wang F, Zhuang L, Liang J, *et al*., 2022, Treatment and prognosis of pleuropulmonary blastoma: A single-center report of 31 cases. *Pediatr Pulmonol*, 57: 2237–2243.

   https://doi.org/10.1002/ppul.25930

10. Grigoletto V, Tagarelli A, Sparber-Sauer M, *et al*., 2020, Inequalities in diagnosis and registration of pediatric very rare tumors: A European study on pleuropulmonary blastoma. *Eur J Pediatr*, 179: 749–756.

    https://doi.org/10.1007/s00431-019-03566-7

11. Bisogno G, Sarnacki S, Stachowicz-Stencel T, *et al*., 2021, Pleuropulmonary blastoma in children and adolescents: The expert/partner diagnostic and therapeutic recommendations. *Pediatr Blood Cancer*, 68(Suppl 4): e29045.

    https://doi.org/10.1002/pbc.29045

12. Duc LA, Vu LT, Ngoc DV, T, *et al*., 2021, Pleuropulmonary blastoma (type III) in a two-year-old: A case report. *Radiol Case Rep*, 16: 2978–2980.

    https://doi.org/10.1016/j.radcr.2021.07.024

13. Mlika M, Anjum F, El Mezni F, 2023, Pleuropulmonary blastoma. In: StatPearls. Treasure Island, FL: StatPearls Publishing. Available from: https://www.ncbi.nlm.nih.gov/books/nbk534211 [Last accessed on 2023 Apr 27].

ACCSCIENCE PUBLISHING

Tumor Discovery

CASE REPORT

A rare clinical observation of ureteral IgG4-related disease in urological practice: A case report

Ekaterina Anikanova[1,2]*, Daniel Yagudaev[1,3], Konstantin Firsov[1,3], Nina Kalyagina[4,5]*, and Arina Plotnikova[5]

[1]Department of Urology and Oncology, Central Clinical Hospital "Russian Railways-Medicine," Moscow, Russia

[2]Department of Oncology and Radiology, Medical Faculty, A.I. Evdokimov Moscow State University of Medicine and Dentistry, Moscow, Russia

[3]Department of Endoscopic Urology, Faculty of Further Education, the Peoples' Friendship University of Russia, Moscow, Russia

[4]Prokhorov General Physics Institute of the Russian Academy of Sciences, Moscow, Russia

[5]Engineering Physics Institute of Biomedicine, National Research Nuclear University MEPhI, Moscow, Russia

Abstract

IgG4-related disease (IgG4-RD) is a systemic immune-dependent pathology marked by infiltration of lymphocytes and plasma cells expressing IgG4 in affected tissues, leading to phlebitis and fibrosclerosis. In urological practice, diagnosing IgG4-RD of the ureter, which may resemble a malignant tumor, presents challenges. We present a unique case: a 64-year-old patient (Patient P.) experienced left lumbar discomfort and a 4 kg weight loss over 2 months. A computed tomography scan revealed a 111 mm tumor obstructing the left ureter, causing hydronephrosis and regional lymphadenopathy. Suspecting ureteral urothelial cancer, the patient underwent a left nephroureterectomy with lymphadenectomy. Microscopic analysis revealed fibrosis and inflammation infiltration (lymphocytes, plasma cells, and eosinophils) in the ureter wall, with no evidence of tumor growth. Immunohistochemistry confirmed IgG4-positive plasma cells. Serum IgG4 rose to 149 mg/dL. Morphological findings led to a diagnosis of IgG4-RD of the ureter. Clinically, it is crucial to recognize IgG4-RD in ureteral neoplasms for early detection, to prevent unnecessary surgical intervention.

Keywords: IgG4-related diseases; IgG4; Ureter; Pseudotumor inflammation; Urothelial cancer

***Corresponding authors:**
Ekaterina Anikanova (Anikanova1801@gmail.com)
Nina Kalyagina (Nina.Kalyagina@gmail.com)

Citation: Anikanova E, Yagudaev D, Firsov K, *et al.*, 2023, A rare clinical observation of ureteral IgG4-related disease in urological practice: A case report. *Tumor Discov*, 2(3): 1766. https://doi.org/10.36922/td.1766

Received: September 5, 2023
Accepted: November 13, 2023
Published Online: November 24, 2023

1. Introduction

IgG4-related disease (IgG4-RD) is a systemic immune-mediated pathology characterized by diffuse or focal infiltration of affected tissues by lymphocytes and plasma cells expressing IgG4, with the absence of neutrophils (a moderate amount of eosinophils may be present). Subsequently, the condition leads to the development of phlebitis and fibrosclerosis, accompanied by an increase in IgG4 content in serum, serving as a laboratory sign[1-3].

Currently, IgG4-RD is defined by systemic involvement, IgG4-association, and common morphological manifestations, including lymphoplasmacytic infiltration and fibrosis. In 2003, a Japanese research group made a pivotal discovery, establishing IgG4-RD as an independent disease with a diverse array of clinical and morphological expressions. These expressions were previously regarded as distinct diseases[4].

In 2011, diagnostic criteria and a three-level classification for IgG4-RD were proposed for the first time[5]. The following criteria are considered essential: (i) The clinical presentation comprises local or multiple lesions with tumor-like inflammatory infiltration of focal or diffuse nature; (ii) the serum IgG4 concentration is elevated above 135 mg/dL; (iii) a histopathological examination reveals lymphoplasmacytic infiltration with fibrosis and obliterative phlebitis and infiltration of IgG4-positive cells (with more than 10 cells visible in the field of view at 400× magnification and a ratio of IgG4/IgG-plasma cells exceeding 40%). To establish a reliable diagnosis of IgG4-RD, it is necessary to combine clinical criteria with laboratory and histological studies. The presence of clinical and histological criteria indicates a probable IgG4-RD, while a combination of clinical and laboratory criteria indicate a possible IgG4-RD. In 2012, the first international nomenclature for this disease was proposed[6].

IgG4-RD affects various organs. Currently, IgG4-RD has been described in the pancreas, biliary tract, liver, stomach, fiber of the retroperitoneal space, mammary, lacrimal and salivary glands, prostate and thyroid glands, and skin[7-9].

Within the urinary system, IgG4-RD is infrequently observed, with a higher prevalence noted in the kidneys and bladder[10,11], while occurrences of ureteral lesions are primarily documented through isolated observations[12,13]. Given that IgG4-RD has only recently been classified as an independent disease, ureteral lesions displaying typical clinical and morphological characteristics were previously labeled as "inflammatory pseudotumor" or "idiopathic segmental ureteritis." The first description of such a lesion dates back to 1978 when Bissada and Finkbeiner first published their findings[14].

The clinical manifestations of IgG4-RD are non-specific, posing difficulties in the differential diagnosis process. This difficulty extends to distinguishing IgG4-RD from various infectious, inflammatory diseases, and tumors. The complexity of differentiation contributes to prolonged periods from the onset of initial clinical manifestations to a definitive diagnosis, leading to the potential adoption of incorrect treatment approaches for affected individuals.

The non-specific clinical manifestations of IgG4-RD present a considerable obstacle in achieving an accurate differential diagnosis, given the potential overlap with infectious, inflammatory, and neoplastic conditions. This overlap often results in delayed diagnosis and the implementation of inappropriate treatment plans for affected individuals.

Here, we present a clinical case of IgG4-RD affecting the ureter, initially misinterpreted as urothelial carcinoma and leading to surgical intervention in the patient.

2. Case presentation

Patient P., a 64-year-old individual, sought medical attention at the hospital, presenting complaints of left lumbar region pain and a weight loss of 4 kg over a 2-month period. A hypervascular tumor, exhibiting a circular shape, was identified during computed tomography (CT) imaging of the abdominal cavity and small pelvis. The tumor was located at the junction of the middle and lower thirds of the left ureter, causing lumen stenosis, with a length measuring 111 mm. Extending into the ureteral wall up to 8 mm, the tumor resulted in hydronephrosis on the left side. Further examination revealed an expansion of the upper third of the ureter to 18 mm, and the pelvis of the left kidney measured 27 mm. Additionally, external iliac lymph nodes on the left exhibited enlargement, measuring up to 18 mm in diameter, while obturator nodes reached up to 13 mm (Figure 1A and B).

The patient underwent an ureteroscopy, during which a circular constriction of the ureter to 2/3 of its lumen was observed at the border of the lower and middle sections of the left ureter. This constriction resulted from the proliferation of whitish tissue covered with fibrin. The shaft of the instrument was passed above the constriction to determine the dilatation of the ureter. The length of the constriction was approximately 100 mm. A biopsy was taken from the affected segment of the ureter. Microscopic examination of the biopsy revealed small fragments of the ureteral wall with induced changes, partially covered with urothelium. The composition consisted of fibrous tissue with plethoric vessels and diffused focal lymphoplasmacytic infiltration, including an admixture of histiocytes and eosinophils. Notably, no conclusive signs of tumor growth were identified within the examined tissue (Figure S1).

Laboratory tests revealed a decrease in blood hemoglobin to 110 g/L, erythrocyte values to 3.39 million/μL, and an increase in blood creatinine to 131 μmol/L and urea to 7.1 mmol/L.

The clinical and radiological findings did not permit the exclusion of a malignant neoplasm of the ureter in the

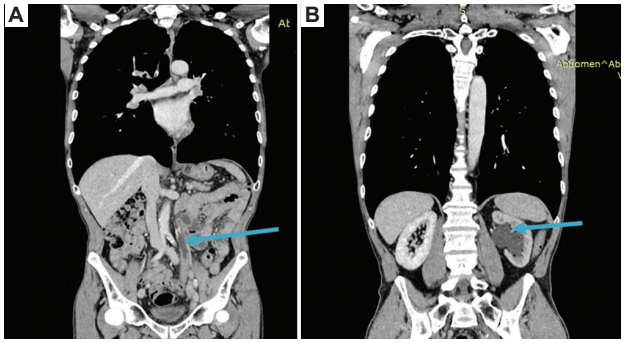

Figure 1. (A) Extended tumor in the middle and lower parts of the left ureter (indicated by the arrow). (B) Pyelokalikoectasis of the left kidney (indicated by the arrow).

patient. Therefore, a laparoscopic left nephroureterectomy with regional lymph node dissection was performed. Following the insertion of working trocars and pneumoperitoneum, the left kidney was mobilized with the ureter to the bladder. Instrumental palpation identified the presence of a whitish-colored, stony formation with a length of up to 100 mm at the junction of the middle and lower thirds of the ureter (Figure 2).

At this level, the ureter was intimately fused with nearby tissues, and enlarged lymph nodes were observed in the left iliac area (Figure S2).

The macroscopic sample consisted of a removed left kidney and left ureter with a tumor and a resected orifice of the left ureter (Figure S3).

Upon macroscopic evaluation, the gross specimen comprised a removed left kidney measuring 100×40×45 mm. The capsule proved challenging to remove. Incisions revealed an expanded calyx-pelvic system with a smooth, pinkish-cyanotic mucous membrane. The boundaries between cortical and medullary regions were indistinct. The left ureter measured 210 mm, exhibiting a significant narrowing of the lumen exceeding 110 mm in the middle and lower thirds, accompanied by up to a 10 mm thickening of the wall. The ureteral wall at this level presented as whitish-gray dense tissue. The distance from the narrowing site to the distal edge of the resection was 30 mm and from the kidney hilum was 90 mm. The removed lymph node varied in diameter from 6 mm to 18 mm (Figure 3A and B).

Microscopic examination revealed a tumor-like thickening of the ureter wall due to extensive moire (storiform) fibrosis (Figure S4). Additionally, there was moderately pronounced, diffuse infiltration of lympho-plasma cells with an admixture of eosinophils (Figure 4).

The muscle wall exhibited fraying, and the muscle fibers displayed hypertrophy. The mucous membrane was

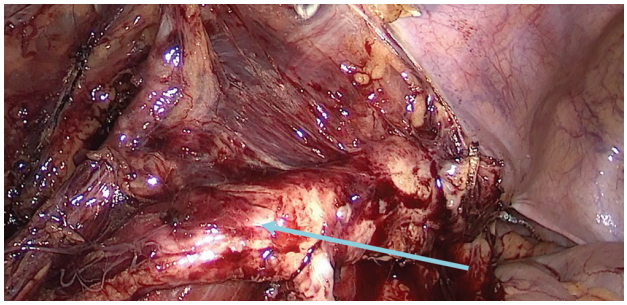

Figure 2. A tumor on the border of the middle and lower parts of the left ureter (indicated by an arrow).

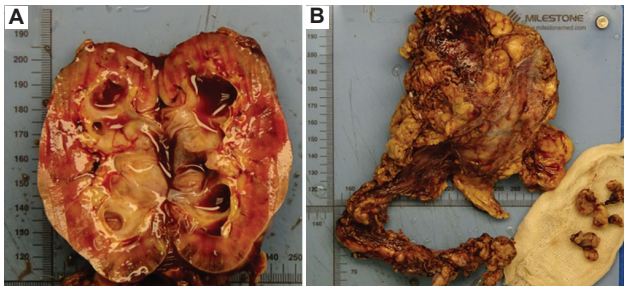

Figure 3. (A) Left kidney. (B) Left ureter dissected with lymph nodes.

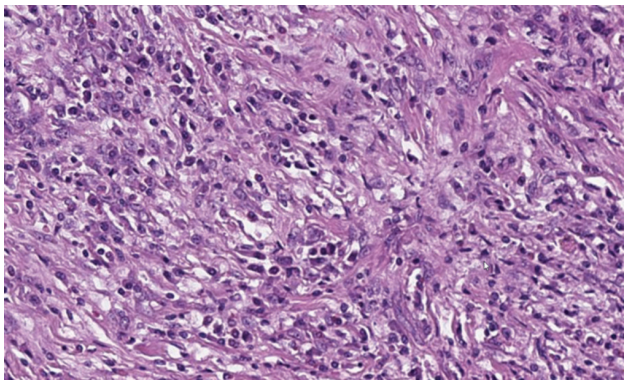

Figure 4. Ureteral wall with diffuse infiltration by lymphocytes, plasmocytes, and eosinophils (hematoxylin end eosin staining, magnification: ×400).

covered with urothelium of normal histological structure, devoid of signs of atypia (Figure S5).

An increased number of venous-type vessels was noted, exhibiting both inflammatory infiltration of the walls without obliteration of the vein lumens and areas with complete obliteration (non-obliterating and obliterating phlebitis). Furthermore, inflammatory infiltration and fibrosis affected the ureteral adventitia and surrounding adipose tissue.

The extracted kidney tissue exhibited typical architectonics with a relatively moderate degree of interstitial infiltration by lympho-plasma cells, interstitial

fibrosis, and sclerosis of individual glomeruli. The renal tubule lumens were dilated, accompanied by dystrophic changes in the tubular epithelium.

Within the lymph node tissue, slight fibrosis was noted with plasticization of the interfollicular spaces and sinuses. Morphological changes were most consistent with tumor-like fibroinflammatory lesions of the ureter, chronic interstitial nephritis, and sinus histiocytosis of the lymph nodes.

For the differential diagnosis of IgG4-RD, immunohistochemistry (IHC) was performed using antibodies against CD138, anaplastic lymphoma kinase (ALK), kappa and lambda light chains, and IgG4. IHC specimens revealed a normal kappa/lambda ratio in the infiltrate, and no ALK expression was observed. Staining with antibodies against CD138 confirmed the presence of an admixture of plasma cells in the infiltrate (Figure 5), the majority of which were IgG4-positive (Figure 6).

The CD138+/IgG4+ ratio exceeded 80%, with over 200 IgG4-positive plasma cells observed in the field of view at 400× magnification.

Morphological and IHC changes corresponded to IgG4-related ureteritis (so-called segmental ureteritis) and IgG4-related interstitial nephritis. No evidence of malignant tumor growth was found in the examined tissue. According to the morphological and IHC results, the patient exhibited a serum IgG4 concentration of 149 mg/dL (reference range: 10 – 135 mg/dL). Thus, based on the clinical, morphological, and laboratory findings, we established the diagnosis of IgG4-RD of the left ureter. The patient is currently under dynamic follow-up, and no signs of disease recurrence have been observed.

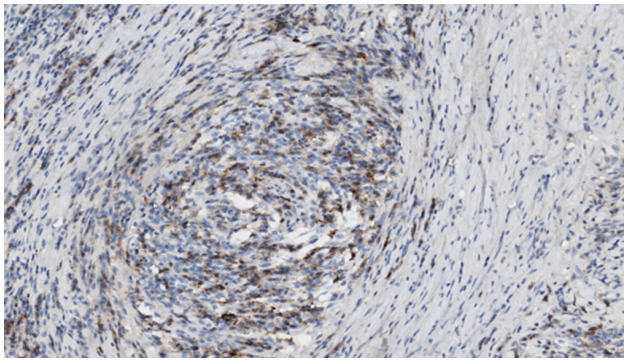

Figure 5. Immunohistochemical image showing periphlebitis. There is a positive reaction with antibodies to CD138 in the cytoplasm of plasma cells. Magnification: ×200.

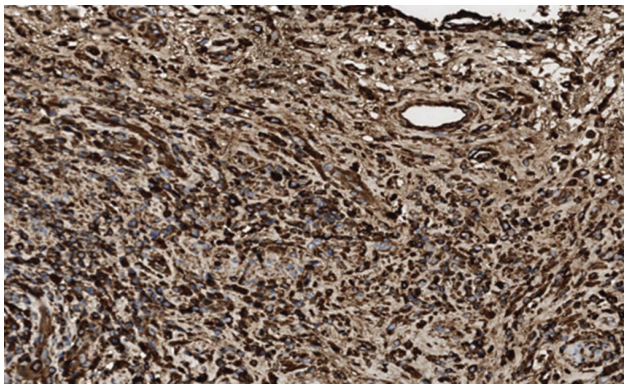

Figure 6. Immunohistochemical study showing positive staining with IgG4 antibodies in the tumor. Magnification: ×400.

3. Discussion

IgG4-RD has recently been identified as an independent disease, characterized by the presence of lymphoplasmacytic infiltration of affected tissues accompanied by hyperproduction of IgG4[1-3]. This condition is observed in various organs, exhibiting a diverse range of clinical manifestations, occasionally mimicking malignant neoplasms[7,8]. While IgG4-related nephritis and retroperitoneal fibrosis have been described in detail in the literature, instances of IgG4-related ureteral diseases have been documented in only 15 clinical cases[12,13,15]. The management of patients with ureteral IgG4-RD remains challenging, given the complexities associated with both diagnosis and treatment.

The complexity of the diagnosis largely stems from the subtle clinical course of the disease and the absence of specific clinical manifestations. Notably, Williams *et al.* describe in their clinical observation the presence of pain in the right quadrant of the abdomen[16], while Lei *et al.* reported in their observation the manifestation of IgG4-related ureteral disease with pain in the left lumbar region[12]. Additionally, Zhong *et al.* describe the manifestations of the disease, including lumbar and abdominal pain, fever, myalgia, and weight loss[13]. In a comprehensive study analyzing treatment outcomes in 65 patients with IgG4 genitourinary diseases, Teng *et al.* reported that at the time of the initial presentation, all patients exhibited varying degrees of renal failure due to impaired urodynamics and damage to the tubular apparatus of the kidneys[10]. In our observation of IgG4-RD of the ureter, the patient's clinical manifestations included left lumbar pain and anorexia, which were also non-specific. Laboratory tests revealed an increase in blood creatinine to 131 μmol/L and urea to 7.1 mmol/L, corresponding to the initial stage of chronic kidney disease.

The complexity of the diagnosis is further compounded by the presence of radiological signs typically associated with ureteral tumor lesions. Lei *et al.* provide a radiographic description of an IgG4-related ureteral lesion

resembling a tumor, characterized by active contrast agent accumulation along the thickened ureteral wall and the presence of enlarged regional lymph nodes[12]. Similar radiological images obtained through multi-slice CT (MSCT) of abdominal organs are presented in the clinical observation by Williams *et al.*[16], which also reported the CT progression of the mass, noting a 1.6-fold increase in size over a 6-week observation period. In addition, through the evaluation of positron emission tomography (PET) with ^{18}F-fluorodeoxyglucose (FDG), Williams *et al.*[16] demonstrated high metabolic activity in the lesion identified through MSCT, as well as in the regional lymph nodes. Analyzing FDG PET-CT results, Ueki *et al.* also reported elevated metabolic activity in the ureteral formation, with up to an 8-fold excess accumulation of the radiopharmaceutical[15]. In our observation, we encountered challenges in interpreting CT results, as the patient presented with an extensive ureteral tumor exhibiting signs of active contrast agent accumulation and an increase in regional lymph nodes. The obtained radiological results did not permit the exclusion of a malignant neoplasm of the ureter.

The question of performing a tumor biopsy for morphological confirmation of the diagnosis remains debatable and unresolved. According to Ueki *et al.*, endoscopic biopsy of lesions should always be performed in controversial clinical situations. In such complicated clinical scenarios, where the outcome of the disease may be affected, Ueki *et al.* suggest performing a biopsy through laparoscopic access or resection of the tumorous ureter with an urgent morphological study[15]. At the same time, the question of endoscopic and intraoperative biopsy remains open, as, in the case of a malignant process, it may lead to its further spread. In our pre-operative clinical observation, the patient underwent ureteroscopy with a biopsy of the pathologically modified parts of the ureter. However, morphological examination revealed fragments of the ureteral wall represented by fibrous tissue with signs of chronic inflammation but without reliable signs of tumor growth. Therefore, pre-operative biopsy is not always informative and may not reveal specific signs of IgG4-RD.

According to established criteria, an important diagnostic parameter for identifying IgG4-related ureteral disease is an elevation in serum IgG4 beyond specified reference values (>135 mg/dL)[6]. In this regard, in contentious clinical scenarios, most authors deem it necessary to examine serum IgG4 levels. In the clinical observation by Ueki *et al.*, the median serum IgG4 level was 384 mg/dL (206 – 965 mg/dL). Zhong *et al.* reported a serum IgG4 increase exceeding 3 times the reference values[13]. In an analysis of a survey involving 65 patients with IgG4-RD of the genitourinary system, Teng *et al.* discovered that, for patients with IgG4-RD affecting the kidney, the mean IgG4 serum level was 9510 mg/L (4295 – 15050 mg/L), while for those with ureteral IgG4-RD, the mean serum IgG4 was 7920 mg/L (3058 – 38150 mg/L). In cases of renal IgG4-RD combined with retroperitoneal fibrosis, mean serum IgG4 levels were maximal, remaining at 14100 mg/L (3200 – 22000 mg/L). Teng *et al.* also reported an established direct correlation between the level of blood serum creatinine and the level of serum IgG4[10]. In our observation, the examination of serum IgG4 was performed after surgical treatment and histological examination. However, we noted a serum IgG4 increase to 149 mg/dL after the primary source was removed.

The pre-operative diagnosis of IgG4-RD is exceptionally challenging due to non-specific clinical manifestations, such as lumbar and abdominal pain, coupled with a radiological image that is frequently misinterpreted as indicative of a malignant neoplasm in the ureter. The determination of serum IgG4 is extremely rare in practice. For this reason, urologists often misdiagnose these diseases as malignant neoplasms, leading to the inadvertent treatment of patients with nephroterectomy. Early diagnosis is imperative to prevent overtreatment.

Treatment strategies for IgG4-associated disease are not well-developed, mainly relying on expert opinions and the results of retrospective studies. While the first prospective studies have been published in recent years, they are mostly small and non-randomized[17].

Glucocorticosteroids (GCS) serve as the primary first-line treatment for IgG4, with most patients responding well to induction therapy. In cases where there is a high risk of recurrence, identified by risk factors such as multiorgan damage, elevated concentrations of IgG4 and IgE, and peripheral blood eosinophilia, additional immunosuppressive drugs (azathioprine, methotrexate, tacrolimus, and cyclophosphamide) may complement the initial GCS therapy. However, their effectiveness has not been convincingly proven. Genetically engineered biologics are usually prescribed when conventional immunosuppressive drugs prove ineffective. Ebbo *et al.* used rituximab in 33 patients diagnosed with IgG4-associated disease[18], achieving a 93.5% clinical response rate and allowing discontinuation of GCS in half of the cases. However, within an average of 19 ± 11 months post-treatment, disease recurrence was observed in 41.9% of patients. Maintenance therapy demonstrated prolonged disease-free survival (P = 0.02). However, it should be noted that rituximab therapy is often associated with the development of severe infections and hypogammaglobulinemia[19]. The

relatively high complication rate associated with rituximab therapy significantly limits its applicability in the treatment of IgG4-associated disease, particularly for maintenance indications. Despite existing recommendations for treating IgG4-associated disease, many experts advocate for a cautious approach in specific clinical situations[20]. In our clinical observation, considering the radical nature of surgical treatment and the absence of disease-related clinical manifestations, the decision was made to opt for dynamic observation. This approach helped minimize the drug burden of the patient and postponed the initiation of drug therapy.

The question of optimal diagnostic methods for actively monitoring patients after treatment is still not fully resolved. PET-CT is considered a promising method for the diagnosis and dynamic monitoring of IgG4-associated disease. An evaluation of 46 PET-CT scans in 21 patients diagnosed with IgG4-associated disease[21] revealed pathological accumulation of FDG in organs commonly affected by IgG4-associated disease at the time of diagnosis or recurrence.

In general, PET-CT has demonstrated greater sensitivity than standard imaging in diagnosing lesions in various organs, particularly in arteries, salivary glands, and lymph nodes. However, in certain cases (e.g., in the presence of small lesions), false-negative results were observed. PET-CT findings before and after treatment generally correlated with the response to therapy and disease activity.

In presenting this clinical observation, our objective is to raise awareness among urologists regarding the potential presence of IgG4-RD in patients with suspected urothelial carcinoma of the ureter. We propose incorporating the determination of serum IgG4 and, in specific cases, biopsy of the formation into the diagnostic algorithm.

4. Conclusion

This uniquely rare clinical case emphasizes the importance for urologists to consider IgG4-RD in the differential diagnosis of ureteral neoplasms. Given that IgG4-RDs can be manifested in various organs and often resemble malignant neoplasms, we advocate for the inclusion of serum IgG4 level determination in the diagnostic algorithm for such polysemantic clinical scenarios. Accurate and timely recognition of IgG4-RD of the ureter facilitates a conservative cure with GSC drugs, potentially averting the need for aggressive surgical treatment.

Acknowledgments

None.

Funding

This research received support from the Ministry of Higher Education and Science of the Russian Federation through a grant (No. 075-15-2020-912) for the creation and development of world-class research centers (Photonics Center).

Conflict of interest

The authors declare that they have no competing interests.

Author contributions

Conceptualization: Ekaterina Anikanova, Daniel Yagudaev
Data curation: Konstantin Firsov
Formal analysis: Nina Kalyagina, Arina Plotnikova
Investigation: Nina Kalyagina, Daniel Yagudaev
Methodology: Daniel Yagudaev, Ekaterina Anikanova, Konstantin Firsov
Resources: Daniel Yagudaev
Supervision: Daniel Yagudaev
Validation: Ekaterina Anikanova, Daniel Yagudaev
Visualization: Konstantin Firsov
Writing – original draft: Ekaterina Anikanova, Nina Kalyagina
Writing – review & editing: Daniel Yagudaev, Arina Plotnikova

Ethics approval and consent to participate

The study was conducted according to the guidelines of the Declaration of Helsinki. Ethical review and approval were waived for this study due to the retrospective nature of the study and the use of de-identified data.

Consent for publication

Informed consent was obtained from the patient involved in the study.

Availability of data

All information that grounded this case report is available within the main text, tables, and figures. Further data are available from the corresponding author upon request.

References

1. Maritati F, Peyronel F, Vaglio A, 2020, IgG4-related disease: A clinical perspective. *Rheumatology* (*Oxford*), 59(Suppl 3): iii123–iii131.

   https://doi.org/10.1093/rheumatology/kez667

2. Zhang W, Stone JH, 2019, Management of IgG4-related disease. *Lancet Rheumatol*, 1: e55–e65.

   https://doi.org/10.1016/S2665-9913(19)30017-7

3. Zykova A, Novikov P, Brovko M, *et al*., 2020, IgG4-related disease: The state of art. *Clin Pharmacol Ther*, 29(3): 4–13. (In Russ).

   https://doi.org/10.32756/0869-5490-2020-3-4-13

4. Kamisawa T, Funata N, Hayashi Y, *et al*., 2003, A new clinicopathological entity of IgG4-related autoimmune disease. *J Gastroenterol*, 38(10): 982–984.

   https://doi.org/10.1007/s00535-003-1175-y

5. Umehara H, Okazaki K, Masaki Y, *et al*., 2012, A novel clinical entity, IgG4-related disease (IgG4RD): General concept and details. *Mod Rheumatol*, 22(1): 1–14.

   https://doi.org/10.1007/s10165-011-0508-6

6. Deshpande V, Zen Y, Chan JK, *et al*., 2012, Consensus statement on the pathology of IgG4-related disease. *Mod Pathol*, 25: 1181–1192.

   https://doi.org/10.1038/modpathol.2012.72

7. Yu KH, Chan TM, Tsai PH, *et al*., 2015, Diagnostic performance of serum IgG4 levels in patients with IgG4-related disease. *Medicine* (*Baltimore*), 94: e1707.

   https://doi.org/10.1097/MD.0000000000001707

8. Vasaitis L, 2016, IgG4-related disease: A relatively new concept for clinicians. *Eur J Inter Med*, 27: 1–9.

   https://doi.org/10.1016/j.ejim.2015.09.022

9. Wallace ZS, Zhang Y, Perugino CA, *et al*., 2019, Clinical phenotypes of IgG4-related disease: An analysis of two international cross-sectional cohorts. *Ann Rheum Dis*, 78(3): 406–412.

   https://doi.org/10.1136/annrheumdis-2018-214603

10. Teng F, Lu H, Zheng K, *et al*., 2020, Urinary system manifestation of IgG4-related disease: Clinical, laboratory, radiological, and pathological spectra of a Chinese single-centre study. *J Immunol Res*, 2020: 5851842.

    https://doi.org/10.1155/2020/5851842

11. Bianchi D, 2016, IgG4-related disease: What urologists should know. *Int Urol Nephrol*, 48(3): 301–312.

    https://doi.org/10.1007/s11255-015-1189-4

12. Lei WH, Xin J, Shao CX, *et al*., 2016, IgG4-related kidney disease mimicking malignant ureter tumor: Case report and literature review. *Medicine* (*Baltimore*), 95(3): e2550.

    https://doi.org/10.1097/MD.0000000000002550

13. Zhong W, Kam J, Beattie K, *et al*., 2018, A rare case of ureteral IgG4 disease masquerading as urothelial carcinoma. *Urology*, 118: e1–e2.

    https://doi.org/10.1016/j.urology.2018.05.019

14. Bissada NK, Finkbeiner AE, 1978, Idiopathic segmental ureteritis. *Urology*, 12(1): 64–66.

    https://doi.org/10.1016/0090-4295(78)90370-9

15. Ueki T, Miyake T, Narita M, *et al*., 2020, IgG4-related focal retroperitoneal fibrosis in ureter suggestive of colon cancer recurrence and resected laparoscopically: A case report. *Surg Case Rep*, 6: 197.

    https://doi.org/10.1186/s40792-020-00964-0

16. Williams IS, Wang N, Bergamin P, *et al*., 2021, Peri-ureteric mass an unusual case of immunoglobin G4-related disease (IgG4-RD). *Urol Case Rep*, 38: 101666.

    https://doi.org/10.1016/j.eucr.2021.101666

17. Lanzillotta M, Mancuso G, Della-Torre E, 2020, Advances in the diagnosis and management of IgG4 related disease. *BMJ*, 369: m1067.

    https://doi.org/10.1136/bmj.m1067

18. Ebbo M, Grados A, Samson M, *et al*., 2017, Long-term efficacy and safety of rituximab in IgG4-related disease: Data from a French nationwide study of thirty-three patients. *PLoS One*, 12(9): e0183844.

    https://doi.org/10.1371/journal.pone.0183844

19. Campochiaro C, Della-Torre E, Lanzillotta M, *et al*., 2020, Long-term efficacy of maintenance therapy with rituximab for IgG4-related disease. *Eur J Intern Med*, 74: 92–98.

    https://doi.org/10.1016/j.ejim.2019.12.029

20. Buijs J, van Heerde MJ, Rauws EA, *et al*., 2014, Comparable efficacy of low-versus high-dose induction corticosteroid treatment in autoimmune pancreatitis. *Pancreas*, 43(2): 261–267.

    https://doi.org/10.1097/MPA.0000000000000044

21. Tang J, Cai S, Ye C, *et al*., 2020, Biomarkers in IgG4-related disease: A systematic review. *Semin Arthritis Rheum*, 50(2):354–359.

    https://doi.org/10.1016/j.semarthrit.2019.06.018

Our Journals

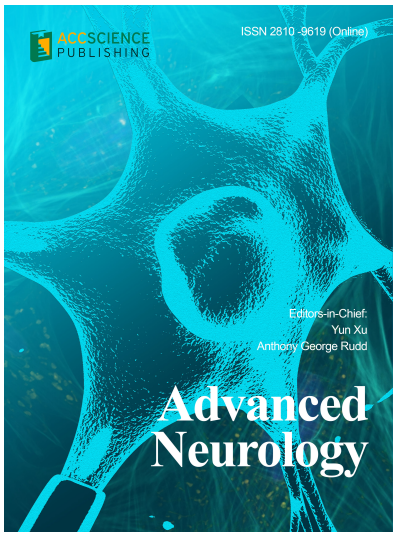

Advanced Neurology is a peer-reviewed and open-access journal that aims to publish and disseminate novel research in the breadth of neurology and neuroscience. The journal aims to advance our understanding in the nervous system and provide a platform to neuroscientists and physicians to showcase their findings in original fundamental and clinical research as well as to present new ideas that highlight the changes in the neurological clinical practice.

Advanced Neurology covers subject areas, including but not limited to the following:

- Neurological disorders
- Neurodegenerative disease
- Cerebrovascular disease
- Epilepsy and movement disorders
- Neuroimmune disease
- Neurological infections
- Muscle disease
- Molecular and cellular neuroscience
- Systems neuroscience
- Cognitive neuroscience
- Computational modeling of nervous system

Global Translational Medicine is a quarterly journal that focuses on medicine, biological sciences, and biomaterials engineering. The goal of *Global Translational Medicine* is to provide a platform to researchers for showcasing their latest research works in translational medicine so as to advance the field towards the betterment of human health. Despite the advancement of omics and new technologies, the process of transforming these technologies and scientific research results into effective therapies and putting them into clinical use still has a long way to go. *Global Translational Medicine* provides a platform to fill the gaps in preclinical and inter-disciplinary research, to promote clinical translation of scientific research results, and to contribute to the conception of new and improved preventive measures as well as diagnostic and therapeutic techniques of diseases.

Global Translational Medicine covers the following themes: cardiovascular disease, metabolism/diabetes/obesity, neuroscience/neurology, cancer, biomaterials and their applications in medicine, proteomics/metabolomics, pharmacogenomics, biomarkers, bioinformatics and data mining, animal and clinical research, and medical methods arising from interdisciplinary crossover.

Start a new journal

Write to us via email if you are interested to start a new journal with AccScience Publishing. Please attach your CV, professional profile page and a brief pitch proposal in your email. We shall inform you of our decision whether we are interested to collaborate in starting a new journal.

Contact: info@accscience.com

https://accscience.com/journal/TD

Contact

www.accscience.com

8 Burn Road, #15-03 Trivex, Singapore 369977

Email: editorial@accscience.com

Phone: +65 8182 1586